

ACTA

UNIVERSITATIS OULUENSIS

*Veijo Lyöri*

STRUCTURAL MONITORING  
WITH FIBRE-OPTIC SENSORS  
USING THE PULSED TIME-OF-  
FLIGHT METHOD AND OTHER  
MEASUREMENT TECHNIQUES

FACULTY OF TECHNOLOGY,  
DEPARTMENT OF ELECTRICAL AND INFORMATION ENGINEERING,  
INFOTECH OULU,  
UNIVERSITY OF OULU

C  
TECHNICAL





*VEIJO LYÖRI*

**STRUCTURAL MONITORING WITH  
FIBRE-OPTIC SENSORS USING  
THE PULSED TIME-OF-FLIGHT  
METHOD AND OTHER  
MEASUREMENT TECHNIQUES**

Academic dissertation to be presented, with the assent of  
the Faculty of Technology of the University of Oulu, for  
public defence in Keckmaninsali (Auditorium HU106),  
Linnanmaa, on January 25th, 2008, at 12 noon

Copyright © 2007  
Acta Univ. Oul. C 291, 2007

Supervised by  
Professor Juha Kostamovaara

Reviewed by  
Professor Brian Culshaw  
Doctor Daniele Inaudi

ISBN 978-951-42-8701-5 (Paperback)  
ISBN 978-951-42-8702-2 (PDF)  
<http://herkules.oulu.fi/isbn9789514287022/>  
ISSN 0355-3213 (Printed)  
ISSN 1796-2226 (Online)  
<http://herkules.oulu.fi/issn03553213/>

Cover design  
Raimo Ahonen

OULU UNIVERSITY PRESS  
OULU 2007

## **Lyöri, Veijo, Structural monitoring with fibre-optic sensors using the pulsed time-of-flight method and other measurement techniques**

Faculty of Technology, University of Oulu, P.O.Box 4000, FI-90014 University of Oulu, Finland,  
Department of Electrical and Information Engineering, Infotech Oulu, University of Oulu, P.O.Box  
4500, FI-90014 University of Oulu, Finland

*Acta Univ. Oul. C 291, 2007*

Oulu, Finland

### ***Abstract***

This thesis deals with the developing of fibre-optic instruments for monitoring the health of civil engineering and composite structures. A number of sensors have been tested for use with different road structures, concrete bridges, fibre reinforced polymer (FRP) containers and other composite specimens, the interrogation methods being mainly based on measuring optical power and time-of-flight (TOF). The main focus is on the development of a fibre-optic TOF measurement system and its applications, but different sensing needs and fibre-optic measurement systems are also reviewed, with the emphasis on commercial devices.

Deformation in a road structure was studied with microbending sensors of gauge-length about 10 cm and a commercial optical time domain reflectometer (OTDR) in a quasi-distributed fashion. The responses of the optical fibre sensors during the one-year measurement period were similar in shape to those obtained with commercial strain gauges but the absolute measurement values typically deviated by several tens of per cent. Low dynamic range, crosstalk and poor signal-to-noise ratio proved to be the main problem when measuring several successive sensors with an OTDR. In another road investigation, microbending and speckle sensors were found useful for providing on/off-type information for traffic control applications.

FRP composite containers were investigated with the focus on developing a continuous monitoring system for improving yield and quality by evaluating the state of cure during the manufacturing process and for assessing damage, e.g. delaminations, during service life. Standard multi-mode and single mode fibres with a typical length of a few hundreds of metres were embedded inside the walls of containers during the normal manufacturing process, and the measurements were carried out using an optical through-power technique and an OTDR. This largely empirical investigation revealed that the coating material and its thickness have an effect on loading sensitivity and on the applicability of the method for cure monitoring. The measurement data also indicated that the end-of-curing process and the location of external damage can be determined with a distributed optical fibre sensor and an OTDR.

Several versions of a pulsed time-of-flight measurement system were developed for interrogating sensor arrays consisting of multiple long gauge-length sensors. The early versions based on commercial electronics were capable of producing relevant measurement data with a reasonable precision, but they suffered especially from poor spatial resolution, low sampling rate and long-term drift.

The high precision TOF system developed in this thesis is capable of measuring time delays between a number of wideband reflectors, such as connectors or fibre Bragg gratings (FBG), along a fibre path with a precision of about 280 fs (rms-value) and a spatial resolution of about 3 ns (0.30 m) in a measurement time of 25 milliseconds. By using a fibre loop sensor with a reference fibre, a strain precision below 1  $\mu\epsilon$  and a measurement frequency of 4 Hz can be achieved. The system has proved comparable in performance to a commercial FBG interrogation system in monitoring the behaviour of a bridge deck, while the fact that it allows static and dynamic measurements with a number of long gauge-length sensors, also embedded in FRP composite material, makes this TOF device unique relative to other measurement systems.

*Keywords:* bridge, civil engineering, container, FBG, FRP composite, health monitoring, microbending, optical fibre, OTDR, road structure, sensor, strain, time-of-flight, TOF



## Acknowledgements

Focusing on research into fibre-optic sensors and their applications to structural monitoring, the work leading to this thesis was carried out in the Department of Electrical and Information Engineering at the University of Oulu over the period 1993–2007.

First of all, I would like to thank Prof. Juha Kostamovaara for supporting, encouraging and believing in me during this challenging work. I also thank him for his patience in waiting for the final manuscript.

I owe my warmest thanks to my wife Kaisu and our children Taru and Ville who have brought meaning and happiness into my life. I also wish to express my deep gratitude to my parents, Kirsti and the late Olavi, and to my sister Pirjo, who have offered unstinting support during my whole life.

I am grateful to my co-workers, Ari Kilpelä, D.Tech., and Guoyong Duan, Lic.Tech., who played a considerable role in the later part of the research work, which represents the main contribution of the thesis. Antti Mäntyniemi, D.Tech., is appreciated for his help with the time measurements and Matti Polojärvi, chief technician, for helping me with the assembly of the electronics and fibre optics.

I wish to thank Prof. Timo Aho at the Research Unit of Construction Technology for giving us a chance to participate in the European Union project “Sustainable Bridges – Assessment for Future Traffic Demands and Longer Lives”.

I also wish to thank previous co-workers, Prof. Harri Kopola, Prof. Risto Myllylä, Prof. Kari Määttä, Seppo Nissilä, Pekka Suopajarvi, Riku Pennala, Mikko Heikkinen, Hannu Lahtinen, Krisztián Kordás and many others, for their participation in the research.

I would also like to convey my appreciation to the entire personnel of the Electronics Laboratory for creating a pleasant working environment. Furthermore, the whole staff of the department’s workshop, especially the operating engineer Pentti Piekkola and the laboratory technician Anssi Rimpiläinen, deserves my warmest thanks for designing and making the mechanical components for the various measurement systems.

Tauno Tönning Säätiö and Tekniikan Edistämissäätiö are gratefully acknowledged for giving financial support.

Last, but not least, I owe my sincerest thanks to our “lunch group”, Juha, Hannu, Ari, Anssi M., Anssi R., Matti, Antero and others, with whom I have had the biggest laughs during working days.

Oulu, December 2007

Veijo Lyöri



## List of terms, symbols and abbreviations

The terms describing the performance of sensors are defined according to the International Vocabulary of Basic and General Terms in Metrology (1994).

Measurement result	is only an approximation or estimate of the value of the measurand and thus is complete only when accompanied by a statement of the uncertainty of that estimate, respectively: $\Delta\varepsilon = 20 \mu\text{m/m} \pm 3 \mu\text{m/m}$ (95%) or $\Delta\varepsilon = (20 \pm 3) \mu\text{m/m}$ (95%). The numerical value following the symbol $\pm$ is the combined standard uncertainty and not a confidence interval. The percentage in parenthesis (here: 95%) informs about the coverage probability, or in other words, about the level of confidence.
Resolution	is defined as smallest difference between indications of the sensor (including the displaying device) that can be meaningfully distinguished. Resolution is related to the achievable measurement uncertainty which should not exceed 10 to 20% of the minimum quantity to be measured; resolution be better than below 10 to 20% of this desired measurement uncertainty. The achievable resolution is always defined by the complete measurement system, not only by the displaying device.
Precision	informs about the closeness of the agreement between the results of successive measurements of the same measurand carried out under the same conditions of measurement (repeatability) or under changed conditions of measurements (reproducibility). Both types of precision may only be expressed quantitatively in terms of the dispersion characteristics of the results (e. g. standard deviation $\sigma$ , variance $\sigma^2$ ).

Accuracy is a qualitative concept and expresses the closeness of the agreement between the result of a measurement and a true value of the measurand. Every still so accurate measurement represents only an estimate; so that accuracy gives the reciprocal information how inaccurate a measurement is due to unavoidable non-linearities, hysteresis effects, environmental influences, vibrations, drifts, and many other effects.

Distributed sensor is a sensor which enables the measurand to be assessed at any point along the fibre to within a spatial resolution determined generally by opto-electronic constraints.

Quasi-distributed sensor is a sensor which enables the measurand to be assessed at a number of predefined locations along the fibre.

A	Ampere
°C	degrees Celsius
Hz	Hertz
K	degrees Kelvin
N	Newton
Pa	Pascal
V	Volt
W	Watt
Ω	Ohm
m	metre, mill, $10^{-3}$
s	second
f	femto, $10^{-15}$
p	pico, $10^{-12}$
n	nano, $10^{-9}$
μ	micro, $10^{-6}$
k	kilo, $10^3$
M	mega, $10^6$
G	giga, $10^9$
dB	decibel
dBm	decibels with respect to a power of 1 mW

$\mu\epsilon$	$\mu$ strain, microstrain, unit of strain (1 $\mu\text{m} / \text{m}$ )
$\mu\text{strain}$	microstrain, unit of strain (1 $\mu\text{m} / \text{m}$ ), $\mu\epsilon$
$\lambda$	optical wavelength
$\lambda_b$	resonance wavelength in an FBG
$\Lambda$	distance between refractive index lines in an FBG
$\Delta$	difference
$\epsilon$	strain
$\tau$	optical time delay
$\nu_B$	frequency shift in Brillouin spectrum
$\sigma$	standard deviation, rms-value, timing jitter, stress
$\phi$	diameter
$a$	strain-optic coefficient ( $\approx -0.2$ )
$c$	speed of light in a vacuum ( $\approx 3 \times 10^8 \text{ m} / \text{s}$ ), cent, $10^{-2}$
$f$	frequency
$h$	hour
$l$	length, gauge length
$n$	group refractive index of an optical fibre ( $\approx 1.47$ )
$t$	time
$A$	transmission loss
$B$	reflection loss
$E$	Young's modulus
$N$	number of measurements used in averaging
$P$	optical power
$R$	reflectivity, reflector
$T$	temperature
ATTN	extra loss in a reflector
$N_{\text{MAX}}$	maximum number of sensors
OPR	optical power range
AGC	automatic gain control
APD	avalanche photo diode
ASIC	application-specific integrated circuit
bin	binary
BOTDA	Brillouin optical time domain analysis system
BOTDR	Brillouin optical time domain reflectometer
CCD	charge-coupled device
CFD	constant fraction timing discriminator
CMOS	complementary metal-oxide-semiconductor

DC	direct current
ECL	emitter-coupled logic
EFPI	extrinsic Fabry-Perot interferometric sensor
EMI	electromagnetic interference
FBG	fibre Bragg grating
FC	standard-type optical fibre connector
FPGA	field-programmable gate array
FRP	fibre-reinforced polymer
FWHM	full width half maximum value
INL	integral nonlinearity
LSB	least significant bit
MEMS	microelectromechanical system
MM	multi-mode
OPGW	optical ground wire
OTDR	optical time domain reflectometer
PC	personal computer, physical contact
ppm	parts per million
rms	root mean square value, standard deviation
SM	single mode
SNR	signal-to-noise ratio
TDC	time-to-digital converter
TDM	time division multiplexing
TOF	time-of-flight, transit time
TTL	transistor-transistor logic
UV	ultra-violet radiation
VIV	vortex induced vibration
WDM	wavelength division multiplexing
WIM	weight in motion

## List of original papers

This thesis consists of an overview and the following nine publications:

- I Lyöri V, Suopajarvi P, Nissilä S, Kopola H & Suni H (1994) Measurement of stress in a road structure using optical fibre sensors. Proc. First World Conference on Structural Control, Los Angeles, USA, 1: WA3 40–48.
- II Suopajarvi P, Pennala R, Heikkinen M, Karioja P, Lyöri V, Myllylä R, Nissilä S, Kopola H & Suni H (1998) Fibre optic sensors for traffic monitoring applications. Proc. SPIE, 5<sup>th</sup> Annual International Symposium on Smart Structures and Materials, San Diego, USA, 3325: 222–229.
- III Suopajarvi P, Lyöri V, Nissilä S, Kopola H & Johansson R (1995) Indicating cure and stress in composite containers using optical fibers. Optical Engineering 34(9): 2587–2591.
- IV Lyöri V, Määttä K, Nissilä S, Kopola H, Englund M & Mitrunen A (1996) A high resolution reflectometer for measuring dynamic strain in a single mode optical fibre. Proc. International Conference on Applications of Photonic Technology 2, Montreal, Canada: 751–756.
- V Lyöri V, Määttä K, Nissilä S, Kopola H & Englund M (1997) A high precision Fresnel-OTDR for distributed fibre-optic sensor network applications. Proc. 12<sup>th</sup> International Conference on Optical Fiber Sensors, Williamsburg, USA: 520–523.
- VI Lyöri V, Määttä K, Myllylä R, Jurvakainen M, Lahtinen H, Peltomäki P, Pramila A, Heikkinen M, Suopajarvi P & Kopola H (2000) A fibre-optic time-of-flight laser radar for measuring integral strain in a composite structure. Proc. SPIE, 14<sup>th</sup> International Conference on Optical Fiber Sensors, Venice, Italy, 4185: 210–213.
- VII Lyöri V, Mäntyniemi A, Kilpelä A, Duan G & Kostamovaara J (2003) A fibre-optic time-of-flight radar with a sub-metre spatial resolution for the measurement of integral strain. Proc. SPIE, International Conference on Smart Structures and Materials, San Diego, USA, 5050: 322–332.
- VIII Lyöri V, Kilpelä A, Duan G, Kostamovaara J & Aho T (2006) Monitoring of a bridge-deck using long-gage optical fiber sensors with a pulsed TOF measurement technique. Proc. 3<sup>rd</sup> International Conference on Bridge Maintenance, Safety and Management (IABMAS), Porto, Portugal, published on CD (ISBN 0 415 40315 4).
- IX Lyöri V, Kilpelä A, Duan G, Mäntyniemi A & Kostamovaara J (2007) Pulsed time-of-flight radar for fiber-optic strain sensing. Review of Scientific Instruments 78(2): 024705.

The papers will be referred to below with the Roman numerals I–IX.

Paper I deals with research into a road structure in which two steel meshes used for reinforcing an asphalt layer were fitted with multi-mode or single mode microbending sensors to produce data on deformation by measuring the strain distribution across the road. The sensors were designed and installed by the author, who was also responsible for the test measurements. The experience

achieved in this study was utilized later for developing various types of microbending and speckle sensors for traffic monitoring applications. The work concerned, which was published in Paper II, was concentrated mainly on providing application-specific advice.

The study of glass composite containers published in Paper III was started during the author's work on his master's thesis (Lyöri 1993), the focus being on developing a continuous monitoring system based on long microbending sensors and optical power measurement techniques for detecting the state of cure during the manufacturing process and for assessing damage during service life. This work was continued by the author and Pekka Suopajarvi, who conducted his own research under the author's supervision.

Papers IV to VI deal with developing a fibre-optic measurement system based on a commercial pulsed time-of-flight (TOF) technique. The author's responsibility in this work was to modify the electronics cards in the device, construct the fibre-optic blocks and carry out the measurements with optical cables and fibre-optic strain sensors embedded in various composite specimens. This work constituted the main part of the author's licentiate thesis (Lyöri 2000).

The research published in Papers VII to IX represents the main contribution of the thesis. Paper VII focuses on introducing a modified TOF device for fibre-optic measurements. The main difference compared with the novice TOF system is the much higher bandwidth of the electronics channel, which, together with the use of a high-speed laser pulser and a new type of time-to-digital converter (TDC), enables much better precision and spatial resolution to be achieved. All the electronics and optics blocks except for the TDC and the software were designed and constructed by the author.

Papers VIII and IX are concerned with the third version of the fibre-optic TOF device developed by the author and others with the objective of improving the system's precision, stability and measurement speed. The device differs in construction from earlier versions in that large computing routines are performed by a programmable FPGA circuit installed in the TOF device rather than in a computer, which considerably improves the measurement speed. As for the TOF sensor, the author's ideas of using a reference fibre in conjunction with a looped sensor structure and a specially polished FC/PC connector as a reflector were found useful from the point of view of stability. The author and others tested the measurement system on a highway bridge, where its performance proved comparable to that of a commercial fibre Bragg grating (FBG) interrogation system.

Paper IX was selected for the March 2007 issue of the Virtual Journal of Ultrafast Science, which is published by the American Physical Society and the American Institute of Physics in cooperation with numerous other societies and publishers and constitutes an edited compilation of links to articles from participating publishers, covering a focused area of frontier research.



# Contents

<b>Abstract</b>	
<b>Acknowledgements</b>	<b>5</b>
<b>List of terms, symbols and abbreviations</b>	<b>7</b>
<b>List of original papers</b>	<b>11</b>
<b>Contents</b>	<b>15</b>
<b>1 Introduction</b>	<b>17</b>
1.1 Background .....	17
1.2 Scope and contribution.....	19
1.3 Organization of the thesis.....	22
<b>2 Structural monitoring with fibre-optic sensors</b>	<b>23</b>
2.1 Sensing needs.....	23
2.1.1 Civil engineering structures.....	23
2.1.2 Composite structures .....	26
2.2 Strain measurement considerations .....	27
2.2.1 Strain, deformation and displacement measurements.....	28
2.2.2 Strain and temperature-induced effects on fibre-optic sensors .....	29
2.2.3 Absolute and relative measurements .....	31
2.2.4 Dynamic and long-term measurements .....	31
2.2.5 Temperature compensation.....	31
2.3 Fibre-optic strain sensors and their interrogation methods .....	32
2.3.1 The fibre Bragg grating measurement system.....	32
2.3.2 Fabry-Perot measurement system.....	35
2.3.3 Microbending measurement system .....	38
2.3.4 Low-coherence interferometer .....	41
2.3.5 Brillouin scattering interrogation systems.....	44
2.3.6 Transit time measurement systems.....	46
2.3.7 Concluding remarks .....	53
<b>3 Experimental work</b>	<b>57</b>
3.1 Measuring of strain in road structures using microbending sensors.....	57
3.2 Traffic monitoring with microbending and speckle sensors .....	61
3.3 Measuring of composite containers with microbending sensors.....	63
3.4 A fibre-optic TOF measurement system based on commercial electronics .....	68

3.4.1	Operation and performance of the novice TOF measurement system.....	68
3.4.2	Measurements with bare TOF sensors.....	70
3.4.3	Application measurements .....	70
3.4.4	Evolution of the TOF system.....	75
<b>4</b>	<b>A high-precision fibre-optic TOF measurement system</b>	<b>77</b>
4.1	Apparatus .....	77
4.1.1	Transmitter.....	79
4.1.2	Receiver.....	79
4.1.3	Timing discriminator .....	80
4.1.4	The time-to-digital converter (TDC) .....	83
4.2	Measurements .....	85
4.2.1	Precision, measurement time and spatial resolution.....	85
4.2.2	Stability.....	86
4.2.3	Dynamic range and sensor networks .....	90
4.2.4	Measurement of strain in a bridge deck using long gauge-length TOF sensors.....	91
4.3	Comparison of the TOF measurement system with commercial devices.....	98
<b>5</b>	<b>Discussion</b>	<b>101</b>
<b>6</b>	<b>Summary</b>	<b>105</b>
	<b>References</b>	<b>107</b>
	<b>Original papers</b>	<b>115</b>

# 1 Introduction

## 1.1 Background

Monitoring of structures such as buildings, bridges, highways, tunnels, dams, pipelines, containers, wings etc. is useful from the economic and security points of view (Inaudi & Vurpillot 1999, Measures 2001: 15). With a proper sensing system it is possible to achieve information about the health of a structure which can be used for designing repair schedules and for giving early warnings of degradation that might lead to a catastrophic failure in the long-term (Measures 2001: 5).

An ageing infrastructure poses an enormous economic challenge for a society. In the USA, for example, more than 200 000 highway bridges were deficient in the early 1990's (Measures 2001: 17). It is estimated that an average of 3% of the newly-built cost of a structure will be invested yearly in its maintenance. With a limited budget, the major challenge lies in finding out which structures need to be repaired first and what interventions should be carried out (Inaudi 2002).

Health monitoring is traditionally based on visual inspection. This method is limited in time and scope, however, as it is only possible to see degradations that are visible and apparent at the time of inspection. Furthermore, one can only see degradations relative to the original state or the state at the previous inspection, but structural deficiencies that might have been hidden in the structure from the start cannot be detected (Inaudi 2002). Fitting the structure with a comprehensive sensor network capable of continuously gathering information on all relevant structural parameters offers a better way of assessing its real behaviour.

Numerous sensor types have been developed during the last 50 years or so for measuring such structural parameters as strain, temperature, pressure, humidity and acceleration, among which strain and its derivatives, such as cracks, deflection and displacement, are the most important parameters for structural monitoring (Inaudi 1997). A strain sensor can also provide information on pressure and temperature, as well as on the corrosion of re-bars, for example (Measures 2001: 423).

Conventional strain sensors such as electrical strain gauges are widely used due to their high accuracy, measurement speed, reliability and low cost (Katz 1998). A precision of  $1 \mu\epsilon$  and measurement frequency of several kHz are typically mentioned on the data sheets of commercial strain gauge systems (OMEGA 1998).

The problem with strain gauges and other conventional sensors is that there is no means of reading several successive sensors with a common interrogation unit, i.e. it is not possible to multiplex the sensors (Measures 2001: 526). As each strain gauge needs two wires for power, two wires for the signal path and an amplifier unit, the sensor system becomes very complex, especially in the case of large buildings. In fibre reinforced polymer (FRP) structures, where it is practical to embed the sensors inside the wall material, the wire harness of a strain gauge network may disturb its operation or even be harmful to the integrity of the structure by causing delaminations, for example. Other problems with strain gauges apart from their poor multiplexing capability are susceptibility to electromagnetic interference (EMI), long-term degradation and in some case a restricted temperature range.

Since the advent of low-loss optical fibres in the mid-1960's (Kao & Hockham 1966) there have been numerous trials devoted to how this unique transmission medium could be used for sensing purposes. The demonstration of the first fibre-optic strain sensor in 1978 (Butter & Hocker) was an essential milestone in this field, as was the invention of a fibre Bragg grating sensor (FBG) and Fabry-Perot interferometric sensor about ten years later (Morey *et al.* 1989, Lee & Taylor 1988). The first commercial products were acoustic hydrophone arrays and gyroscopes (Udd 1991a) for military and other special applications, but as general-purpose strain and temperature sensors emerged onto the market in the mid-1990's, technicians started to use fibre-optic technology in ordinary measurement applications as well. This was due to the many advantages that fibre-optic sensors can offer over their conventional counterparts, among which their extreme multiplexing capability is obviously the most prominent. With a proper multiplexing technique, such as time division multiplexing (TDM) or wavelength division multiplexing (WDM), it is possible to read responses from tens or even hundreds of sensors along a single fibre path, which enables the building of comprehensive sensor networks in a relatively simple manner (Kersey 1995). The growing interest in fibre-optic sensors is also due to properties such as their light weight, small size, immunity to electromagnetic interference (EMI), high-temperature performance, large bandwidth, environmental robustness with respect to vibration and shock, high sensitivity and dielectric nature (Culshaw 1988, Udd 1991a).

There are a number of commercially available fibre-optic interrogation systems which are based on amplitude measurement with a microbending sensor (OSMOS) or spectrum measurement with a fibre Bragg grating (Micron Optics, Insensys, Smart Fibres, Blue Road Research, see reference list for [www](http://www) ad-

resses). There also exist measurement systems which utilize interferometry, such as the Fabry-Perot system (Fiso Technologies, Roctest), or a low coherence interferometer (Smartec, Fox-Tek, Fogale Nanotech). Furthermore, some systems are based on measuring frequency changes in Brillouin backscattered radiation by means of Brillouin optical time domain reflectometry (BOTDR, Yokogawa Electric) or Brillouin optical time domain analysis (BOTDA, Omnisens).

Fibre-optic measurement systems differ in gauge length, which can range from a few millimetres in a typical FBG system up to several metres in a low-coherence interferometer. There is also a wide range of sampling rates, starting from the DC of a Brillouin scattering system and progressing up to several kilohertz in an FBG system. The measurement precision of each system is typically of the order of one microstrain or below, except that of a Brillouin scattering system, which is about 10–20 microstrains. Brillouin systems have one advantage over the others, that they provide a distributed form of measurement.

The work carried out in this thesis deals with the developing of microbending and other amplitude-based sensors for various civil engineering and FRP composite applications. It will be shown that simple microbending sensors together with an optical time domain reflectometer (OTDR) or a low-cost amplitude measurement system can produce relevant information for many applications. The thesis also introduces a new interrogation method for fibre-optic sensing based on time interval measurement. It will become apparent that the pulsed time-of-flight (TOF) measurement system developed here has a performance comparable to that of commercial interrogation methods. Moreover, it is able to measure both dynamic and static phenomena with multiple long gauge-length sensors, including ones embedded inside an FRP composite structure, which makes it unique relative to other measurement systems.

## **1.2 Scope and contribution**

Focusing on research into fibre-optic sensors and their applications to structural monitoring, the work leading to this thesis was carried out in the Department of Electrical and Information Engineering at the University of Oulu over the period 1993–2007.

The work started, for the author's master's thesis, with a number of laboratory tests and field trials using long optical sensor fibres in conjunction with an OTDR. It was assumed that telecommunication fibres together with a standard multi-mode OTDR would offer a relatively easy and low-cost means of construct-

ing large sensor networks. After some preliminary elongation tests it became apparent, however, that due to the poor spatial resolution of the particular OTDR measurements could not be carried out in the time domain but only in the amplitude domain, which greatly restricted the expected field of applications. Strain measurement with a reasonable precision of about  $100 \mu\epsilon$  nevertheless proved successful for a few sensors connected in a quasi-distributed way with the aid of a microbending structure built into the fibre.

The resulting microbending sensor was used for measuring deformation in a road structure, as described in Paper I. The responses of the optical fibre sensors in two field trials which both extended over one year were rather similar in shape to those of commercial resistive strain gauges, but the absolute measurement values typically deviated by several tens of per cent. The main problems when carrying out measurements with several successive sensors proved to be the low dynamic range, crosstalk between the multi-mode sensors and a poor signal-to-noise ratio in the OTDR. In another road experiment, presented in Paper II, a measurement system based on an optical through-power technique and a continuous microbending or speckle sensor was found useful for producing on/off-type information in traffic monitoring applications such as traffic counts and the control of traffic lights.

Composite containers were also investigated, with the focus on developing a continuous monitoring system for evaluating the state of cure during the manufacturing process and for assessing potential damage during service life (Paper III). Standard multi-mode and single mode fibres with a typical length of a few hundred metres were embedded inside the walls of containers during the normal manufacturing process, and the measurements were carried out using an optical through-power technique and an OTDR. Although the investigation was largely empirical, it revealed that the coating material and its thickness have an effect on the loading sensitivity and the applicability of the method to cure monitoring. The measurement data also indicated that the end-of-curing process and the location of external damage can be determined with distributed optical fibre sensors and an OTDR.

According to the experiments, the main problems with the monitoring system based on an OTDR and quasi-distributed microbending sensors were a low signal-to-noise ratio and a poor multiplexing capability. This was due to the low dynamic range of a typical OTDR and the cumulative attenuation modulated by the sensors (Measures 2001: 552). A typical OTDR also has a low spatial resolution, of the order of several metres, which restricts its use in distributed sensing appli-

cations. On the other hand, a high-resolution OTDR based on a sampling technique offers a much better spatial resolution, of a few millimetres. With a time measurement resolution of a few picoseconds, it also allows measurements in the time domain, which considerably improves the multiplexing efficiency and simplifies the sensor structure (Zimmermann *et al.* 1990). A high-resolution OTDR nevertheless employs highly sophisticated electronics with an ultra-high bandwidth, which makes it too costly for most measurement applications (Measures 2001: 554). Also, due to inherent jitter in the sampling circuit, the strain resolution is limited to a few hundred microstrains for a gauge-length of a few metres (Kercel & Muhs 1992, Habel *et al.* 1999), which is an inadequate value for most practical measurements. In addition, OTDR systems have a low measurement speed, which makes them suitable only for static measurement applications (Zimmermann & Claus 1991).

It was assumed in the course of this work that a much better performance in terms of resolution, precision and measurement speed could be achieved with a pulsed time-of-flight (TOF) measurement technique. The idea was based on the wide experience of the author's supervisors in developing TOF technology for various applications in the academic field and for commercial products (Myllylä 1978, Kaisto *et al.* 1983, Kostamovaara & Myllylä 1986, Nissilä *et al.* 1991, Määttä *et al.* 1993). Use of a time-to-digital converter (TDC) in conjunction with a constant fraction timing discriminator (CFD) would enable a high time measurement precision to be achieved with a considerably lower bandwidth than in the case of a high-resolution OTDR. This would simplify the electronic structure and substantially reduce manufacturing costs. By using averaging, the time measurement precision could be improved to the level of a few hundred femtoseconds or even below, corresponding to a few tens of micrometres in fibre length. Dynamic measurements would also be possible with the aid of fast electronic circuits.

With these ideas in mind, research into a fibre-optic TOF measurement system started in 1994. The first prototype was based on the measurement technique that had been developed at Electronics Laboratory of the University of Oulu for commercial rangefinders (Määttä *et al.* 1993). The precision and sampling rate of the novice system were of the order of 1 ps (100  $\mu\text{m}$ ) and 1 Hz, respectively, slightly better than in a high-resolution OTDR. The performance was found to be adequate for the pull testing of telecommunication cables (Paper IV), but it suffered especially from long-term drift in sensor applications (Paper VI).

After this preliminary work, several versions of the TOF system were developed with the aim of improving its stability, precision, sampling rate and spatial

resolution (Papers VII–IX). The most recent TOF system developed in this connection is capable of measuring time delays between a number of wideband reflectors, such as connectors or fibre Bragg gratings, along a fibre path with a precision of about 280 fs (rms value) and a spatial resolution of about 3 ns (0.30 m) in a measurement time of 25 ms. By using a fibre loop sensor with a reference fibre, a strain precision below 1  $\mu\epsilon$  and a measurement frequency of 4 Hz can be achieved. The system has proved comparable in performance to a commercial FBG system in measuring static and dynamic phenomena in a highway bridge.

To the best of the author's knowledge, the results achieved, in terms of precision, stability and measurement speed, far exceed the performance of all the earlier fibre-optic TOF systems used for structural monitoring (Zimmermann *et al.* 1990, Kerckel & Muhs 1992, Habel *et al.* 1999). As a truly integrating measurement approach, this TOF system is also a potential candidate for a commercial market. The fact that it allows dynamic and static measurements to be derived from multiple long gauge-length sensors, including ones embedded inside an FRP composite structure, makes this TOF system unique relative to other measurement approaches, including an FBG system. This ability makes it an attractive tool for the composite industry, but as a cost-effective alternative it may also attract wider interest e.g. in the safeguard and telecommunication applications.

### **1.3 Organization of the thesis**

This thesis consists of six chapters. Following the Introduction, Chapter 2 explains the theory and provides background information on fibre-optic sensors and their interrogation methods, with the emphasis on commercial systems and their applications to civil engineering and composite structures. Chapter 3 summarizes the experimental work, which is discussed in more detail in the appended papers, while Chapter 4 reviews comprehensively the most recently developed version of the TOF measurement system, its operation principle and performance in relation to commercial measurement systems. Chapter 5 discusses the significance of the results, while Chapter 6 provides a summary of this work.

## **2 Structural monitoring with fibre-optic sensors**

The topics presented in this chapter are comprehensively treated in a number of books and other publications, which cover the whole area of fibre-optic sensing and smart structures (Dakin & Culshaw 1988, Udd 1991b, Udd 1995, Culshaw 1996, Rastogi 1997, Measures 2001, López-Higuera 2002). Only strain-related topics that directly support the scope of the thesis will be discussed here, and then only briefly. Special consideration will be given to commercial strain sensors and their interrogation methods. Transit time systems will be explained in more detail in order to form a basis of comparison for the TOF measurement system developed here. Application measurements will also be reviewed.

### **2.1 Sensing needs**

The potential area of application for fibre-optic sensors in structural monitoring is vast, comprising aviation, marine and automotive applications and those to be found in connection with civil engineering structures. There are different sensing needs throughout the life span of a structure, i.e. during manufacturing, testing and service life. Civil engineering and FRP composite structures are obviously the most important potential areas of application for fibre-optic sensors, and these will be explained in more detail in the following sections.

#### **2.1.1 Civil engineering structures**

The term civil engineering structures usually means large concrete or steel structures such as bridges, tunnels, dams, geostructures, power plants, high-rise buildings and historical monuments. Civil engineering structures in particular can benefit from structural health monitoring techniques, as these can improve safety and reduce maintenance costs (Inaudi & Vurpillot 1999, Measures 2001: 15).

It is possible with the aid of a monitoring system to study the behaviour of a structure under dynamic loading conditions and also follow its long-term deterioration (Figure 1). There is a large diversity of monitoring techniques suitable for civil engineering structures, including electrical and optical methods as well as techniques that rely on acoustical (Jaeger *et al.* 1997, Pospisil *et al.* 2003) and geodetical processes (Jacobs 2004, Roberts *et al.* 2006).

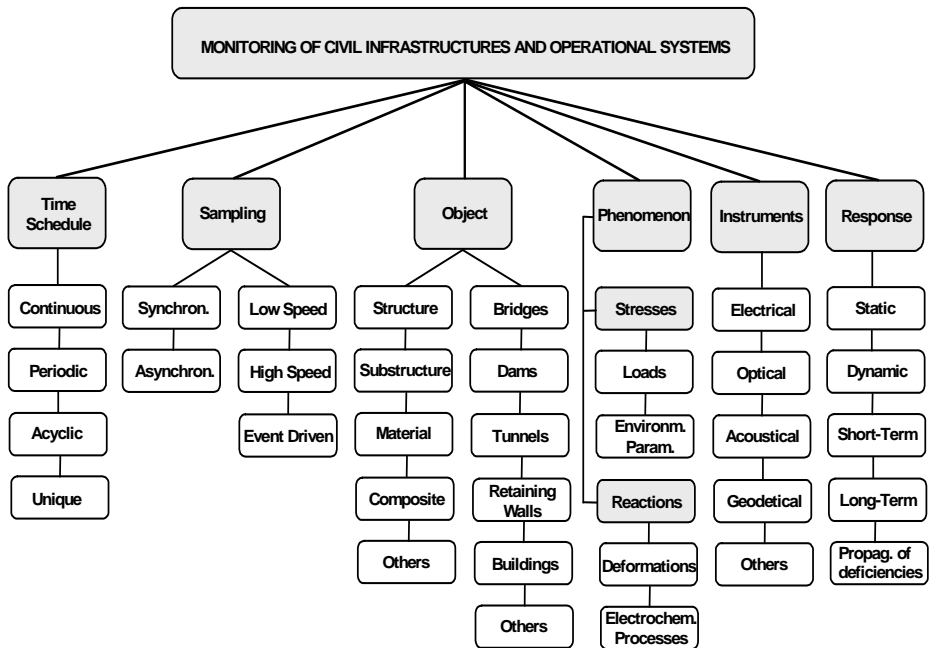


Fig. 1. Classification of monitoring techniques and objects (ISHMII 2002: 2).

Electrical sensors such as strain gauges and accelerometers are widely used in civil engineering structures to provide information on loading capacity and structural eigenfrequencies, for instance (Katz 1998, OMEGA 1998). Electrical sensors are a proven technology and they are well suited for dynamic and short-term measurements, but being susceptible to corrosion (Measures 2001: 233), they may not produce reliable information in the long term, which is a prerequisite when monitoring the integrity of a structure throughout its life-span. Nevertheless, environmentally immune, passive optical fibre-sensors offer a better means of performing this measurement task. In contrast to their electrical counterparts, fibre-optic systems also allow serial or parallel multiplexing of sensors with a measurement base of up to several metres, which together can facilitate the building of comprehensive sensor networks into or onto structures with characteristic dimensions of several hundreds of metres or even kilometres. The most relevant parameters to be measured in civil engineering structures are (Inaudi *et al.* 2000):

- Physical quantities: position, deformation, inclination, strain, force, pressure, acceleration, vibration
- Temperature
- Chemical quantities: humidity, pH, chlorine concentration
- Environmental parameters: air temperature, wind speed and direction, irradiation, precipitation, snow accumulation, water levels and flow, pollutant concentration

Figure 2 introduces potential applications for fibre-optic sensors in bridges. A comprehensive database on structural health monitoring techniques for civil engineering structures can be found on the website of the International Society for Structural Health Monitoring of Intelligent Infrastructure ([www.ishmii.org](http://www.ishmii.org)).

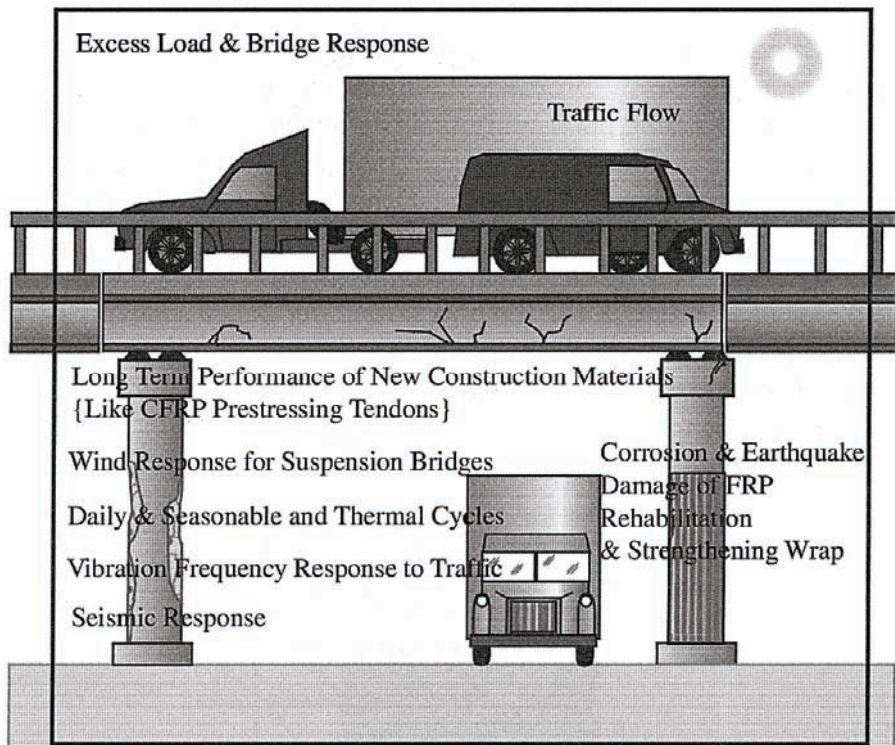
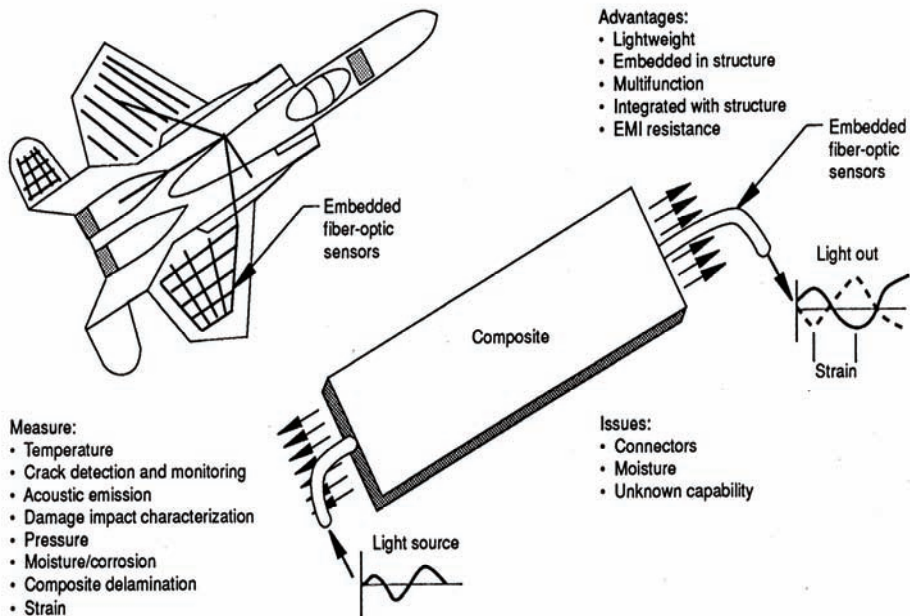


Fig. 2. Potential applications for fibre-optic sensors in the case of bridges (Measures 2001: 40).

### 2.1.2 Composite structures

The term composite structure usually means a multilayer structure that consists of a polymer and reinforcing elements. These are manufactured with the aid of a mould by filament winding, pultrusion or prepreg techniques. The most common reinforcing elements are glass, carbon and aramid fibres, while the polymer is typically a polyester or epoxy resin. Fibre-reinforced polymer composites (FRP) are extremely stiff structures in relation to their light weight, which makes them an attractive choice for aviation and space applications (Figure 3, Talat 1990). Other applications are various types of cylinders, pipes, containers, ropes, wires and turbine blades, for example. Due to their rustproof nature, FRP composites are also good candidates for repairing ageing infrastructures such as concrete bridges (Meier 2000, Bakis *et al.* 2002, Rizkalla & Hassan 2002).



**Fig. 3. Potential applications of fibre-optic sensors in FRP composite structures (Talat 1990).**

Despite the many benefits of composites, their material properties may vary significantly depending largely on the manufacturing process. The integrity of a structure may suffer from resin eyes, for instance, and residual stresses may arise

during curing. As a consequence, the layers can become detached from each other, causing what are known as delaminations. In addition, composite structures may be subject to matrix cracks and fibre breaks caused by heavy impacts (Measures 2001: 27), and their strength can be reduced by certain chemicals, especially in the long term (Kajorncheappunngam *et al.* 2002).

The uncertainties regarding material properties are a significant barrier to the wide acceptance of composite structures (Measures 2001: 26) and have led officials to place restrictions on their use in some critical applications such as underground oil containers. The risk of failure can nevertheless be minimized with a continuous monitoring system that gathers measurement data from the structure through its life-span, including the manufacturing phase (Measures 2001: 38). To obtain appropriate information, the whole structure should in principle be assembled with a comprehensive sensor network, which is only possible using fibre-optic sensors of various types. The potential for fibre-optic sensors in FRP composite structures, particularly in aviation, is illustrated in Figure 3. Most of the issues found in the figure are nevertheless common to the whole composite industry. A state-of-the-art report on health monitoring in the case of composite structures has been produced by Fixter & Williamson (2006).

## **2.2 Strain measurement considerations**

The propagation of a strain signal in an optical fibre sensing system is illustrated in Figure 4. Strain in the host structure is transferred to the sensor fibre via some form of bondline. The resulting change in the fibre-optic sensor measurement parameter (e.g. amplitude or wavelength) is converted from an optical signal in the optical fibre to an electrical signal by the demodulation unit. The electrical signal is then interpreted as a strain measurement by the computer (Measures 2001: 264).

In a practical strain measurement situation the strain in the host structure is relevant but may not correspond to the observed strain in the optical fibre, which necessitates some sort of calibration procedure (Measures 2001: 264) in which a known strain and temperature will be imposed on the host structure. The calibration experiment permits the system parameters to be characterized, so that when an unknown strain is imposed on the host structure, the electrical signal can be used to determine its magnitude (Valis *et al.* 1992).

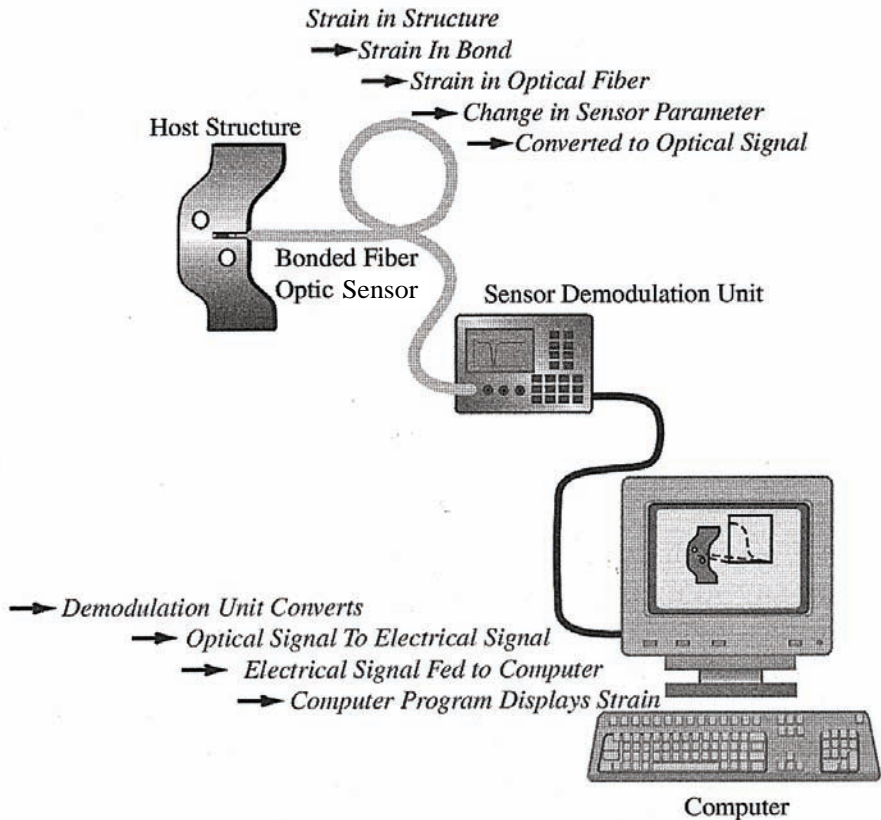


Fig. 4. Schematic illustration showing the signal path in fibre-optic strain sensing (Measures 2001: 264).

### 2.2.1 Strain, deformation and displacement measurements

Strain, deformation and displacement constitute the most interesting parameters to be monitored in the vast majority of structures (Inaudi 1997).

Strain sensors are deformation sensors with a very short measurement base of a few millimetres. Strain measurements are best suited to monitoring of the local behaviour of a material rather than the global behaviour of a structure. Strain sensors will therefore be placed at critical points in a structure, where high strains are expected that could exceed the resistance of the material.

Deformation refers to internal variation in the shape of a structure and is usually accompanied by a change in the strain field. It is usually measured with a long gauge-length sensor that integrates the strain over its measurement base,

which can extend from a few metres up to several hundreds of metres in the case of some geostructures or long, suspended bridges. Deformation measurements are particularly useful in structures that have to show dimensional stability, where the load state is usually far lower than the material failure limit, so that local strain measurements are not of interest (Inaudi 1997). Long gauge-length deformation sensors are useful for measuring and monitoring the following phenomena (Measures 2001: 498):

- Deformation of concrete during setting
- Pre-stressing
- Neutral axis evolution
- Concrete-steel interaction
- Post-seismic damage evaluation
- Spatial displacement (curvature analysis)
- Crack opening
- Creep-flow
- Long-term deformation
- Restoration

Displacement refers to a movement between different parts of a structure, which can occur without any change in strain distribution (Inaudi 1997). A displacement sensor monitors the distance variations between two given points. Examples of displacement measurements are the monitoring of rocks sliding with respect to another or movement in a bridge with respect to the ground. Most sensors used for deformation can also be used for displacement measurements.

### **2.2.2 Strain and temperature-induced effects on fibre-optic sensors**

Strain ( $\varepsilon$ ) is related to the internal compressive, tensile and shear state of a material. If the strain state of a structure is constant along the measurement path  $L$ , the measured deformation ( $\Delta L$ ) will be given by

$$\varepsilon = \frac{\Delta L}{L} . \quad (1)$$

By measuring  $\Delta L$ , it is therefore possible to obtain an indirect measurement of  $\varepsilon$  (Inaudi 1997). In fibre-optic sensing the fundamental parameter lying behind most sensor approaches is the optical path length of the sensing section (Measures 2001: 265). The sensor optical path length (*SOP* $L$ ,  $\zeta_L$ ) is expressed as

$$\zeta_L = nL, \quad (2)$$

where  $n$  is the refractive index of the fibre core. In general, the *SOPL* is a function of the applied stress and temperature ( $\sigma$ ,  $T$ ). It can be shown that (Measures 2001: 267)

$$\frac{\Delta \zeta_L}{\zeta_L} = S_\varepsilon \Delta \varepsilon + S_T \Delta T, \quad (3)$$

where  $\Delta \varepsilon$  and  $\Delta T$  represent the changes in strain and temperature from the reference values. The strain and temperature sensitivities  $S_\varepsilon$  and  $S_T$ , respectively, are of the form

$$S_\varepsilon \equiv \left\{ 1 + \frac{1}{n} \left[ \frac{\partial n}{\partial \varepsilon} \right]_T \right\}; \quad S_T \equiv \left\{ \alpha_F + \frac{1}{n} \left[ \frac{\partial n}{\partial T} \right]_\sigma \right\}, \quad (4)$$

where the second term in  $S_\varepsilon$  is a strain-optic coefficient, whereas  $\alpha_F$  in  $S_T$  is the coefficient of thermal expansion for the optical fibre ( $\approx 0.5 \cdot 10^{-6} \text{ }^\circ\text{C}^{-1}$ ). Representative values for the fibre-optic strain and temperature sensitivities are  $S_\varepsilon = 0.8 \cdot 10^{-6} \mu\varepsilon^{-1}$ ; and  $S_T = 6.0 \cdot 10^{-6} \text{ }^\circ\text{C}^{-1}$ , respectively, but there are some variations depending on the sensor type and the wavelength used (Morey *et al.* 1994, Alavie *et al.* 1995, Russell & Archambault 1996, Sørensen *et al.* 2006).

It becomes apparent from Equations 3 and 4 that, due to the strain-optic effect, the measured strain is about 20% smaller than the real strain undergone by the structure. It should also be noted that a temperature change of  $1^\circ\text{C}$  causes a measurable change of about  $6 \mu\varepsilon$  in an unstrained fibre. This is mainly due to a temperature-induced change in the fibre refractive index, as the actual thermal strain is only  $0.5 \mu\varepsilon$ .

It should also be noted that the above treatment is valid only for an axially loaded sensor. When embedded inside a material, a fibre sensor is usually subject to transverse strain and other strain components, as a consequence of which the strain-optic coefficient may vary in an unexpected way. One should therefore measure three principal strains, three shear strains and temperature for a reliable characterization of the strain state of a material (Van Steenkiste & Springer 1997). In most practical applications, however, there is some priori knowledge of the loading state of the structure, and thus the number of sensors needed is considerably smaller. Strain and thermal effects on fibre-optic sensors are comprehensively introduced in the textbooks by Measures (2001) and Van Steenkiste & Springer (1997).

### **2.2.3 Absolute and relative measurements**

The difference between an absolute strain measurement result and a relative one resides in the fact that an absolute value is relative to the unstrained state of the material, while a relative measurement result is relative to that measured at the time of sensor installation. If sensors are installed on an already loaded structure (even only by its own weight), a reading merely indicates variation in the load on the structure, whereupon it is difficult to estimate whether the material is approaching its failure limit (Inaudi 1997). If an absolute measurement result is important, the sensors should be installed on (or in) an unstrained material or on a material that is in a predictable strain state. This is usually possible in newly-built structures only.

### **2.2.4 Dynamic and long-term measurements**

Dynamic measurements are usually related to acoustic vibration or deflection of a structural element under dynamic loading conditions. The requirement for the sampling rate depends on the application and may vary from a few Hertz up to several kilohertz. As the strain variation is usually appreciable, drift in the measurement system is not a concern (Inaudi 1997).

In a long-term or static measurement the measurement period may vary from weeks up to several years. This places high demands on the stability of the measurement system and the durability of its components, i.e. fibres, optoelectronic devices, mechanical parts etc. Redundancy, modularity and self-testing capabilities are important issues to be addressed in this time domain.

### **2.2.5 Temperature compensation**

Generally speaking, all strain sensors are also sensitive to temperature variation. To perform a reliable strain measurement, it is therefore necessary to use some form of temperature compensation technique. One can use a sensor with a thermal behaviour that is negligible in relation to the desired accuracy, for example, or else measure both strain and temperature and eliminate the temperature effect by means of a calibration curve or table.

One common means of temperature compensation in fibre-optic sensing is to use two similar sensors, one attached firmly to a structure and the other loosely somewhere in its proximity. As both sensors are subject to temperature variation and only one is strained, it is possible to deduce the temperature-induced change from the fibre refractive index. A comprehensive review of compensation techniques can be found in the book “Structural Monitoring with Fiber Optic Technology” (Measures 2001: 263–324).

## 2.3 Fibre-optic strain sensors and their interrogation methods

### 2.3.1 The fibre Bragg grating measurement system

A fibre Bragg grating (FBG) is a wavelength filter that is photo-induced into a fibre core using an intense UV light and a phase mask (Figure 5). Bragg gratings are generally used in telecommunications for wavelength division multiplexing (WDM), for example, but they can also be applied to strain sensing (Morey *et al.* 1989, Kersey *et al.* 1997).

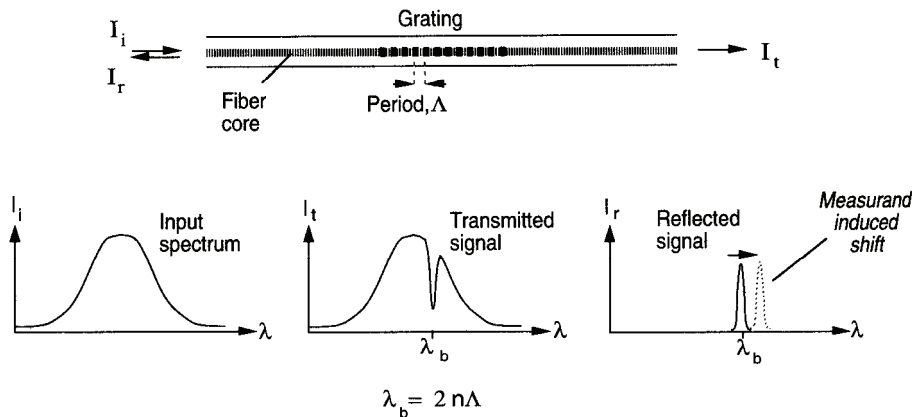


**Fig. 5. Principle of fibre Bragg grating (Kersey 1997a).**

As shown in Figure 5, the small refractive index changes that form the grating reflect light at certain wavelengths defined by the period  $\Delta$ , while the remainder of the spectrum remains unchanged. When the fibre is stressed the period of the grating changes, and as a consequence the central wavelength of the reflection

spectrum shifts to another wavelength that can be determined by spectral measurement techniques.

There are a number of demodulation schemes for FBGs (Measures 2001: 371–402). Commercial devices, e.g. those from Micron Optics, typically employ a scanning Fabry-Perot tuneable filter, as it allows sub-microstrain measurement precision for a series of FBGs multiplexed in the wavelength domain, as shown in Figure 6.

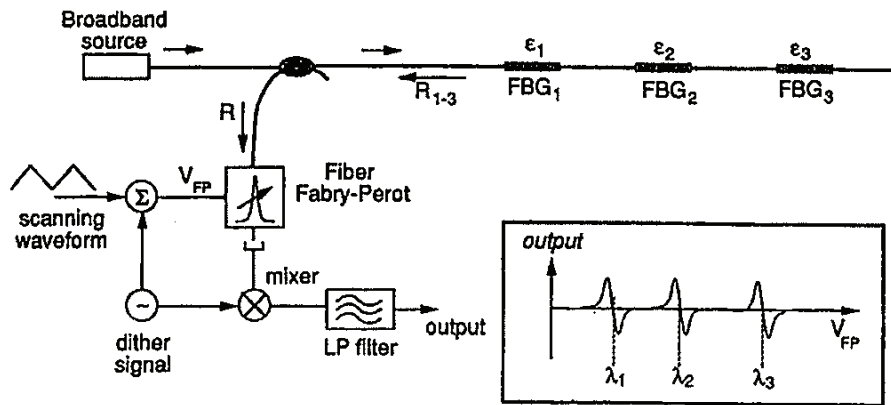


Fig. 6. FBG interrogation method based on a Fabry-Perot tuneable filter (Kersey *et al.* 1993).

Due to the spectral limitation on the light source used in the WDM approach,  $< 80$  nm, there is a trade-off between the number of sensors and the measurement range of an FBG. As  $1 \mu\epsilon$  corresponds to  $1.2$  pm in wavelength (Doyle 2003), it is possible to measure roughly 6 gratings with a maximum strain of  $10\,000 \mu\epsilon$  [ $(80 \text{ nm} / 1.2 \text{ pm} \cdot 1 \mu\epsilon) / 10\,000 \mu\epsilon \approx 6.7$ ], 12 gratings with  $5\,000 \mu\epsilon$ , and so on. Nevertheless, by using a time-division-multiplexing (TDM) technique the number of FBGs can be greatly increased up to 100 units per sensor fibre without any limitation on the measurement range. In a TDM system all the FBGs with a low reflectivity of about 1–5% (in contrast to  $\approx 90\%$  in the WDM approach), operate at the same wavelength, which substantially simplifies the architecture of the sensor fibre. As all FBGs are equal, it is relatively easy to manufacture sensors automatically in large series, which greatly reduces costs. TDM-based FBG interrogation systems are commercially available from Insensys Ltd, UK (Bogue 2005, Everall & Lloyd 2006) and from Smart Fibres Ltd, UK (Doyle 2003), for example.

There are a number of research groups that have used FBG sensors for structural monitoring (Idriss *et al.* 1997, Kunzler *et al.* 2003, Calvert & Mooney 2004, Doornink *et al.* 2004, Lin *et al.* 2004, Chan *et al.* 2006, Zhang *et al.* 2006). Most of these experiments have been based on wavelength division multiplexing, but the TDM technique has gained ground during the last couple of years (FOS 2004).

In order to test the potential of a fibre-optic monitoring system, Idriss *et al.* (1997) assembled a comprehensive sensor network on the I-10 highway bridge over Las Cruces, New Mexico. This bridge has spans of length 36 m comprising a concrete deck supported by welded steel plate girders. As many as 32 wavelength-division multiplexed FBGs were surface-mounted at various locations along the girders to measure static and dynamic loads. One FBG was used to provide temperature compensation for the remaining 31. The sampling rate of the interrogation system was 45 Hz and the minimum detectable strain was about 10  $\mu\epsilon$ , being restricted by electronic noise in the system.

In the dynamic measurement the maximum strain was noted in the middle of the girder. The response for a truck was about 80  $\mu\epsilon$ , whereas that for a passenger car was considerably smaller, about 25  $\mu\epsilon$ . It was also noted that, unlike a truck, a car does not induce any noticeable bridge vibrations. An important observation to be drawn from this work was the absence of slow strain drifts, indicating that the temperature reference sensor compensates for the thermal drifts in the strain monitoring FBG sensors.

Idriss concluded that such a fibre-optic monitoring system is a very effective tool for use by a bridge engineer. Traffic information such as vehicle weight and speed can be extracted from the strain signature, and the statistical pattern of strain response in the bridge can be used to give warnings about any abnormal conditions and to provide a record of the loading history of the structure, which could be valuable from a maintenance point of view.

Time division multiplexing offers a great potential when a large number of sensors need to be interrogated at a high sampling rate. Such measurement applications are typically found in energy production, e.g. in oil and gas fields and wind farms. A joint industry project “DeepStar” was started to study vortex-induced vibration (VIV) in riser pipes used in offshore oil and gas production (Insensys 2005). VIV contributes to fatigue in the risers and reduces their safe working life, resulting in a major expense for the operators.

In order to complete the measurement task, a miniaturized model of a riser pipe was manufactured using a composite material. This composite pipe was

about 150 m long and 3.5 cm in diameter and instrumented along its entire length with 280 embedded FBG sensors to enable the curvature of the pipe to be measured continuously on two axes along its whole length at very high resolution. During the experiment each sensor was scanned at around 60 Hz using an interrogation system from Insensys Ltd. that allows curvatures as small as  $6 \cdot 10^{-5} \text{m}^{-1}$  to be detected.

The test yielded a large volume of flow-induced vibration data. It was stated in conclusion that TDM-based FBG technology has major advantages over traditional sensors such as accelerometers: no electrical power is transmitted to the sensors, a greater spacing density can be achieved and strain can be measured directly, allowing direct estimation of the fatigue damage rate. This is likely to be an increasingly important technology for investigating the response of riser systems to VIV both experimentally and in the monitoring of full-size risers in operation.

### **2.3.2 Fabry-Perot measurement system**

An Extrinsic Fabry-Perot sensor (EFPI) is a point-type fibre-optic strain gauge that involves a small air gap between two reflective surfaces installed in a micro-capillary tube (Lee & Taylor 1995). A schematic diagram of a commercial low-coherence interferometer from FISO Technologies Inc. which uses an optical cross-correlation technique to evaluate the absolute strain experienced by an EFPI sensor is shown in Figure 7. The broadband light modulated and reflected by the EFPI sensor is passed through a cylindrical lens and analysed by a wedge-shaped Fizeau interferometer (Measures 2001: 461–463), which transmits minimally at the exact location along the wedge where its spacing matches the EFPI cavity length. When the EFPI sensor is subjected to strain the cavity length changes, whereupon the position of the minimum in transmission shifts along the linear CCD array accordingly. Knowledge of the slope of the wedge, the unstrained cavity length and the gauge length is used to calculate the strain experienced by the EFPI sensor (Measures 2001: 461–463).

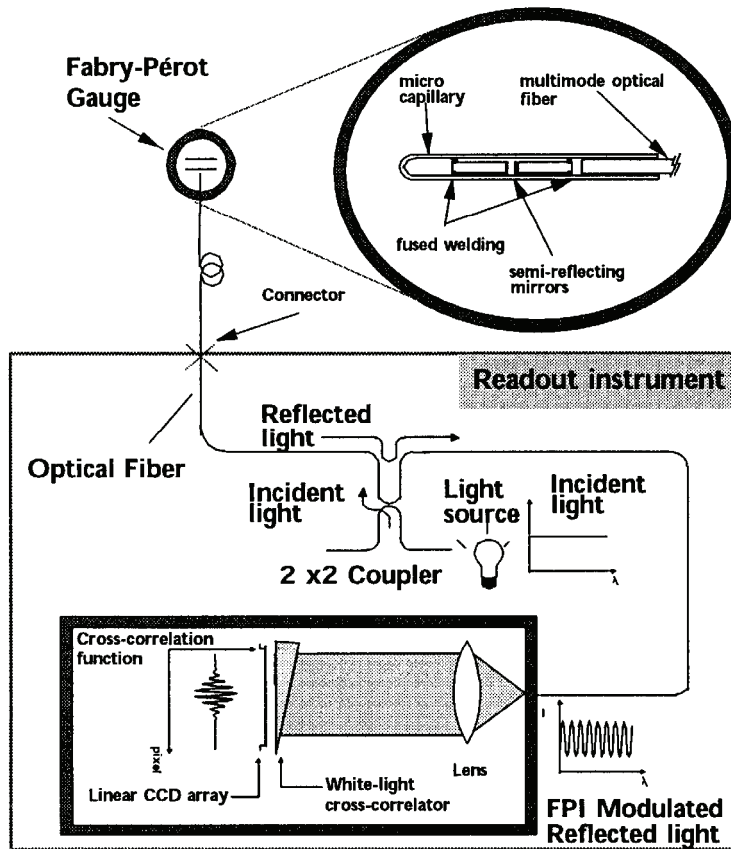


Fig. 7. Schematic diagram of a commercial fibre-optic Fabry-Perot measurement system. Reprinted by courtesy of FISO Technologies Inc.

FISO's measurement systems provide a sampling frequency that typically exceeds 10 Hz and has a precision of less than  $0.3 \mu\epsilon$ . The inherent gauge length of the EFPI sensor is of the order of 1 cm, but with a suitable package it can be enlarged to 10 cm. The strain range depends directly on the gauge length and can be chosen between  $\pm 1\,000 \mu\epsilon$  and  $\pm 10\,000 \mu\epsilon$ . The Fabry-Perot measurement system is inherently a single-channel approach, but the number of sensors can be increased markedly by means of an optical fibre switch. Immunity to transversal strain is the main benefit of the EFPI sensor over the FBG, accompanied by reduced sensitivity to temperature changes (Measures 2001: 456).

Morin *et al.* (1996) assembled 54 EFPI sensors on a propeller blade of a Polar Class icebreaker and used instrumentation from FISO Technologies to obtain a

detailed map of the location and distribution of the ice impact loads acting on the propeller. The primary objective of this work was to validate theoretical models of propeller/ice interaction against experimental data and to use the knowledge gained to improve the design of ships.

The performance of the fibre-optic blade instrumentation of the Polar Star during its first use under ice-breaking conditions substantially exceeded early expectations. A large set of useful measurements were obtained even though the vessel encountered unusually severe ice-breaking conditions. With regard to the strain measurement, a number of very high-amplitude blade impact loads were monitored but in only a few of these extreme events did the strain rate in the blade approach the design capability, and then only for one or two milliseconds during the rising edge of the impact strain wave form. The most significant difference between the performance of the fibre-optic measurement system and those based on resistive strain gauges in similar applications were the much better signal-to-noise levels and the absence of long-term drift in the fibre-optic system.

Lawrence *et al.* (1997) used EFPI sensors and instrumentation from FISO Technologies for cure monitoring in the case of FRP composites. They embedded two EFPI sensors and a thermocouple into a composite specimen which had a special layout to enable a study to be made of residual stresses that form inside the structure during curing. This method offers the advantage of non-destructive determination of residual stresses and can account for the effects of chemical and thermal shrinkage and viscoelastic stress relaxation. The conclusion was that residual stresses can be monitored in real time during curing, allowing this information to be used for process monitoring and control.

Habel *et al.* (1997) used EFPI sensors to measure the deformation of mortars at early ages and of large concrete components on site. He demonstrated that these highly sensitive fibre-optic strain gauges can be used without failure in the raw environment of structures. Also, EFPI sensors allow one to obtain more information about building reactions than ordinary strain gauges or displacement meters, and they are unaffected by electromagnetic interference.

Measures *et al.* (2001: 514–525) used Fabry-Perot sensors for monitoring the integrity of a natural gas vehicle tank made of a carbon FRP composite material and for measuring hoop strain in composite wraps used for repairing corroded concrete columns. Their experimental setup deviated from FISO's approach in that the reference optical path was realized with an adjustable Michelson interferometer and the Fabry-Perot cavity was made of a length of optical fibre and a pair

of wideband Bragg gratings. This arrangement allows longer gauge-lengths of up to several metres to be used, and it also enables serial multiplexing of the sensors.

### 2.3.3 Microbending measurement system

The microbending sensor is one of the earliest fibre-optic measurement approaches, having originally been demonstrated by Fields and Cole (1980) for acoustic measurements. In a microbending sensor a change in the strain field affects the light power that propagates inside a fibre core. Operation is based on modulating the bend radius of the fibre with a corrugated structure, as shown in Figure 8. In this arrangement a sensor fibre is installed between two plates with saw-shaped edges. Upon elongation the plates attached to the structure draw away from the fibre, leading to an increase in the light level, while in compression the effect is the opposite.

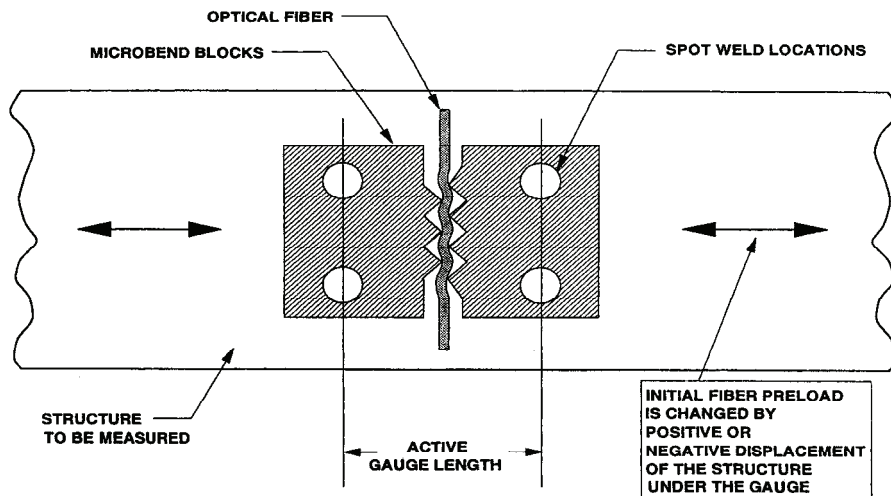
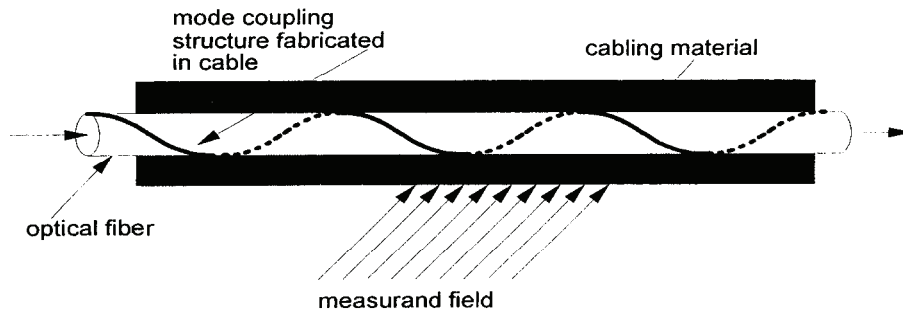


Fig. 8. Point-type strain sensor based on microbending effect (Berthold 1997).

Another way of implementing a microbending structure in a fibre is presented in Figure 9. In this configuration a spiral wire is wrapped around the whole length of the fibre to enable distributed pressure measurement, but it is also possible to measure the integral strain between the anchoring points with a suitable package.



**Fig. 9. Distributed microbending sensor for measuring pressure (Horiguchi *et al.* 1997).**

Microbending sensors are manufactured commercially by the French company OSMOS SA, for instance. In their setup, an optical fibre is twisted with one or more fibres along its sensing length. As the sensor is subjected to elongation the fibres will induce bending in each another and cause part of the light to escape the fibre. It is therefore possible to obtain the deformation of the structure by measuring the intensity of the transmitted light. The precision and sampling rate of the OSMOS system are typically  $1\ \mu\epsilon$  and 100 Hz, respectively, for a single sensor with a gauge-length of 10 cm – 10 m.

OSMOS deformation sensors have been widely used throughout the world for monitoring bridges, tunnels, buildings and historical monuments, for example. Braunstein *et al.* (2002) assembled eight OSMOS sensors, each 5 m long, on the Skovdiget Bridge in Denmark to measure longitudinal deformations in the girders and transversal deformations in the ribs. The dynamic deformation was  $28\ \mu\epsilon$  and  $75\ \mu\epsilon$  for the girders and ribs, respectively, as a heavy truck passed over the bridge. Braunstein *et al.*, also studied Herrenbrücke Bridge in Lübeck, Germany, where they used OSMOS sensors for measuring deformation and weight in motion (WIM). A comprehensive study of various structural parameters showed that microbending deformation sensors provide information on the status of an object and allow for the early detection of structural problems. Additionally, the monitoring system leads to a reduction in maintenance costs and significantly facilitates management of the structure.

Commercial microbending systems, e.g. those manufactured by OSMOS SA, are typically single-sensor approaches, but it is possible to implement serially multiplexed sensor networks by using an OTDR as an interrogation device. The OTDR technique, which is commonly used for analysing telecommunications

links, utilizes an inherent Rayleigh scattering process to derive losses in an optical fibre and its connectors, splices and so forth (Barnoski & Jensen 1976). The capability of OTDR techniques for analysing small losses in a fibre can be used to form distributed (or quasi-distributed) sensor systems, in which losses intentionally introduced into a fibre via a transducing element can be monitored (Figure 10).

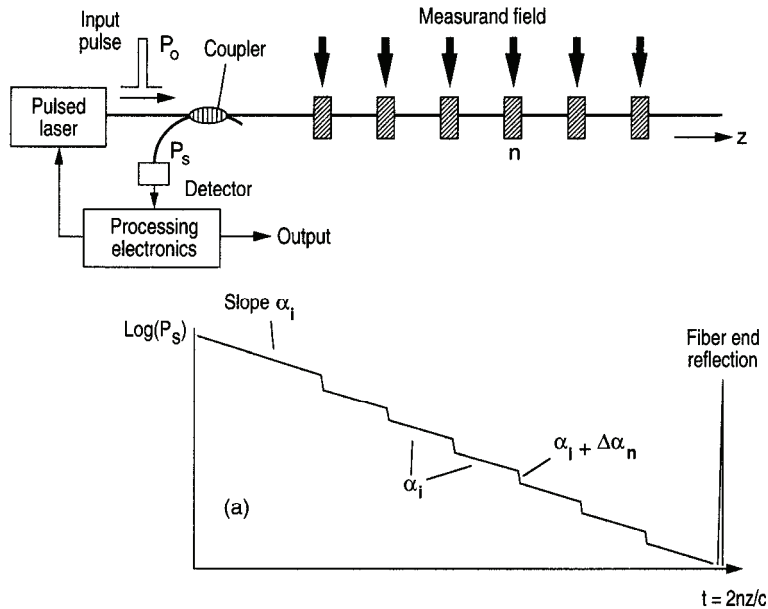


**Fig. 10. Quasi-distributed measurement approach based on an OTDR (Kersey 1997a).**

With a typical OTDR providing a dynamic range and resolution of 20–30 dB and 0.01 dB, respectively, distributed microbending sensors can operate at ranges of up to a few kilometres with up to 1000 effective interrogated sections along the fibre (Horiguchi *et al.* 1997). Measurements to about 10% accuracy are feasible in principle, but the concept is usually best suited to operation as a distributed alarm, especially since the sensitivity is a function of position, due to increasing loss along the fibre, and is also a function of the actual measurement field applied (Horiguchi *et al.* 1997). Nevertheless, a quasi-distributed OTDR approach allows a better performance for a considerably smaller number of sensors (Pinto *et al.* 2006).

OTDR techniques have been used to develop a range of intrinsic distributed and quasi-distributed sensor systems (Dakin 1993, Niewisch & Bartelt 1994,

Bennett & McLaughlin 1995, Michie *et al.* 1995, Rogers 1999, Gu *et al.* 2000, MacLean *et al.* 2001, Culshaw 2004, Pinto *et al.* 2006). Bennett and McLaughlin (1995), for example, used a quasi-distributed approach for monitoring corrosion on large steel structures. In their sensor setup a multi-mode fibre is tightly bent onto the specimen and secured with a “corrosion fuse”. When the fuse corrodes, it eventually breaks and allows the fibre to straighten. The resulting difference in optical intensity emerging from the fibre is measurable using an OTDR or other optical detector. This idea was tested using three serial sensors in a simulated corrosive atmosphere, confirming that this cheap and easily implemented monitoring scheme could be used to infer the presence of corrosion at different locations or the degree of corrosion at a single location.

Michie *et al.* (1995) developed a distributed microbending sensor which enabled the detection of water along the length of an optical fibre. The sensing capability was realized through a combination of an OTDR and a microbending transducer activated by chemically swellable polymers (hydrogels). Experiments with a water sensor prototype showed that the detection of wetted sections less than 50 cm in length in cables longer than 100 m is possible. It was expected that other chemical parameters such as pH or ionic concentration could also be detected with an appropriate hydrogel.

Pinto *et al.* (2006) have recently demonstrated a quasi-distributed displacement sensor that utilizes a single mode fibre and a commercial OTDR. Attenuation of 9 dB has been measured for a displacement of 120 mm, which corresponds to about 0.027 dB/mm. The system performance has been approved with four sensing heads, but according to authors the interrogation system has a potential for larger sensor networks.

#### **2.3.4 Low-coherence interferometer**

In the commercial fibre-optic interrogation system presented in Figure 11, which is a modification of a traditional Michelson interferometer, a single mode optical fibre is illuminated with a DC-type broadband light that is evenly divided between a sensor fibre and a reference fibre in an optical fibre coupler. The sensor fibre is pre-tensioned and mechanically coupled to the structure at two anchorage points in order to follow its deformations, while the reference fibre is free and acts as a temperature reference (Inaudi *et al.* 2000). If the fibres are of equal length, constructive interference is seen in a photo detector. If there is a mismatch between the optical path lengths a movable mirror is used to compensate for the

imbalance. Due to the short coherence length of the broadband source the maximum signal is easily detectable.

The measurement system is manufactured by a Swiss company, Smartec SA, and carries the product name SOFO. The strain precision of the SOFO sensing system is typically about  $1 \mu\epsilon$ , the measurement time a few seconds and the sensor length 20 cm – 20 m. The SOFO sensing system can measure one sensor at a time, but allows a substantial increase in the number of sensors if an optical fibre switch is used. The SOFO sensing system is widely used in various civil engineering and other applications such as bridges, tunnels, piles, anchored walls, dams, historical monuments and nuclear power plants (Inaudi *et al.* 2000).

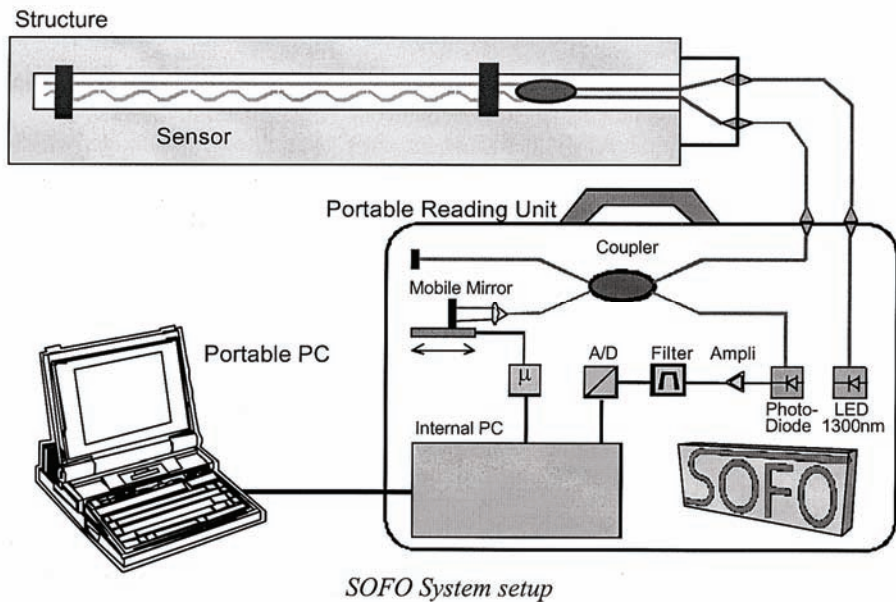


**Fig. 11. A commercial measurement system based on low-coherence interferometry (Inaudi *et al.* 2000). Reprinted by courtesy of Smartec SA.**

Inaudi & Vurpillot (1999) embedded more than 100 SOFO deformation sensors into the renovated Versoix Bridge in Geneva, Switzerland, with the aim of measuring displacements in the fresh concrete during the setting phase and long-term deformation in the bridge after renovation. Sensors were installed at various positions in the girder cross-section at multiple locations along the bridge span to obtain vertical and horizontal curvatures in an earth-bound coordinate system. By

taking a double integral of the curvatures and respecting the boundary conditions it was then possible to retrieve deformations in the bridge.

Inaudi's research group also applied the same methodology to the Lutrive Highway Bridge in Switzerland to measure the variation in vertical displacement when the bridge was subject to a static load (Inaudi & Vurpillot 1999). The results obtained with 30 SOFO deformation sensors were compared with the displacements achieved with an optic levelling system, pointing to a discrepancy of less than 7% between the two systems.

Another commercial device based on low-coherence interferometry is available from a Canadian company, FOX-TEK, Inc. Cauchi *et al.* (2007) used this for monitoring bending in a buried gas pipeline due to ground movement. In this experiment they installed several linear and coiled fibre sensors and reference vibrating wires to produce information on the longitudinal strain necessary for computing the maximum bending and its direction. The gauge-lengths of the linear sensors and vibrating wires were 1 m and 10 cm, respectively, while the size of the coiled sensor was 10 cm in one direction.

After a few months of measurement the results obtained using the three sensor types were in a good agreement despite an offset between the measurement curves. According to Cauchi this was due partly to the different sensor lengths, as a longer sensor can average out local abnormalities, and partly to the different sensor layouts, as a coiled sensor is susceptible to both longitudinal and hoop strain. The conclusion was that fibre-optic interferometric sensors offer benefits over conventional sensors due to their larger dynamic range and larger customizable sensor size. Furthermore, monitoring programs can lead to increased safety and throughput, fewer unplanned shutdowns and a reduced threat of environmental damage.

Zhao & Ansari (2001) also developed a low-coherence interferometer and tested it under laboratory conditions. Their experimental interrogation device differed from the measurement systems discussed above in that it provided for serial multiplexing.

A low-coherence interferometer capable of measuring a number of long gauge-length serial sensors is commercially available from a French company, Fogale Nanotech. This system has been tested by Delepine-Lesoille *et al.* (2006), who report on the design and realization of a wave-shaped optical fibre sensor for continuous measurement of concrete strains over very long distances.

### 2.3.5 Brillouin scattering interrogation systems

Brillouin scattering is an inelastic form of scattering generated by photon/phonon interaction in an optical fibre. In a spontaneous Brillouin process thermally excited acoustic waves (phonons) produce a periodic modulation of the refractive index. Brillouin scattering occurs when light propagating in the fibre is diffracted backwards by the moving grating, giving rise to a frequency-shifted component through a phenomenon similar to Doppler shift (Inaudi 2002). The usefulness of Brillouin scattering for optical fibre sensing resides in the fact that the frequency shift depends on the silica density, which is a function of strain and temperature.

While the efficiency of spontaneous Brillouin scattering is extremely low, stimulated scattering allows much stronger signals to be produced. The first Brillouin scattering concept utilizing this phenomenon was demonstrated by Kurashima *et al.* (1990) and was termed Brillouin optical time domain analysis (BOTDA). In their configuration, as shown schematically in Figure 12, a short pump pulse is sent into the sensor fibre at one end, while a continuous wave probe beam with a frequency offset corresponding to the nominal Brillouin shift ( $\nu_B$ ) is launched into the fibre at the other. The continuous wave probe light experiences Brillouin gain at the fibre locations where the frequency offset is matched to the peak Brillouin gain (Kersey 1997b). The time dependence of the detected continuous wave light thus provides the gain profile experienced by the probe light as the pump pulse passes along the fibre. Measurements carried out with a wide range of frequency offsets allow a full picture of the Brillouin frequency for each fibre location to be achieved (Kersey 1997b). As a consequence the distribution of strain and temperature can be derived within the spatial resolution determined by the width of the pump pulse.

A distributed interrogation system based on stimulated Brillouin scattering is available from a Swiss company, Omnisens SA, for example. The structure of this device deviates from Figure 12 in that the pump and probe signals are generated from a single laser source with the aid of an integrated optics modulator (Nikles *et al.* 2004). This kind of arrangement improves the stability and also allows a single-end measurement. Omnisens' device allows both strain and temperature measurement with typical precisions of  $10 \mu\epsilon$  and  $0.3^\circ\text{C}$ , respectively, a spatial resolution of 1 m over a fibre length of 10 km and a typical measurement time of about 2 min.

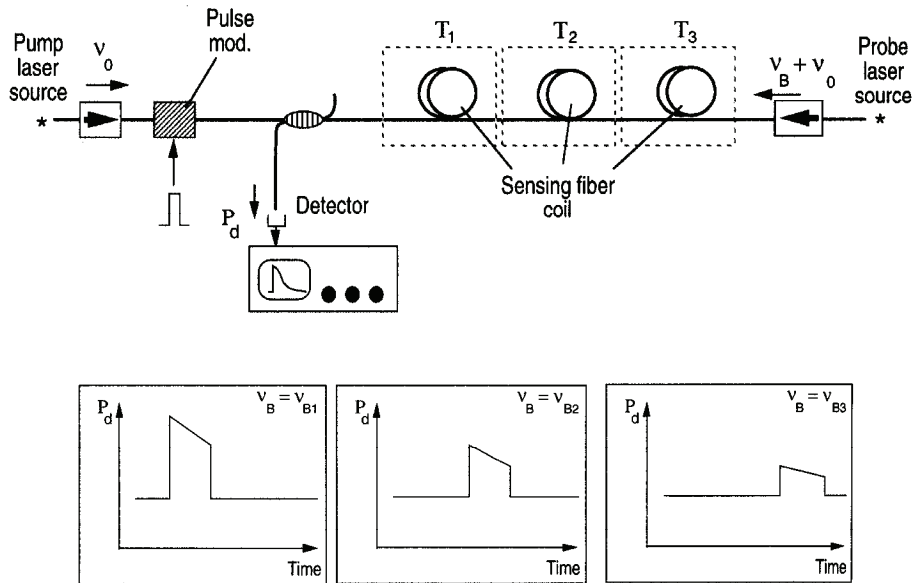


**Fig. 12. A distributed measurement system based on stimulated Brillouin scattering (Kersey 1997b).**

Due to their distributed nature, Brillouin scattering systems are especially suited for monitoring very large structures with characteristic dimensions that can extend up to a matter of kilometres, as in the case of oil and gas pipelines or geo-structures, for example. The main advantage of a distributed approach resides in the fact that as the whole fibre length serves as a sensor, no a priori knowledge of structurally highly loaded areas or weak points is necessary.

Inaudi & Glisic (2005) used a Brillouin scattering system from Omnisens to identify high strain areas, crack onset, leakage and temperature distributions in structures such as dams, bridges and pipelines. According to Inaudi the use of distributed fibre-optic sensors for the monitoring of civil structures and infrastructures opens up new possibilities that have no equivalent in conventional sensor systems. Using an appropriate sensor design it is possible to successfully install distributed sensors on large structures and obtain useful data for their evaluation and management.

Inaudi & Glisic (2006) also used the Brillouin measurement system for monitoring composite coiled tubing as used in hydrocarbon reservoirs. For this purpose they developed a special sensor design, a SMARTprofile™, which consists

of temperature and strain sensor fibres embedded in a polyethylene thermoplastic profile. These sensors were integrated into the liner of the tubing over its entire length in order to measure well parameters and produce structural integrity information.

Gao *et al.* (2006) used a Brillouin optical time domain reflectometer (BOTDR) from Yokogawa Electric Co. to monitor the stress in post-tensioning cables. Yokogawa's approach is different from Omnisens' system in that it makes use of spontaneous Brillouin scattering for measurement purposes. Gao's experiment showed that the fibre-optic distributed sensor possesses high accuracy, as the relative deviation of the measurement results between the fibre-optic sensors and electrical strain gauges was less than 2.7%. According to Gao, the stress distribution of a post-tensioning cable under all loads can be used to evaluating the state of health of the beam.

Brillouin scattering systems have also been used for structural monitoring by researchers such as Bao & DeMerchant (2001) and Li *et al.* (2006).

### **2.3.6 Transit time measurement systems**

Fibre-optic interrogation systems based on the measurement of transit time were subject to intensive research in the 1980's. Optical cable manufacturers and telecommunications operators were particularly active in this field, proposing the measurement of dispersion, axial strain and pulse delay stability by methods such as time delay oscillators (Johnson & Ulrich 1978, Brininstool 1987), time delay resonators (Brininstool 1987), the phase shift measurement technique (Tateda *et al.* 1980, Kashyap *et al.* 1982, Bergman *et al.* 1983) and the pulse delay measurement technique (Hartog *et al.* 1978, Tateda *et al.* 1980, Tatekura *et al.* 1982, Shibata *et al.* 1983, Hornung *et al.* 1983).

#### *Time delay oscillator*

A measurement system based on a time delay oscillator which was developed by Brininstool (1987) is shown schematically in Figure 13. In this arrangement a start button initiates a closed-loop square-wave oscillator that is composed of the optical fibre to be measured and an electronic regeneration circuit. A frequency counter measures strain-induced changes in oscillation frequency, which is inversely proportional to the optical fibre transit time plus the electronic delay in the circuitry. It is important in order to yield highly accurate results with this

measurement configuration that the electronic delay should be relatively constant and much smaller than the fibre delay.

The relationship between the change in optical time delay due to strain and the oscillation frequency is given by (Brininstool 1987):

$$\Delta\tau = \frac{|f_0 - f_1|}{2f_0f_1} \approx \frac{\Delta f}{2f_0^2}, \quad (5)$$

in which  $f_0$  is the initial frequency at zero strain and  $f_1$  is the frequency at strain.

The system was tested with a 70 m multi-element cable subjected to tensile load cycling. In this experiment the initial frequency was 1.25 MHz, whereas the frequency fluctuation due to electronic delay drift was within  $\pm 100$  Hz. Using Equation (5), this corresponds to a minimum resolvable resolution of  $\pm 30$  ps and an axial strain resolution of  $\pm 0.01\%$ .

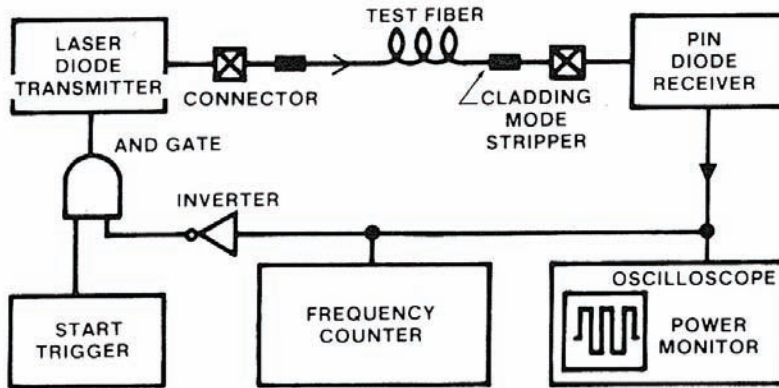


Fig. 13. Schematic diagram of a time delay oscillator (Brininstool 1987).

### *Time delay resonator*

A time delay resonator was developed by Brininstool & Garcia as a backup approach to the time delay oscillator discussed above (Brininstool 1987). As in the case of the time delay oscillator, the loop frequency of the time delay resonator is inversely proportional to the transit time. The main difference between the two systems is that the time delay resonator does not include any electronic regeneration circuitry, as shown in Fig. 14. As there is no electronic drift in the resonator design, changes in loop frequency are due solely to changes in fibre transit time.

During operation, narrow optical pulses are injected into the test fibre and pass out of it via fibre-optic couplers. The closed-loop configuration means that a single pulse makes successive passes around the loop and causes a decaying oscillation in the output of the APD. To measure the loop frequency, the laser pulse repetition frequency is adjusted until resonance occurs, which happens when a given pulse and all of its multipass echoes arrive at the detector simultaneously. The fibre strain can be measured by tuning the pulse repetition rate and reading the loop frequency from a counter. The corresponding change in the time delay is given by an expression similar to that of the time delay oscillator, but from which the factor 2 has been dropped (Brininstool 1987).

The resolution of the measurement depends on the Q-factor, which is a function of the loop transmission loss. The resolution of the system with a transmission factor of 0.5 (-3 dB) was determined to be 3 cm over 30 m, or  $\Delta\epsilon = \pm 0.1\%$  but it was estimated that by improving the transmission factor to 0.75 (1.25 dB loss) an improved length resolution of 5 mm, or  $\Delta\epsilon = \pm 0.02\%$  could be achieved.

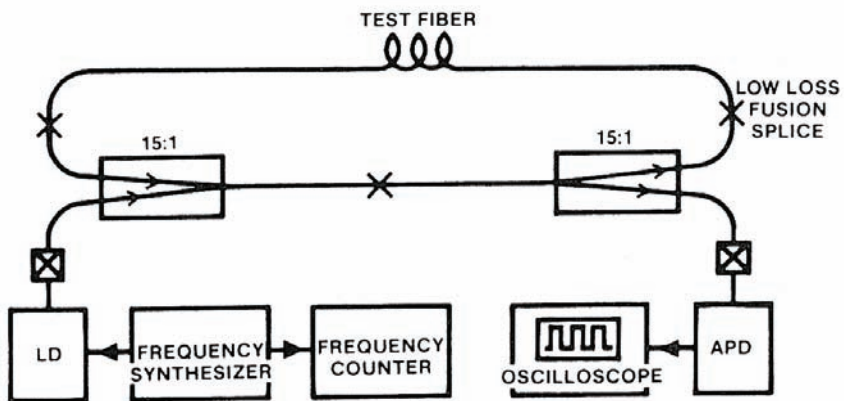
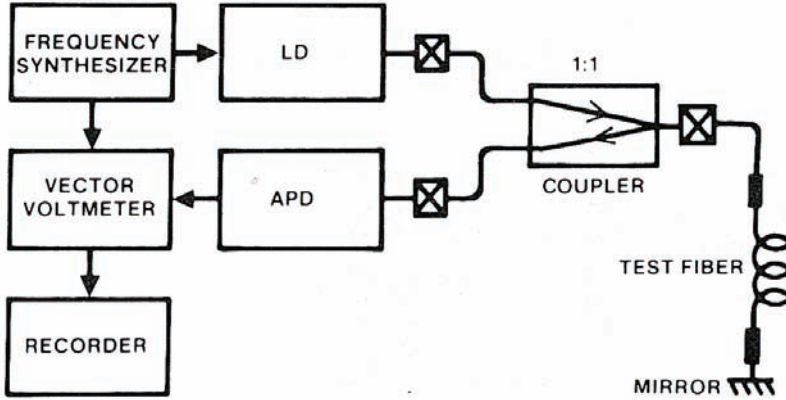


Fig. 14. Schematic diagram of a time delay resonator (Brininstool 1987).

### *Phase shift measurement technique*

The arrangement of a phase shift measurement technique is shown schematically in Fig. 15. The frequency synthesizer modulates the laser diode sinusoidally, and the vector-volmeter measures the relative phase between the APD output and an electrical reference signal applied directly from the synthesizer (Brininstool 1987).



**Fig. 15. The phase shift measurement setup (Brininstool 1987).**

An approximate expression relating strain to relative phase ( $\phi$ ), fibre time delay ( $\tau$ ) and modulation frequency ( $f$ ) is

$$\varepsilon = \left( \frac{1}{L} \right) \left( \frac{\Delta L}{\Delta \tau} \right) \left( \frac{\Delta \phi}{360^\circ f} \right), \quad (6)$$

where  $L = l_0$  for double-ended attachment,  $L = 2l_0$  for the mirrored, single-ended approach and  $l_0 =$  gauge length.

In actual measurements the modulation frequency can be freely chosen to provide a simplified readout directly from the vector voltmeter. The term  $(\Delta L/\Delta \tau)$  can be derived from a reference table or by performing a calibration test. The strain resolution of the measurement system is limited to 0.001% by the readout resolution of the vector voltmeter ( $0.1^\circ$ ) and by drift in the frequency synthesizer.

As the phase shift system provides only a relative measurement, the fibre cannot be detached from the system without losing the reference point (Brininstool 1987). This proves to be a major drawback in practical situations. This problem can be overcome by using a differential phase shift measurement technique (Kashyap & Reeve 1980). The oscillator techniques discussed earlier are also insensitive to test discontinuities.

Phase shift measurement instrument allowing a millimeter resolution has been commercially available e.g. from EG&G Fiber Optics with a product code SPL 300. Quite recently Guoliang *et al.* (2007) published an oscillator interrogated time-of-flight optical fibre interferometer which is essentially similar to the system discussed above. Providing a length resolution of 9.5 mm and range of 1.39 m this system is especially suited to strain measurements of very large struc-

tures. Results from static loading tests of a FRP strengthened concrete beam with embedded fibre ribbons have shown the feasibility of this technique for monitoring infrastructure systems.

### *Pulse delay measurement technique*

Its high precision and multiplexing capability makes the pulse delay measurement technique the most attractive transit time method for structural monitoring (Zimmermann *et al.* 1989). In the pulse delay measurement setup based on a sampling method presented in Figure 16, a short laser pulse is sent into the fibre. After a certain delay, the sampling circuit is triggered by means of a precise time delay generator. Following the first sampling process, a new laser pulse is sent into the fibre and sampled with a small difference at the starting point compared with the previous measurement. By performing the sampling process a number of times it is possible to reconstruct optical pulses precisely. The use of an extremely stable time base in conjunction with very short probe pulses allows this system to discriminate closely spaced discontinuities such as reflective connectors and to measure their distance with high precision.

In the pulse delay approach fibre strain can be determined using the formula (Zimmermann *et al.* 1990)

$$\varepsilon_j = \frac{\Delta t_j - \Delta t_{j-1}}{2l_j n / c} \left[ \frac{1}{1+a} \right], \quad (7)$$

where  $\Delta t_j$  and  $\Delta t_{j-1}$  are the pulse delays of the far and near-end reflections from the  $j_{th}$  segment,  $c$  is the speed of light in a vacuum,  $n$  is the group refractive index of the fibre ( $\approx 1.47$ ),  $l_j$  is the length of the  $j_{th}$  segment and  $a$  is the strain-optic coefficient of the fibre ( $\approx -0.2$ ). According to Equation (7), a time measurement precision of 1 ps corresponds to a fibre strain of about 127  $\mu\epsilon$  or 0.0127% (rms value) for a gauge-length of 1 m.

A pulse delay measurement instrument allowing picosecond resolution, known as the Millimeter Resolution OTDR System, was commercially available from Opto-Electronics Inc. (Fig. 16). This company no longer exists, but a somewhat similar OTDR is available from Tempo Ltd. with the product code OFM20. According to the product specification of the Opto-Electronics system, the time measurement resolution depends on the signal-to-noise ratio being typically 1–10 ps (0.1–1.0 mm) in an SNR range of 50–5. The corresponding spatial resolution

should vary between 0.2 and 1.2 mm. Timing jitter in the time delay generator places the fundamental limit on performance.

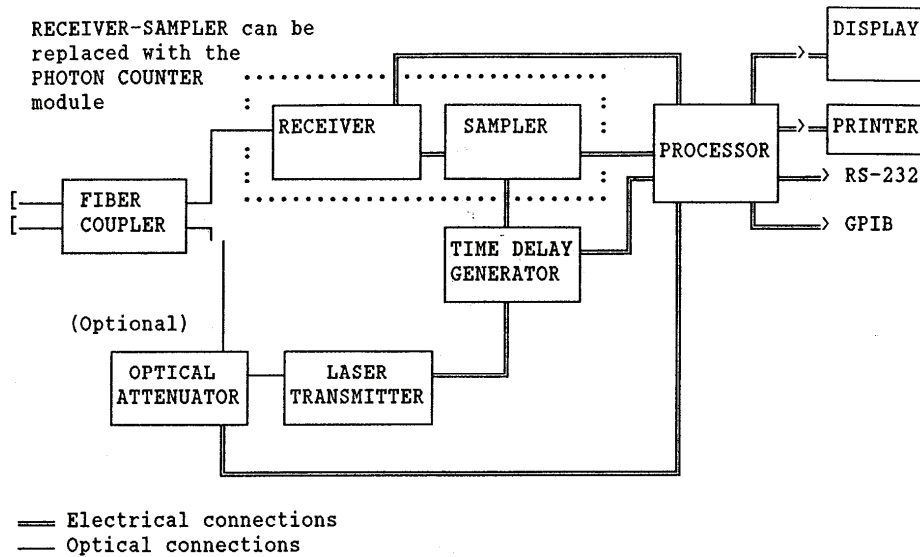


**Fig. 16. Pulse delay measurement setup. Block diagram of the Opto-Electronics Millimeter Resolution OTDR.**

Of all the transit time measurement systems discussed above, the pulse delay approach is obviously the only method which, in addition to telecommunication applications, has also been widely used for structural monitoring. Zimmermann *et al.* were especially active in this field in the early 1990's, using Opto-Electronics' high resolution OTDR for monitoring various structures such as composite anchoring tendons (1993), the wings of an aircraft (1991), composite jackets for retrofitting bridge columns and other composite specimens (Lou *et al.* 1994, 1995). The resolution of Zimmermann's system was of the order of  $\pm 250 \mu\text{m}$ , but it could be improved to  $10 \mu\text{m}$  by means of a fibre re-entrant loop (Zimmermann *et al.* 1990). The gauge-length in these measurements was typically from about 0.5 m up to several metres, the number of serially multiplexed sensors could be as great as 10 and the minimum measurement time was 4 s.

Habel *et al.* (1999) used a high resolution OTDR from Opto-Electronics for monitoring the long-term behaviour of anchoring tendons bonded to the rock foundation of a gravity dam. He equipped 10 anchors of length around 71 m with serial-type sensor arrays, each of which had 10 measurement segments with

gauge lengths varying in the range 0.5–2 m. These sensors were used to measure the strain distribution during the tensioning procedure and to monitor long-term loading capacity. After four years of measurements it was stated that the system is able to provide results in such a harsh environment, but that the ingress/egress conditions for the cables and the source-to-fibre coupling have to be adapted to the latest OTDR devices in order to ensure the expected resolution of  $\leq 0.3$  mm. Questions concerning the temperature-induced error in strain results and the long-term stability of the reflectors should also be investigated.

Smith & Williams (2002) also used pulse delay measurement techniques for structural monitoring, employing polymer optical sensor fibres in conjunction with a high resolution OTDR from Opto-Electronics to derive large strains in synthetic fibre mooring ropes used on offshore floating oil platforms. This experiment revealed that commercially available polymer fibres exhibit a linear response to large strains of up to several per cent, but the main drawback was the high attenuation of the fibres. Nevertheless, with proper integration, instrumentation and techniques, polymeric optical fibres appeared to offer a high potential for measure large strains on long mooring rope segments. The method for the direct measurement of large strains in ropes in situ using a plastic optical fibre and an OTDR or other light time-of-flight measurement instrument has now been patented by Williams *et al.* (2006).

Kercel & Muhs (1992) constructed various high resolution OTDRs from off-the-shelf components and studied their repeatable sensitivity in strain measurement. Kercel's system was different from the measurement approaches discussed above in that it used single mode fibres and a high bandwidth sampling oscilloscope for interrogation. The conclusion after a comprehensive measurement procedure under laboratory conditions was that the strain sensitivities in Fresnel and loop setups were  $400 \mu\epsilon$  and  $200 \mu\epsilon$ , respectively. The predominant limit on performance was the  $\pm 2$  ps jitter and a secondary limit was the 6.4 GHz bandwidth of the detector.

Hampshire & Adeli (2000) demonstrated a pulse delay measurement technique for monitoring the behaviour of steel structures using distributed optical fibre sensors. Their interrogation system was based on the use of a Hewlett Packard HP53310A Modulation Domain Analyzer which has the ability to make precise measurements of the time interval between two electrical signals (commonly referred to as "data-to-clock" jitter analysis). This function is used for a variety of purposes including measurement of the time interval between optical pulses. The

averaged accuracy of these time measurements can be of the order of a few femtoseconds.

In the actual measurement a simply supported w-shaped test beam was loaded by bending it with a hydraulic jack, whereupon the results obtained with surface mounted optical fibre sensors typically deviated by about 10% from the direct reference measurements. The differences between the measurement systems were mainly attributed to the poor stability and accuracy of the emitter, detector and analyser electronics. In addition, it was unlikely that the light pulse signals during the experiment were pure square waves, as a consequence of which any lag or lead time in the light pulse signals could have been a potential source of error. It was concluded that future researchers may wish to consider using an alternative method for determining the strain in an optical fibre, such as a Fabry-Perot or Michelson interferometer or the Bragg grating technique.

Zumberge *et al.* (1998, 2002) used time-of-flight sensors to derive borehole strains in Siple Dome, Antarctica. The round-trip length of the sensor fibre, stretched and fixed at both ends, could be measured using a commercial electronic distance meter (EDM) designed to determine the time-of-flight of light pulses in the atmosphere, which had to be modified with focusing optics to allow fibre-optic measurements. After correction for the refractive index of the fibre, and with appropriate optics to accommodate dispersion in the fibre, the fibre length could be determined with a precision of about 2 mm, allowing the strain in a 1 km sensor fibre to be identified with a precision of 2  $\mu\epsilon$ . The stability of the measurement system was shown to be 1 mm over 3 years.

### **2.3.7 Concluding remarks**

This section summarizes the main features of commercially available fibre-optic strain measurement systems and comments on their potential for structural monitoring. Some comments presented here are the author's own opinions and do not necessarily have any wider acceptance.

To sum up, there exist six types of fibre-optic sensor that have been widely used for structural strain monitoring: a fibre Bragg grating (FBG), an external Fabry-Perot interferometric sensor (EFPI), a low-coherence interferometric sensor, a microbending sensor, a Brillouin scattering-based sensor and an OTDR-based time-of-flight sensor.

The fibre Bragg grating is the most promising sensor technology for most applications, including FRP composite, concrete and metal structures. With sub-

micron precision and high sampling frequency, typically exceeding 100 Hz, it allows precise measurements to be made in both the static and dynamic time domain. An FBG system provides an extremely high serial multiplexing capacity, especially when working in TDM mode, allowing sensor systems in excess of 100 units to be built in a relatively simple manner. As a point-type sensor, a fibre Bragg grating is especially suitable for strain measurement, but with an appropriate package its inherent gauge-length of a few millimetres can be enlarged to several metres, thus allowing deformation measurements as well.

The external Fabry-Perot interferometric sensor was one of the earliest fibre-optic sensor approaches to become commercially available. The performance of a point-type EFPI sensor resembles that of a fibre Bragg grating, and the gauge-length of an EFPI sensor can similarly be increased with a suitable package. A typical EFPI interrogation system only allows parallel multiplexing, however, which makes the structure of a sensor system rather complicated with respect to the FBG approach. The main benefit of an EFPI sensor over an FBG is its immunity to transversal strain and the possibility of compensating for thermal effects by using an appropriate package. Due to their poor multiplexing capability and costly sensors, EFPI systems will obviously lose their popularity relative to FBG systems.

Low-coherence interferometric sensors have been widely used in various civil engineering and other applications such as bridges, tunnels, piles, anchored walls, dams, historical monuments and nuclear power plants. Achieving a high precision of the order of  $1 \mu\epsilon$  with a wide range of gauge-lengths from about 20 cm up to 20 m, a low-coherence fibre-optic interferometer is capable of monitoring concrete deformation during setting, pre-stressing, crack opening and long-term deformation, for instance. This inherently single-channel measurement approach allows DC-type measurements to be made with a number of sensors by means of an optical fibre switch.

Commercial microbending systems are usually single sensor approaches in which the number of sensors can be greatly increased by using an optical fibre switch. Allowing a precision and sampling rate of  $1 \mu\epsilon$  and 100 Hz, respectively, for gauge-lengths up to several metres, microbending systems have been widely used, especially for the measurement of deformation in various structures such as bridges. A microbending system is a cost-effective competitor, especially for a low-coherence interferometer.

Of all the fibre-optic measurement systems, only the Brillouin scattering techniques, BOTDA or BOTDR, allow distributed strain sensing. With a typical

spatial resolution in the range of 1–2 m, they allow the static measurement of strain with a precision of about 10–20  $\mu\epsilon$  for a sensor fibre exceeding 10 km in length. Due to their very complex architecture, Brillouin scattering systems are extremely costly devices, but their capability for producing strain information for thousands of locations along a sensor fibre makes them nevertheless the best choice for monitoring very large structures such as pipelines and geostructures with characteristic dimensions extending for a matter of kilometres.

OTDR-based time-of-flight sensors were subjected to extensive research in the 1980's and early 1990's, but only a few articles have been published in this field during the last ten years (Habel *et al.* 1999, Zumberge *et al.* 2002, Pluciński *et al.* 2005). Although the reason for this lack of interest is not known, it is obvious that their complex design and high cost made such systems unattractive for monitoring purposes. Furthermore, stability problems with multi-mode fibres and reflectors may have ruled out their use in long-term measurement applications.



## 3 Experimental work

The research work carried out in this thesis can be roughly divided into three main categories: field tests with custom-made microbending sensors, as summarized in Sections 3.1 to 3.3, the development of a fibre-optic TOF measurement system based on commercial electronics, presented in Section 3.4, and the development of a high precision TOF interrogation system, which is described in more detail in Chapter 4. The following sections give a summary of this work, while more comprehensive discussions can be found in the appended papers.

### 3.1 Measuring of strain in road structures using microbending sensors

The information given here is reported in more detail in Paper I.

Frost is one of the key elements which cause damage to road structures in the north, where, especially in springtime, a road can be subject to frost damage in the form of cracks along the centre line. The damage can be reduced by using frost-free materials, thermal isolators or reinforcing elements, e.g. steel meshes. The use of a steel mesh has proved to be the most attractive and least expensive means of repairing old road structures. When using such a mesh it is important to determine the actual amount of stress, in order to avoid over-design and reduce material costs. This can be done by measuring the strain profile of the mesh across the road.

This project entailed field installations in two frost-susceptible roads in the central part of Finland. In the first case a steel mesh was assembled in the base course of a road, about 20 cm under the surface, and in the second a steel mesh was integrated into the levelling mix just under the asphalt concrete. The former was fitted with multi-mode (MM) microbending sensors, whereas the latter was equipped with single mode (SM) microbending sensors. Both of the meshes were also equipped with strain gauges to provide reference information. As the experiments and results were essentially similar, only the approach with single mode sensors will be explained here.

The principle of a microbending sensor is presented in Figure 17. Setting out from the saw-tooth plates shown in Fig. 8, the microbending structure was introduced into a fibre by bending it along a suitable pin modulator and fixing it to the structure to be measured. In this sensor configuration varying loading conditions alter the distances between the attachments, which affects the initial tension of the fibre. As a consequence the bend radius of the fibre is modulated, which can be

detected as changes in microbending loss. This loss can be measured with a simple through-power technique or with an OTDR, as shown in Fig. 10, which also allows multi-sensor measurement in a quasi-distributed fashion.

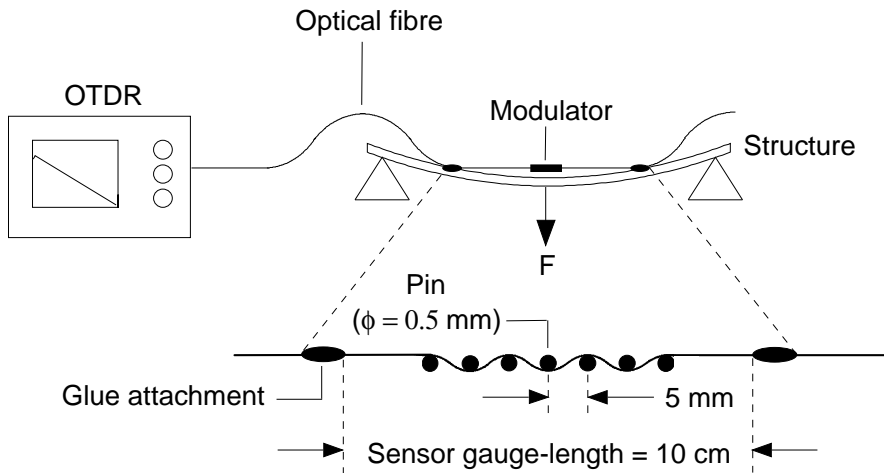


**Fig. 17. Principle of a microbending sensor used for measuring a road structure.**

The prototype sensor was tested and calibrated with a universal material testing machine by stressing a piece of steel rod ( $\phi = 7$  mm), to which a sensor was attached, and measuring the attenuation of the sensor as a function of the force. Prior to the test the sensor fibre was glued to the rod at both ends of a modulator using Epotek 353ND adhesive of high thermal durability. The single mode fibre used was  $9/125$   $\mu\text{m}$  in diameter and it had a heat-resistant polyimide coating for tolerating temperatures of up to  $150$   $^{\circ}\text{C}$  during the asphalt laying process. This type of thin, tightly-buffered fibre ( $\phi = 145$   $\mu\text{m}$ ) was also mechanically stable and as such ideal for sensor applications. According to experimental tests a microbending modulator which had 7 pins ( $\phi = 0.5$  mm) with distortion periodicity of 5 mm allowed a reasonable precision for a few serial sensors.

When using a wavelength of 1310 nm the slope of the microbending sensor proved to be  $\approx 8$  kN / 0.45 dB in the linear region, implying a stress resolution ( $\sigma$ ) of about 23 MPa using an OTDR with 0.05 dB amplitude resolution ( $\sigma = [8\text{kN} \cdot (0.05 \text{ dB} / 0.45 \text{ dB}) / (\pi \cdot 3.5 \text{ mm})^2] = 23 \text{ MPa}$ ). The corresponding strain resolution ( $\epsilon$ ) defined from the well-known relation  $\sigma = E \cdot \epsilon$ , where  $E$  is the Young's modulus of steel ( $\approx 200$  kN /  $\text{mm}^2 = 0.2$  MPa), was 115  $\mu\epsilon$ .

Altogether five microbending sensors and reference strain gauges were assembled on the mesh in a direction pointing across the road, as shown in Fig. 18. The fibre-optic sensor network consisted of two separate sensor arrays, each of which had three sensors in cascade form (with the outermost sensor on the right-hand side serving as a reference). The housing at each sensor point was made of a steel pipe covered with a heat-shrinking sleeve (see Paper I, Fig. 5). The fibres between the sensor points were placed in a hydraulic tube. Each sensor was about 10 cm in length.

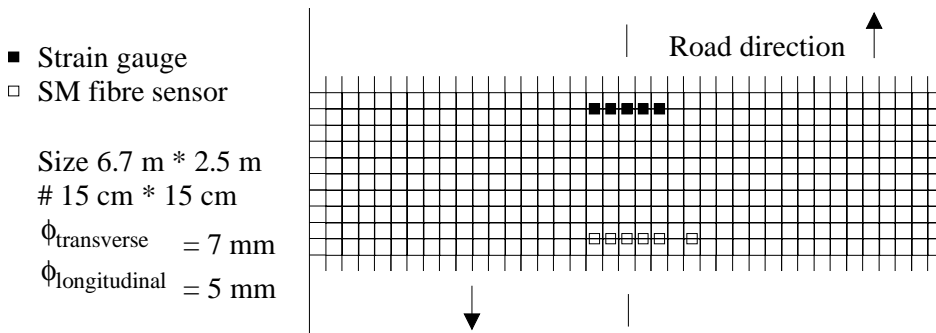


**Fig. 18. Scheme for the steel mesh assembled under the asphalt layer. The fibre-optic sensors and reference strain gauges were installed close to the centre line in a direction pointing across the road.**

Data was collected for more than a year with measurement periods of about three months. A comparison between the results obtained with the single mode microbending sensors and the corresponding strain gauges is shown in Figure 19. The curves are rather similar in shape but apart from the first sensors on the left-hand side there is a noticeable offset between them varying from  $-45 \mu\epsilon$  in minimum up to  $555 \mu\epsilon$  in maximum. This can be partly explained by the different locations of the fibre sensors and the reference strain gauges. Due to the cumbersome pre-tension process it is also possible that some sensors were not working in the most linear region of the calibration curve. A further likely reason is that there were unintended points of microbending, e.g. in the interconnection fibres between successive sensors.

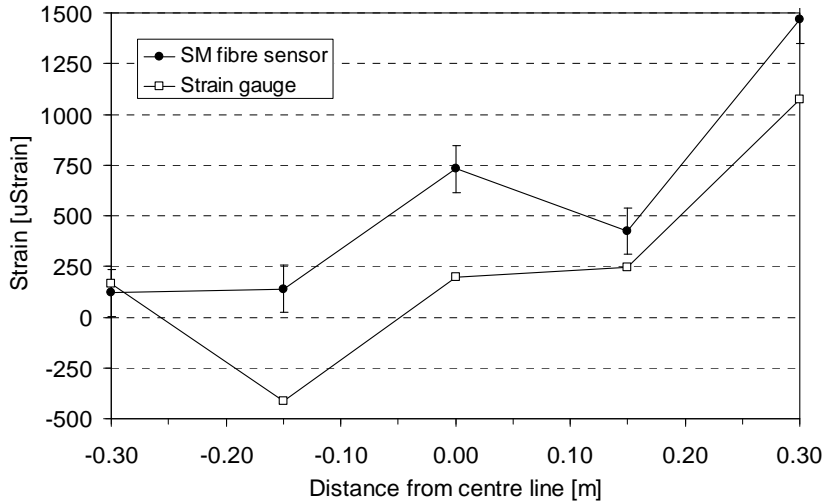


**Fig. 19. Comparison between the measurement results obtained with the single mode fibre optic sensors and the corresponding strain gauges (Paper I).**

Despite the anomalies between the measurement curves, the experiment showed that microbending sensors can be used for structural strain monitoring in a harsh environment. It has been shown in the literature that, with a proper sensor design, it is possible to achieve a strain resolution of about  $1 \mu\text{m}$  when using a single sensor and a through-power technique (Braunstein *et al.* 2002).

The major limitation of an OTDR-type approach is that the attenuation is cumulative. The light level in the extreme distal sensor depends on the measurand at each sensor along the fibre, and this places severe requirements on the dynamic range of the OTDR detection system and means that considerable averaging needs to be done to achieve a good signal-to-noise ratio. Due to the limited dynamic range of a standard telecommunication OTDR ( $\approx 30 \text{ dB}$ ) the number of multiplexed sensors will inevitably remain small, a maximum of 5–10, making this approach uneconomic for strain sensing. Nevertheless, the combination of an OTDR and a distributed microbending sensor is a powerful tool for detecting on/off-type alarm situations.

### 3.2 Traffic monitoring with microbending and speckle sensors

This research work focused on the developing and testing of fibre optic sensors for traffic monitoring applications, as reported in more detail in Paper II. Such sensors are useful for monitoring the traffic entering and leaving guarded areas, counting traffic on public roads and determining lane occupancy at traffic lights. The sensors may also provide information about the speed of a vehicle and its wheel base, together with the number of axles, vehicle type and weight.

The sensors developed here were based on the microbending principle and speckle phenomenon, while interrogation was performed by means of an optical through-power technique and an analogue data acquisition card installed in a computer. The microbending sensor used for measuring pressure required a special fibre and set-up. The speckle sensor was based on a standard telecommunication cable and was more suitable for vibration measurement.

The principle of the microbending sensor is presented in Figure 20 (a) and a cross-section of the final assembly in Figure 20 (b). The microbending sensor used in this experiment was a commercial product that is typically used in safety applications. It consists of a standard telecommunication fibre and a plastic spiral wire which forms a continuous microbending structure on the fibre. When in operation the sensor is subject to lateral pressure, as a consequence of which the spiral wire is pressed against the fibre. This introduces sharp microbends in the fibre which allows part of the light power to escape from the core. This can be detected as attenuation in the receiver.

A schematic diagram of the speckle sensor is provided in Figure 20 (c). In this approach a coherent light from a laser source is launched into a multi-mode fibre. Due to interference of propagating modes, a speckle pattern appears in the far field of the sensor fibre. The distribution of the speckles changes randomly over time, but the total intensity of the pattern remains unchanged. By placing a small detector in the far field so that it covers only a small part of the illuminated area, the changes in speckle pattern can be made to modulate the intensity at the detector. When the fibre is perturbed, the speckle pattern changes, which modulates the output of the detector at the perturbation frequency. This pattern change is due to changes in the propagation constants of different modes caused by modifications in the fibre refractive index.

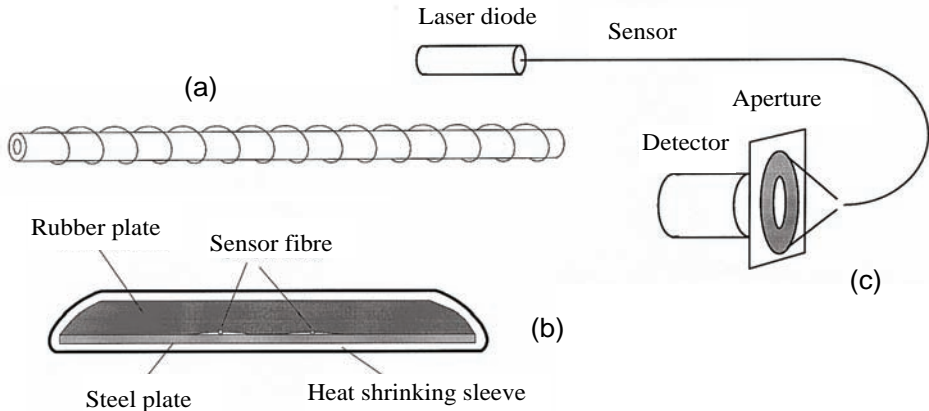


**Fig. 20. (a) Principle of the continuous microbending sensor. (b) Cross-section of the complete microbending sensor. (c) Schematic diagram of the speckle sensor (Paper II).**

In order to find a proper cable for the speckle sensor, several cable types were tested on a vibration test bench in a frequency range of 5–150 Hz. The most appropriate cable in terms of vibration sensitivity and ease of mounting in a road structure proved to be a 7 mm thick flexible duct cable which tolerated temperature and humidity changes and was mechanically stable.

The field installations were carried out on a motorway in northern Finland. In order to install these sensors which were up to 6 m long in the road structure, a cut of suitable size had to be made in the existing asphalt for each sensor. Two microbending sensors, placed 2 m apart, and one speckle sensor were assembled on the bottoms of grooves sawn across the lane (Paper II). After adding a protective sand layer on top of the sensors the grooves were filled with an asphalt concrete.

Following the assembly, tests were carried out with different vehicle types and at different speeds in order to characterize the sensors. The majority of the measurements were performed with microbending sensors, and only some preliminary tests involved the speckle sensors. Speed was measured using the microbending sensors and the results were confirmed with a calibrated speed indicator. Some examples of recorded pulses are presented in Fig. 21.

The measurements made with the microbending sensors indicated that the pulse shapes differed notably between the vehicle types and it was possible to identify these. The speed and wheel base of a vehicle could be measured with an

accuracy of 1.5 km/h and 5 cm, respectively, and the number of axles could be counted easily.

The experiments suggested that both microbending and speckle sensors are capable of producing on/off-type information which is adequate for many road applications such as traffic counts and traffic light control, but more precise measurements are needed for categorizing vehicles or measuring weight in motion (WIM). In this sense the well established microbending principle offers a higher potential than an approach based on the somewhat random speckle phenomenon. The main advantage of the speckle approach is that a standard cable with no special housing can be used as a sensor.

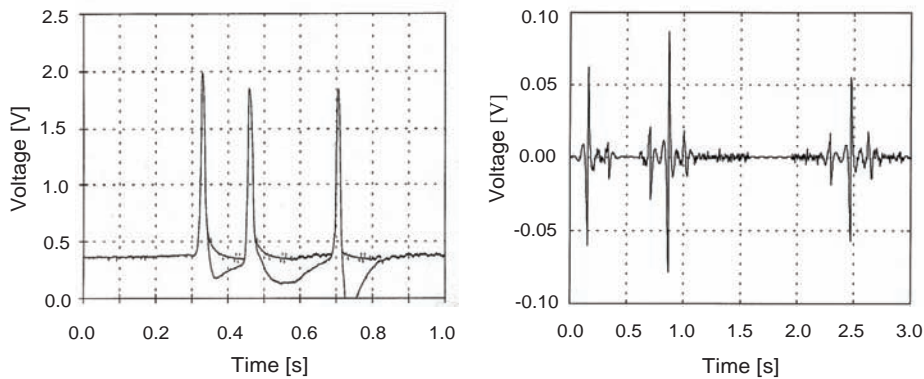


**Fig. 21. (Left) High-pass filtered and unfiltered signals from the detector when a passenger car with a caravan crossed the microbending sensor. (Right) Signal from the detector when three passenger cars crossed the speckle sensor (Paper II).**

### **3.3 Measuring of composite containers with microbending sensors**

Composites offer economical and advanced alternatives to metals for many structures. Their applications have been of special interest to aerospace designers because of their low weight, but their industrial and commercial applications are also expanding. Composite containers for toxic and dangerous chemicals or petrol, for example, are critical structures from an environmental safety point of view, which means that the process by which composites are manufactured and monitoring of the integrity of the structures are very important aspects.

The main aims of this experimental work, discussed in Paper III, were to investigate the integration and embedding of optical fibre sensors inside the com-

posite material during the manufacture, to study the possibilities for cure monitoring during fabrication, and to construct simple condition monitoring systems based on microbending sensors. The costs entailed versus the additional business value and the savings achieved by optimization of the manufacturing process were also important aspects for the industrial partner.

The measurements were carried out for three composite containers 5 m in length, 1.4 to 1.6 m in diameter and with walls approximately 5 mm thick. These were manufactured using a semiautomatic spooling machine, by reeling resinous reinforcing glass fibres and fibreglass matrix on a cylindrical mould, as illustrated in Fig. 22.

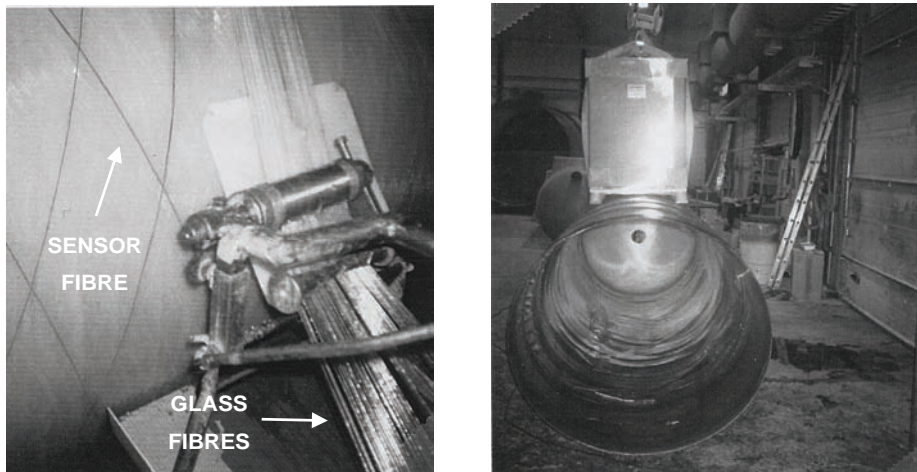


**Fig. 22. (Left) Photograph of the spooling process showing the location of a thick nylon coated sensor fibre. (Right) A semi-finished container subjected to transversal loading.**

To find the best response for cure and condition monitoring, different types of optical fibres were installed in different layers of the container wall. Both multi-mode and single mode telecommunication fibres with different coatings, such as nylon and acrylate, were tested using fibre lengths from 150 m to 300 m.

The optical fibres were installed inside the wall material during the manufacturing process by winding the sensor fibres in with the glass fibres and fibreglass matrix. This was a simple, time-saving procedure and it also ensured that the optical fibres were positioned exactly parallel to the reinforcing fibres, which minimizes the reduction in composite strength. In this kind of assembly microbends

are formed when optical and reinforcing fibres of different turns cross each other, as shown in Figure 22.

The optical power loss in the sensor fibres was measured either by a through-power technique, using an EXFO FOT-902-G optical power source and receiver unit, or by OTDR, using a multi-mode model AOC10 8/13M50 from Antell Optonics and a single mode device FCS-123B from EXFO. Cure measurement began directly after the mould had stopped revolving and it was continued until the attenuation was no longer changed that typically lasted about 5–15 hours depending on the container (Figure 23).

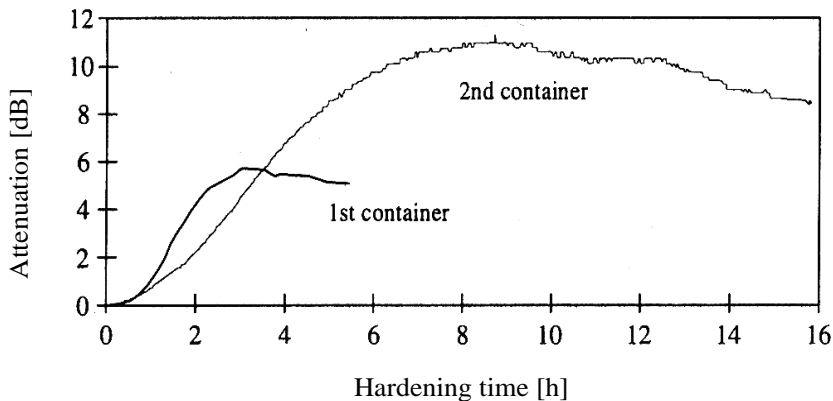


**Fig. 23. Changes in attenuation during cure monitoring in an acrylate-coated graded-index multi-mode sensor fibre in two experiments (Paper III).**

The most sensitive response in monitoring the state of curing was achieved with a single-layer acrylate-coated graded-index multi-mode fibre with dimensions of 50/125/250  $\mu\text{m}$ . As presented in Fig. 23, the attenuation increases exponentially at the beginning of curing but less markedly as curing proceeds, and eventually it ceases to increase and then starts to decrease slowly after the hardening process has ended.

The maximum attenuation (17 to 30 dB/km) and the time in which it was achieved (3 to 8 h) differed between the experiments. These parameters depend on the amount of hardener used in manufacturing and on the lay of the composite and sensing fibres, which varies because of manufacturing tolerances. Variations in fibre lay cause differences in microbending structure and thus also in maximum attenuation. The amount of hardener was smaller than normal in the second container, which is the reason why the time scales of these two curves are so different.

Loading tests were carried out with a hydraulic jack fastened to the side of the container and used to press a steel bar 10 mm in diameter against the side wall. Such loading is expected to occur in the case of an underground container buried in frost-susceptible ground, where sharp-edged stones may damage the container wall, especially in spring time. The experiment was repeated three times for each fibre, and each time the pressure was directed at a different point but still directly against the fibre to be studied. After that the same measurement was repeated by pressing on a spot that had already been loaded once. Finally, the effect of the distance between the fibre and pressing position on the attenuation was studied.

The most sensitive fibre in the loading measurement proved to be a dual-layer acrylate-coated ( $\phi = 250 \mu\text{m}$ ) single mode telecommunication fibre, the results of which are presented in Figure 24.

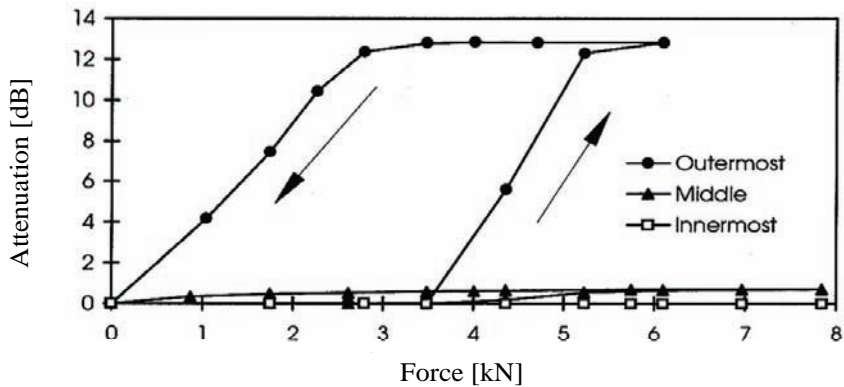


**Fig. 24. Attenuation during loading measurements in thin acrylate-coated single mode fibres embedded in different layers of a container wall (Paper III).**

As shown, the sensor fibre embedded closest to the outside surface of the wall was the most sensitive to external loading, whereas that installed near the inside surface was almost immune to the same load. The maximum attenuation value changed as the measuring point was moved along the fibre because of variation in the microbending structure. The threshold value at which the attenuation started to grow quickly was almost the same in each measurement, 3.5 kN. The pressure threshold was smaller, however, when the same point was stressed for a second time, but even in this case the attenuation was restored to its original value with

the hysteresis effect when the load was removed. Both these effects, hysteresis and decrease in the threshold value, can be explained by delaminations, i.e. permanent damage to the composite structure caused by pressure. A visual inspection ensured that there were permanent damages of about 1 mm in depth on the outside surface while the interior of the container was unchanged. This explains the difference between the results of the outer and innermost sensors shown in Figure 24. The attenuation declined rapidly with increasing distance between the loading point and the fibre, and when the distance was about 20 mm, the stress no longer affected the transmission in the fibre at all.

According to these experiments, the end of the cure and curing speed can be determined from the shape of the attenuation curve. One can therefore expect the results obtained in cure monitoring to be applicable for optimizing the manufacturing time and possibly also the product quality, which may be related to the hardening speed.

As regards health monitoring, the best sensitivity can be achieved when the sensor fibre is embedded as close to the outer surface as possible. In this respect the distance between adjacent fibres is also of great importance. Standard single mode and multi-mode telecommunication fibres with thin acrylate coatings are feasible sensors when assembled parallel to the reinforcing fibres. Both through-power and OTDR techniques can be used for cure monitoring but an OTDR is a better alternative for health monitoring as it also provides spatial data.

While microbending and other amplitude-based measurement systems offer an easy and cost-effective means of setting up simple on/off type sensor networks, they do not allow precise measurement for many serially multiplexed sensors, as FBG systems can do, for example. Apart from spectral measurement techniques, serial multiplexing and demodulation can also be performed with a pulsed time-of-flight technique (TOF), as described in the following section.

### **3.4 A fibre-optic TOF measurement system based on commercial electronics**

The novice fibre-optic TOF measurement system was based on a pulsed TOF laser range finding technique that was originally developed in the Electronics Laboratory at the University of Oulu (Kostamovaara & Myllylä 1986, Määttä *et al.* 1993) and later commercialized by such companies as Noptel Oy, Prometrics Oy and Rautaruukki New Technology, whose products are intended for profiling hot surfaces in the steel industry and for determining the three-dimensional shapes of ship blocks in a shipyard, etc. The TOF measurement system discussed here is adapted from these commercial devices to allow for long-haul fibre-optic measurement (Papers IV–VI).

#### **3.4.1 Operation and performance of the novice TOF measurement system**

As shown in Fig. 25, the basic blocks of the TOF measurement system are a laser transmitter, optics for the transmitted and received optical signals, optical gain control, a common receiver channel for the start and stop pulses, a constant fraction timing discriminator (CFD) and the time interval measurement electronics. The method involves sending 10 ns optical pulses ( $\lambda = 1310$  nm) into the fibre and measuring the propagation time from the laser transmitter to a reflective feature along the fibre path and back to the receiver. A small fraction of the outgoing pulse is taken straight to the receiver via an optical fibre coupler to trigger the time measurement electronics. The optical pulse is converted in an avalanche photo diode (APD) to an electrical current pulse, which is in turn converted to a voltage pulse in a transimpedance-type amplifier. The amplified voltage pulse is taken to a CFD, which transforms the alternating analogue timing pulse to an accurate digital timing pulse for use in the time measurement electronics. The digital timing pulse is derived from the analogue one by a constant fraction timing discrimination method in which the timing threshold is a certain fraction of the maximum value of the pulse amplitude, about 0.5. This principle makes it possible to keep the timing threshold stable despite variation in the amplitude of the upcoming pulses, provided that the amplitude variation is within the 1 : 10 dynamic range of the CFD. If the signal amplitude is very high and exceeds this value, an optical attenuator is used to adjust it to the appropriate level.

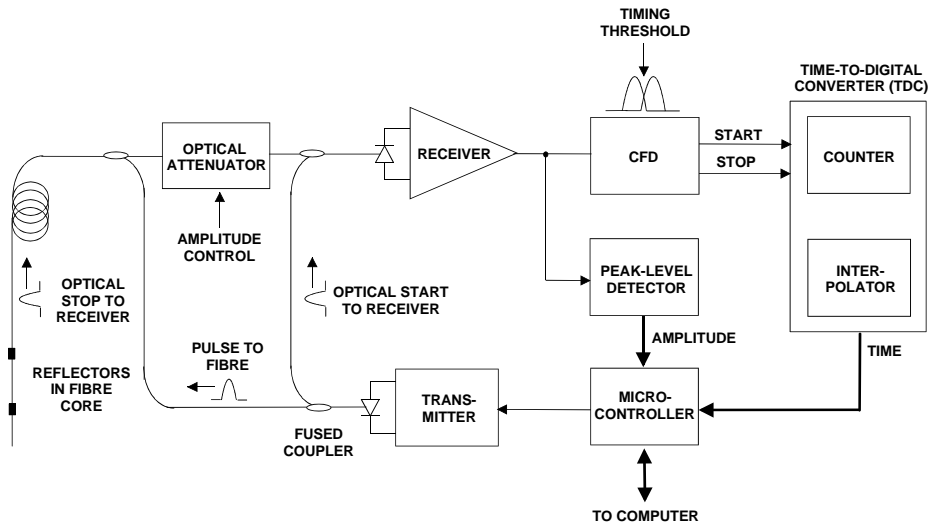


**Fig. 25. Block diagram of the novice TOF measurement system.**

The time delay between the start and stop pulses coming from the CFD is measured by time measurement electronics based on a time to digital conversion (TDC), which is a combination of a digital counting method and an analogue interpolation technique. The digital block of the TDC uses a 100 MHz oscillator to increment a 16-bit counter which produces a measure of the time interval with a precision of  $\pm 1$  clock cycle, i.e.  $\pm 10$  ns in time. The precision is improved to a fraction of  $1/241$  of its original value by using fast analogue interpolation, and thus the final time measurement precision is about 41.5 ps. This is an inherent value for the time measurement electronics and does not include the error sources of the receiver channel, such as the noise of the pre-amplifier and timing jitter of the comparator and logic circuits.

In practical measurements the single shot precision was typically about 60 ps, which corresponds to 6 mm in fibre length. This measurement precision was further improved by averaging the measurement results over a number of successive pulses, whereupon the precision improved in proportion to  $1/\sqrt{N}$ , where  $N$  is the number of the measurements to be averaged. Thus, the number of measurements needed to produce a precision of 1 mm was about 30, and the precision achieved by averaging 3000 measurements was about 0.1 mm. The corresponding measurement time was about 1 s and the spatial resolution about 5 m, being restricted by the jitter of the stop pulse selection logic and by the use of relatively long probe pulses of about 10 ns.

### **3.4.2 Measurements with bare TOF sensors**

Prior to the application tests a bare TOF sensor was loaded in terms of tensile stress, transverse pressure and temperature, as presented in more detail in Papers IV–VI. The tensile tests showed that the response of the TOF sensor was linear and repeatable with a precision of  $100 \mu\epsilon$  (0.01%), derived from Equation (7). Moreover, the effect of elongation on the refractive index of the fibre proved to be constant ( $a \approx -0.2$ ) within the elastic range of 0–1% for a glass optical fibre, which is in good agreement with other observations (Section 2.2.2).

Several TOF sensors with different protective jackets such as acrylate, polyimide and aluminium were used in the tests. A sensor with a polyimide coating proved most appropriate for practical applications. The explanation is that this coating forms a strong connection with the optical fibre, a necessary characteristic in strain measurements. In addition, its diameter is very small, around  $140 \mu\text{m}$ , and it is thermally stable up to  $380 \text{ }^\circ\text{C}$ .

A TOF sensor can be subjected to a severe transversal load by embedding it in FRP composite material, for example. Such transverse loading was induced in the sensor fibre by changing oil pressure in a tube so that the maximum pressure was 150 bar. The test demonstrated that the effect of pressure on transit time was negligible.

The response of an uncoated TOF sensor was also measured in a thermally controlled environment. This experiment, described in Paper VI, revealed that temperature change has a strong effect on the refractive index of the optical fibre and is thus a potential source of error unless appropriate techniques for thermal compensation are used, as discussed in Section 2.2.5. It also revealed that the temperature sensitivity ( $S_T$ ) of the TOF sensor was  $\approx 6.9 \cdot 10^{-6}$ , a typical value, as shown in Section 2.2.2.

### **3.4.3 Application measurements**

During the work three slightly different versions of the novice fibre-optic TOF measurement system were manufactured for monitoring fibre elongation in optical cable testing and assembly (Paper IV) and for determining strain in composite structures (Paper VI). The majority of the experiments were single-sensor approaches in which the start pulse was taken directly from the laser transmitter while the stop pulse was reflected from a cleaved fibre end. The measurement setup in which two TOF sensors are glued to the surface of a structure is illustrated in Figure 26.

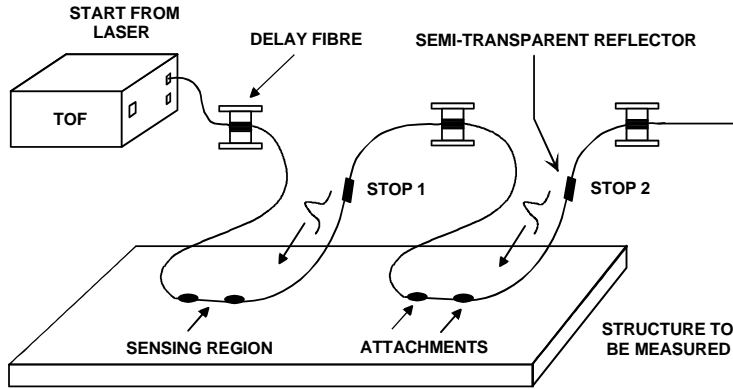


**Fig. 26. A simplified TOF measurement setup showing the sensor principle and the arrangement of a serial-type sensor network.**

### *Cable pull testing*

The monitoring of fibre strain during a pull test on an optical cable was the first application for the newly developed interrogation system (Paper IV). This was the main object of interest for the industrial partner and the experiment revealed that the measurement approach based on the pulsed TOF technique also has potential for telecommunication applications.

Optical fibre cables are frequently installed in places where they are subject to very high tensile stress, e.g. waterway crossings where the distance between pylons can be several hundreds of metres and places with sub-zero temperatures where a thick ice layer can form on the cable in winter. Optical cables for use in harsh environments place major demands on the manufacturer, since their structure should be robust enough to tolerate stress and avoid excessive elongation, which can be harmful in long-term use. Thus a large number of laboratory tests are needed before a new cable type can be recommended for use under field conditions.

An optical cable is normally tested by pulling it with a material testing machine and measuring the elongation of the fibres as a function of the pulling force. Due to the short cable length of 10–20 m typically used in this test, the elongation is usually too small to be detected by an optical time domain reflectometer (OTDR) that is normally used for optical link testing. More sophisticated and typically highly expensive means such as Brillouin scattering measurement sys-

tems and high-resolution OTDRs are therefore needed to derive fibre elongation (Sections 2.3.5 and 2.3.6). As shown in this experiment, fibre elongation can also be monitored using a much simpler pulsed TOF method.

The results of an experiment in which a metallic optical ground wire (OPGW,  $\phi \approx 19$  mm) was stressed with a material testing machine by increasing the force in 4 kN steps from 0 kN to about 80 kN, which was far beyond its maximum permitted tension value of  $\approx 35$  kN, are shown in Figure 27. Also presented in Fig. 27 is a photograph of a typical OPGW cable and its cross-section showing the locations of the optical fibres (2), various aluminium strength members (1,4,5) and the plastic buffer tubes (3).

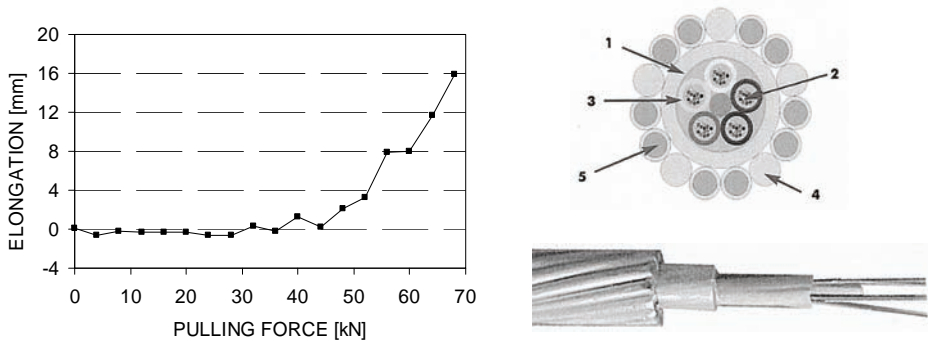


**Fig. 27. (Left) Elongation of an optical fibre as a function of cable pulling force. (Right) Photograph and cross-section of a typical OPGW cable (Paper IV).**

The length of the cable used in the test was 15 metres and the strain sensitivity was improved by fusing all the fibres in cascade form so that the entire length under stress was about 180 m. The result, presented in Figure 27, shows that, the fibre begins to elongate when the pulling force is around 30–35 kN, which is in good agreement with the manufacturer’s product specification. When the force is increased beyond this threshold value the extent of elongation increases rapidly and finally, at a force of about 80 kN, the fibre breaks (not seen in the figure).

### *Laboratory tests with composite specimens*

Composite specimens with embedded TOF sensors were tensile-tested in the axial direction using a universal material testing machine (Paper VI). The composite plates made of polyester resin and glass fibres were rectangular in shape with dimensions of about 880 mm  $\times$  20 mm  $\times$  5 mm, as presented in Fig. 28. Also shown in Fig. 28 is the result obtained with an embedded TOF sensor with a polyimide

coating, which is in good agreement with that given by the reference extensometer. Similar tests with an acrylate-coated sensor also showed an adequate response. When the loading was reversed, i.e. to produce pressure, both sensor types always disengaged from the laminate and the response measured was approximately a third of the actual change in length. This was probably due to extensive chemical shrinkage and thermal expansion of the polyester resin during the manufacturing process, a condition sufficient to cause a large initial shear stress in the resin at the sensor surface. Experiments were also carried out with cylindrical specimens, whereupon it became evident that neither transversal nor torsional load had any effect on the response of an axially assembled sensor, whereas a radially mounted TOF sensor was sensitive to torsional loading, showing a similar response to the reference device.

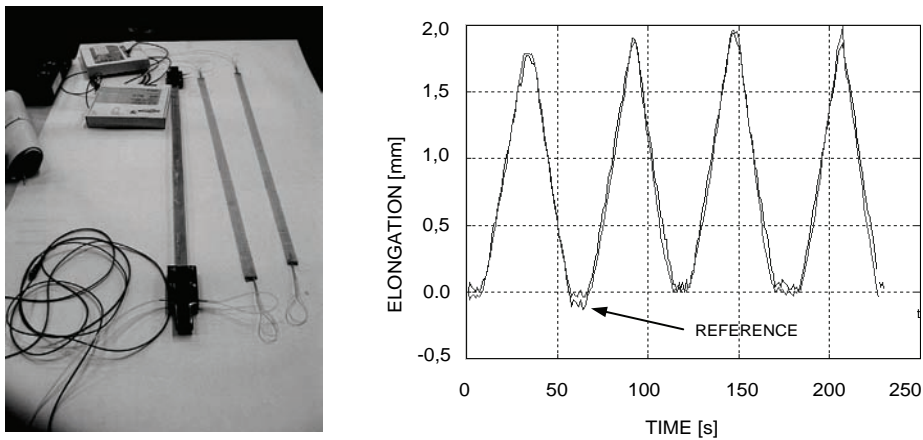


**Fig. 28. (Left) Photograph of glass resin composite plates used in tensile tests. (Right) Response obtained with a polyimide-coated TOF sensor embedded axially in a composite plate subjected to tensile loading (Paper VI).**

In general, the most disturbing effect in the laboratory tests was the weak bonding strength of the coating of the fibres with the surrounding plastic material. Acrylate coating fails to attach either to the plastic resin (polyester or epoxy) or to the optical fibre, while polyimide coating remains fastened to the optical fibre but bonds weakly to the resin. The peeling of the sensor is particularly pronounced with plastic specimens. Laminate specimens, on the other hand, do not suffer from the problem due to the compression effect of the reinforcing fibres. Perfect bonding between a sensor and the surrounding material can be achieved only by removing the coating.

### *Field test with a carbon/epoxy cylinder*

The TOF measurement system was also tested in an industrial environment with a carbon/epoxy cylinder used with a paper machine, as discussed in Paper VI. The industrial partner's intention was to determine the amount of residual stresses caused by the manufacturing process, as this might influence the long-term integrity of the structure.

The experiment was conducted on a miniaturized model of the actual draw roll, as shown in Figure 29. The measurements were performed during a manufacturing process in which filament winding was first followed by pre-curing with an external heat source and finally curing in an autoclave. Equally spaced polyimide-coated TOF sensors were embedded in the cylinder in the axial and the radial (layer) directions relative to the specimen.

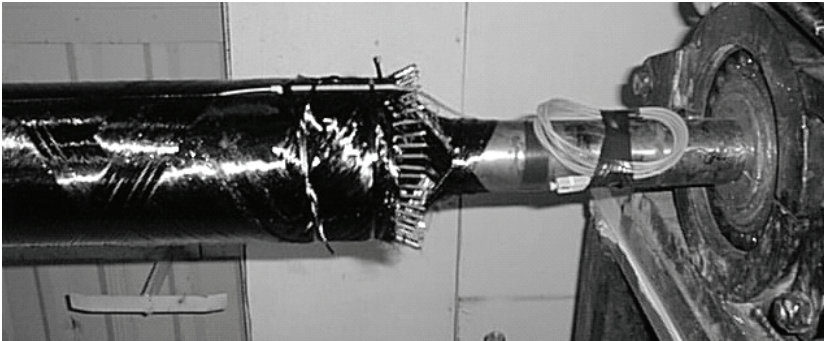


**Fig. 29. Photograph of the carbon/epoxy cylinder used in the experiment.**

During the measurement the reflection pulses showed a dramatic continuous change in attenuation along the sensor fibres. This was probably due to the microbending effect in the optical fibre caused by the pre-stressed reinforcing fibres. The signal level continued to decrease during curing of the resin owing to chemical shrinkage, which further compressed the material. In addition, temperature changes altered the volume of material, which in turn influenced the signal level.

As the signal level was small and variable, the residual strain in the cylinder could not be measured reliably, but the assembly of the sensors during the manufacturing process was successful and some sensors also survived the extremely hostile environment of the autoclave. The attenuation problem could obviously also be overcome by using a more powerful laser with an appropriate gain control.

### **3.4.4 Evolution of the TOF system**

Although the early fibre-optic TOF measurement system was capable of producing strain information with a precision adequate for many applications e.g. to optical cable testing, it suffered from poor spatial resolution, low measurement speed and long-term drift which are important issues to be addressed in fibre-optic strain sensing.

The first step towards a more practical measurement system was to improve the spatial resolution and measurement precision by drastically increasing the bandwidth of the receiver channel, as explained in Paper VII. Another improvement in performance was achieved through the use of a new type of digital TDC circuit implemented on a CMOS chip. Besides offering better single-shot precision, spatial resolution, measurement speed and power consumption, the new TDC was an order of magnitude smaller in size, thus enabling a much more compact design than in the previous system.

This new TOF measurement system provided better spatial resolution and measurement precision, but its measurement speed was still only at a moderate level and long-term drift was still a major problem. As the low measurement speed was mainly attributed to a slow transfer rate between the measurement device and the PC, it was assumed that this problem could be solved by reducing the amount of data transfer by re-processing the measurement data in the TOF device. It was calculated that the measurement speed could be improved by a factor of 100 with a programmable FPGA circuit.

The major problem regarding the long-term drift was temperature-induced changes in the optical properties of the sensor fibre, especially in the refractive index, and also in the electrical properties of the interrogation device, especially in the TDC. Due to the fact that temperature changes are common in a single-channel measurement approach such as a TOF system, it was assumed that temperature drift and other common mode errors could be effectively eliminated by means of a reference fibre. In order to test these ideas a new version of the fibre-optic TOF measurement system was developed, which will be discussed in the next chapter.



## 4 A high-precision fibre-optic TOF measurement system

Since the high-precision TOF measurement system developed here represents the main contribution of this thesis, a whole chapter is dedicated to a detailed description of its operation, performance and application measurements. The majority of the information given here can be found in Papers XIII and IX, apart from the section which compares the system with commercial devices.

### 4.1 Apparatus

The high-precision TOF measurement system consists of a laser transmitter, receiver, timing discriminator, time-to-digital converter (TDC), programmable logic circuit (FPGA) and computer, as shown in Figure 30.

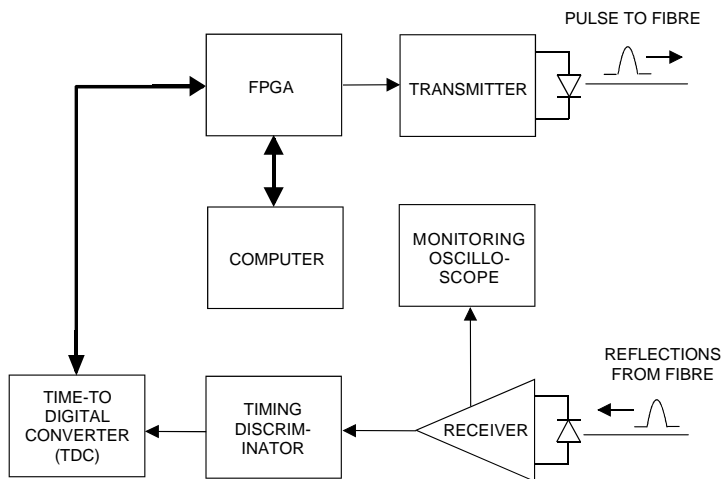


**Fig. 30. Block diagram of the high-precision TOF measurement system.**

During a measurement sequence a short optical pulse is sent into a single-mode fibre which has wideband, low-reflectivity semitransparent reflectors such as fibre-optic connectors to produce timing pulses. The reflected pulses are detected by the receiver, from which they are transferred to the timing discriminator, which changes the alternating analogue timing pulses it receives to accurate digital pulses for the TDC used to measure the time delays between the pulses. These measurement data are processed by the FPGA to enable dynamic measurements

to be achieved. In this system the computer serves as a mass storage unit and user interface, while the oscilloscope is used only for monitoring purposes.

The principle of TOF measurement with several sensors connected in series is presented in Figure 31. Each sensor consists of a sensor fibre and an equally long reference fibre, as shown with dashed lines. Reflectors are attached to the fibre ends e.g. R1, R2 and R3. The actual sensor fibre is in tension, while the reference fibre is loosely attached. The role of the reference fibre is to eliminate common mode errors arising from temperature effects, for instance.

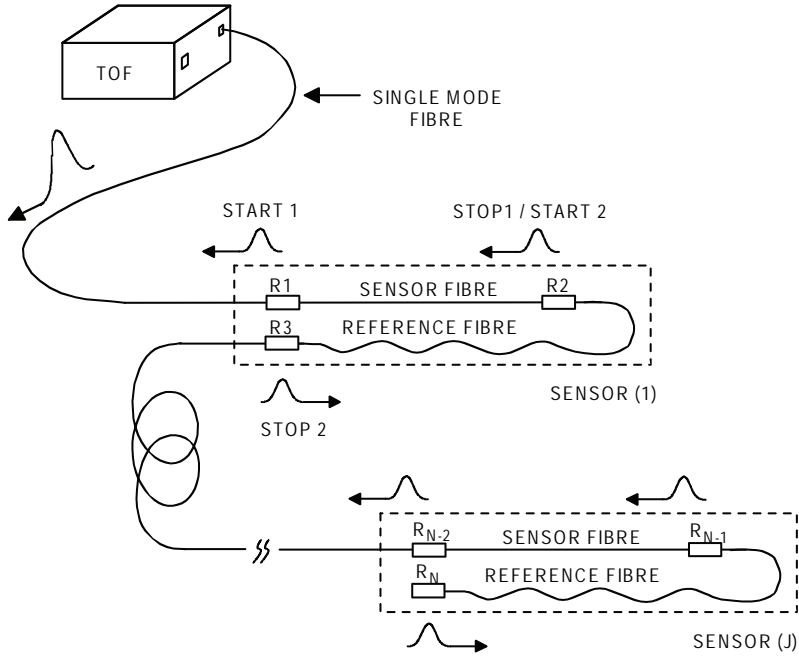


**Fig. 31. The TOF measurement principle.**

A measurement result is achieved as the difference in time delay between the sensor and reference fibre, e.g.  $\Delta t_{START1 \rightarrow STOP1} - \Delta t_{START2 \rightarrow STOP2}$ . The strain ( $\epsilon_j$ ) in the  $j$ th sensor is derived from the formula

$$\epsilon_j = \frac{1}{2l_j \frac{n}{c}(1+a)} \cdot [\Delta t(R_{N-2} \rightarrow R_{N-1}) - \Delta t(R_{N-1} \rightarrow R_N)], \quad (8)$$

which is an adaptation of the formula presented in Zimmerman's paper (1990). In Equation (8)  $\Delta t(R_{N-2} \rightarrow R_{N-1})$  represents a change in the pulse delay between the start and stop pulses of the sensor fibre,  $\Delta t(R_{N-1} \rightarrow R_N)$  is a change in the pulse delay between the start and stop pulses of the reference fibre,  $c$  is the speed of light in a vacuum,  $n$  is the group refractive index for the fibre ( $\approx 1.47$ ),  $l_j$  is the length of the  $j$ th sensor and its reference fibre and  $a$  is the strain-optic coefficient ( $\approx -0.2$ ).

#### **4.1.1 Transmitter**

The length of a probe pulse sets the limit for the spatial resolution. A spatial resolution of 0.50 m, for example, corresponds to about 5 ns in time. To ensure the necessary recovery time for the components in the signal path, however, and to minimize overlap between adjacent pulses, the optical probe pulses used are considerably shorter, about 2 ns (FWHM).

The transmitter is a simple avalanche transistor pulser (Kilpelä & Kostamovaara 1997, Paper VII), which drives a laser diode manufactured by Mitsubishi Electric with the product name FU-17SLD-F1. This is a low-cost Fabry-Perot type laser with an FC-connector package. The data sheets specify a typical centre wavelength of 1300 nm, rise and fall times of about 300 ps and an operating current of a few tenths of a milliamp, producing a minimum continuous optical power of 1 mW. It has been found, however, that when driving the laser with very short current pulses ( $< 2$  ns) at a relatively low repetition frequency ( $< 1$  MHz), much higher current levels in excess of 100 mA can be used, yielding an optical pulse power of 10 mW or more. High power levels are needed to achieve detectable reflection pulses from a fibre containing a series of reflectors with a low reflectivity of 0.1% or less.

#### **4.1.2 Receiver**

The receiver consists of a pre-amplifier module and a post-amplifier. The pre-amplifier module is a commercial device for telecommunication links manufactured by OKI Electric with the model number OF3610B-C2, offering a bit rate of 622 Mbit/s. It includes an avalanche photo diode (APD) with a typical responsivity and sensitivity of 9 A/W and  $-40.5$  dBm, respectively ( $\lambda = 1310$  nm), a transimpedance pre-amplifier and a fibre pigtail with an FC-type connector.

The post-amplifier is used to amplify the pulses to a sufficient voltage level for the timing discriminator, i.e. 100 mV, and it is realized in the form of a high-frequency operational amplifier (AD8009) with a gain of about 5 and an upper  $-3$  dB corner frequency of 500 MHz. The noise voltage in the output from the post-amplifier is 0.9 mV (rms) measured with a URV-5 mill-voltmeter using a measurement bandwidth of 0–1 GHz. Actual probe pulses have demonstrated that using an APD bias voltage of 55 V, the rise and fall times and pulse width measured from the output of the post-amplifier are 800 ps, 1.2 ns and 1.5 ns, respectively.

The receiver has differential outputs with 50 ohm impedances, one of which, the inverting output feeds the actual measurement signal to the timing discriminator, while the non-inverting output is used for pulse train monitoring with the oscilloscope.

### **4.1.3 Timing discriminator**

As explained earlier, the timing discriminator converts a timing pulse of varying shape and amplitude to a logic pulse that is precisely related in time to the occurrence of a particular event. Time-pickoff circuits can be roughly divided into leading-edge discriminators and constant-fraction discriminators (Kilpelä *et al.* 1998). In a leading-edge discriminator, the timing moment represents the point when the leading edge of the input pulse crosses a fixed threshold level and is consequently a function of the amplitude and rise time of the input signal. In a constant-fraction timing discriminator (CFD), as used in this work, the timing moment is always located at a fractional point of the leading and trailing edges of the input pulse, making it more immune to amplitude variations (Figure 32).

The time-pickoff circuit is realized using a delay cable and a comparator, so that an inverted signal coming from the receiver is fed directly to the negative input of an ultra-fast ECL comparator, while its delayed replica is connected to the positive input, as shown in Figure 32. The slew rate, open loop gain and bandwidth of the comparator are 10 V/ns, 66 dB and 900 MHz, respectively, and it is manufactured by Signal Processing Technologies under the product name SPT9689. The signal from the inverting output of the comparator is taken to a flip-flop circuit, which converts the short timing pulses to standard ECL logic pulses. These are subsequently transferred to an ECL/TTL translator, from which they are finally fed to the time-to-digital converter (TDC).

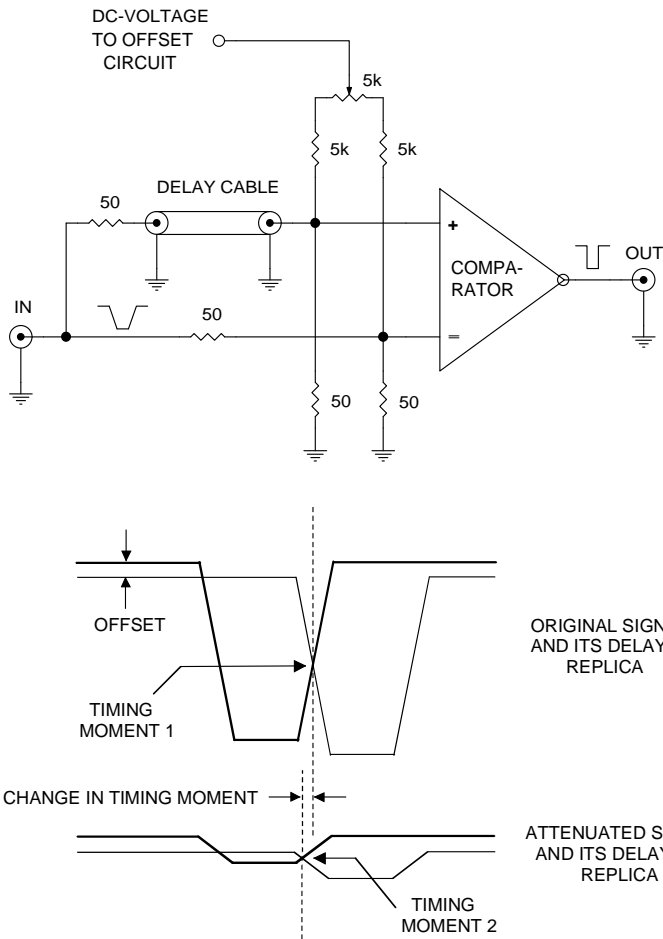


**Fig. 32. Schematic diagram of the constant fraction timing discriminator and a simplified pulse diagram showing the effect of offset voltage on the timing moment.**

The performance of the timing discriminator is measured in terms of three parameters: walk error, drift and timing jitter. Walk error arises mainly from the fact that the propagation delay of the comparator depends on the slew rate and amplitude of the input pulse. It has been established that a higher slew rate results in a smaller propagation delay (Kilpelä *et al.* 1998).

Walk error can be partly compensated for by advancing the timing moment with a small offset voltage connected to the reference input to the comparator, as shown in Figure 32. The optimal offset voltage can be found by measuring the time delay as a function of stop pulse amplitude while the start pulse amplitude

remains constant. Carrying out the measurement for different offset voltages allows a set of walk error curves to be collected, from which the curve with the minimum variation is selected and the offset voltage is adjusted accordingly.

The optimal offset voltage in a CFD is typically in the same range as the noise voltage of the receiver channel, which may lead to false triggers unless an additional noise comparator is used (Kilpelä *et al.* 1998). In the current implementation, however, no noise comparator is needed, since the optimal offset voltage is high enough to prevent the timing comparator from being triggered by noise pulses.

Three walk curves for the TOF measurement system obtained with different offset voltages are illustrated in Figure 33. As shown, the walk error varies from about 0 ps to  $-5$  ps for an offset value of 7.6 mV in a range of about 65–140 mV, while the walk errors at other offset voltages are somewhat larger. Although, according to Figure 33, the optimum amplitude region is slightly different for each offset voltage value, an offset voltage of 7.6 mV still gives the best result. It is worth noting here that the offset voltages given in the chart do not include the inherent offset voltage of the comparator, which is about  $-2.0$  mV at room temperature.

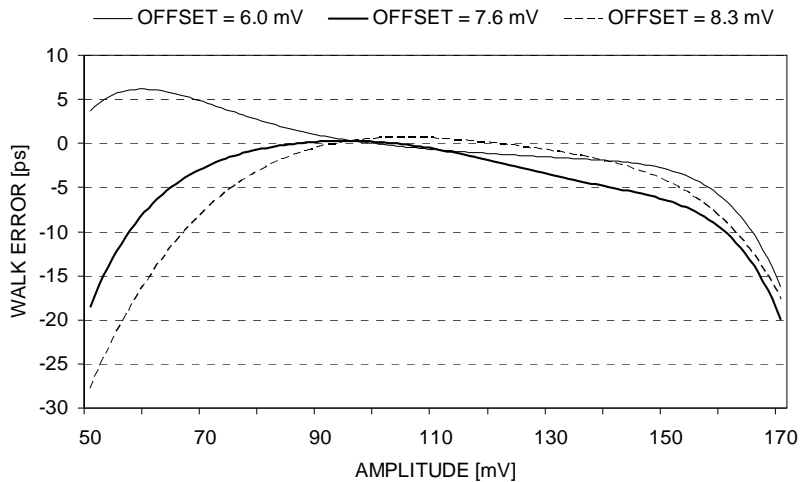


**Fig. 33. Walk error of the TOF measurement system (Paper IX).**

Walk error can usually be cancelled out by means of automatic gain control (AGC), which can be either electrical or optical. The AGC of the present TOF

system is based on controlling the bias voltage of the APD and is designed to keep pulse amplitudes within a few millivolts in the most stable region of the walk curve. This has proved a good technique and produces only a negligible timing error provided that the attenuation arises from a common mode effect such as temperature variation in the photo-detector. This kind of AGC is not fast enough, however, to equalize the amplitudes of closely-spaced single reflection pulses, which may vary due to such effects as microbending. Effects of this type necessitate the use of a time-pickoff circuit with a low walk error that is capable of adapting to two successive pulses with varying amplitudes.

The timing jitter ( $\sigma_t$ ) of the measurement result, which is expressed by means of the term precision, depends on the slew rate and noise of the input pulse, as expressed by (Bertolini 1968)

$$\sigma_t^2 = \frac{\sigma_n^2}{(dV/dt)^2}, \quad (9)$$

in which  $\sigma_n$  is the rms noise at the input to the timing discriminator and  $dV/dt$  is the slew rate of the signal at the timing moment. By substituting the measured values of 0.9 mV and 100 mV/ns, respectively, for the noise voltage and slew rate, a timing jitter of 9 ps is obtained for a single pulse and 12.7 ps for a pair of pulses including start and stop pulses ( $\sigma_t = \sqrt{\sigma_{START}^2 + \sigma_{STOP}^2} \approx 12.7\text{ps}$ ,  $SNR \approx 100$ ). Being a statistical error, timing jitter can be reduced by averaging several successive measurement results.

#### 4.1.4 The time-to-digital converter (TDC)

The time-to-digital converter used in this work is a full-custom ASIC fabricated in a 0.6  $\mu\text{m}$  CMOS process (Mäntyniemi *et al.* 2002a, 2002b, Mäntyniemi 2004). Its block diagram is shown in Figure 34.

The time interval measurement principle of the TDC is based on a synchronous counter and three-stage asynchronous delay-locked delay line interpolation within a clock period. A single 15-bit 50 MHz counter is used to expand the dynamic range of the TDC to several hundred microseconds. The counter digitizes time intervals at a resolution of 20 ns clock cycles. The counter is enabled by the start pulse and its state is sampled by the stop pulses, as shown in Figure 34.

The first, coarse interpolation is based on a 16-bin delay-locked delay line. The timing signals sample the state of the delay line, which represents the moment of arrival of the timing signals within the clock period with a resolution of

1.25 ns (= 20 ns / 16). The coarse interpolator also provides a difference signal proportional to the moment of arrival of the timing signal with respect to the clock phases propagating in the coarse delay line. This difference signal is used as a residue that is digitized with a two-stage 32-bin fine interpolator based on a delay-locked delay difference between delay cells and has an LSB resolution of 39 ps (= 20 ns / 16 / 32). The 24-bit time interval measurement is a combination of 15-bit data from the counter registers and 4-bit and 5-bit data from the interpolators. The three-stage interpolation principle makes it possible to integrate multiple measurement channels with the high interpolation ratio of 512, i.e. how many fractions the clock cycle can be digitized to, on a single chip.

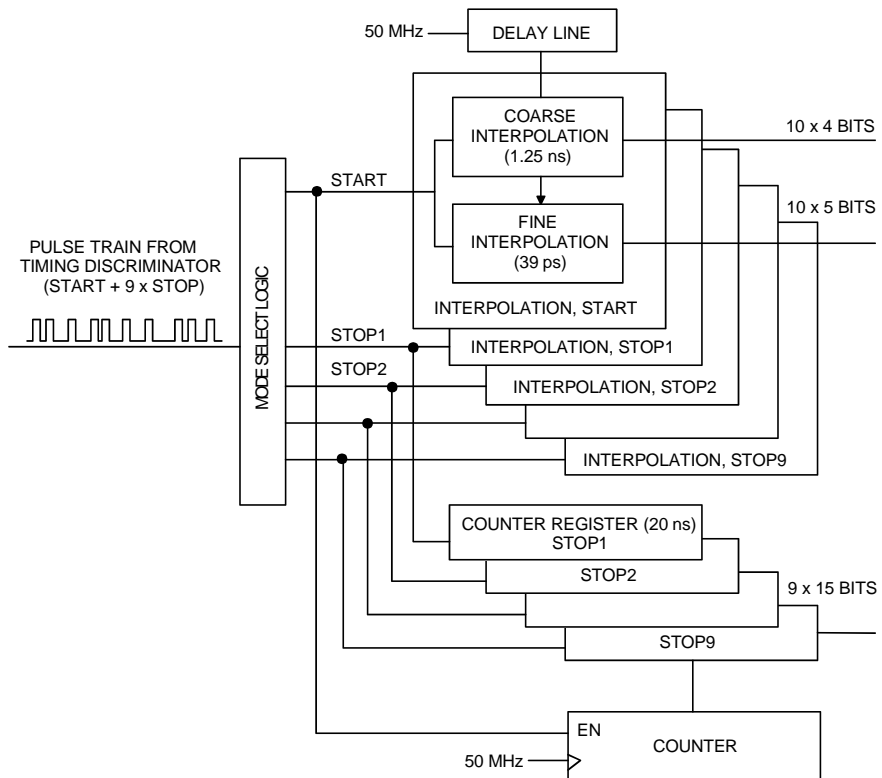


**Fig. 34. Block diagram of the TDC.**

The TDC has two operating modes. It can be used either as a multi-channel TDC with a common start and nine independent stop channels, or it can be used as a single-channel multi-hit TDC with ten multi-hits with a typical double-pulse reso-

lution of 2 ns. The high double-pulse resolution required by the specified spatial resolution of 0.5 m is achieved by utilizing all the measurement channels in the multi-hit mode. The mode select logic of the TDC distributes the timing pulses that appear as a pulse train to the measurement channels, as seen in Figure 34. The moment of arrival of the first timing pulse is measured in the start channel and each subsequent pulse is treated as a stop pulse.

As the LSB resolution of the TDC is 39 ps, its ideal single-shot precision should be  $\leq 0.5 \cdot \text{LSB} = 19.5$  ps, depending on the measured time interval. The rms single-shot precision of the TDC itself should be  $\text{LSB}/\sqrt{6} = 15.9$  ps, because it is limited by the quantization noise of the two digitized timing signals in the time interval measurement. The actual single-shot precision has proved to be somewhat larger than the theoretical value, however, due to the integral nonlinearity (INL) of the interpolators. A comprehensive description of INL and the TDC used has been provided by Mäntyniemi *et al.* (2002a, 2002b) and Mäntyniemi (2004).

## 4.2 Measurements

### 4.2.1 Precision, measurement time and spatial resolution

The precision of the TOF measurement system was studied using a standard single mode telecommunication fibre with an acrylate coating as a sensor. No reference fibre was used in this test. The fibre, measuring 20 m in length, was loosely looped on a test bench to form a 2 m sensor.

Both ends of the fibre were assembled with FC-connectors to produce reflection pulses for the time measurement unit. Having been industrially polished in a modified FC/PC process, the connectors provide adequate reflectivity of about 0.1% and a small loss of 0.2 dB. In contrast to flat-polishing method used earlier PC polishing eliminates interference effects between the ferrules, allowing the pulse amplitudes to remain stable at varying temperatures.

The theoretical single-shot precision of the apparatus is about 20 ps, which can be calculated directly from the corresponding values of the CFD and TDC, assuming that these values are independent ( $\sigma_t = \sqrt{12.7^2 + 15.9^2} \approx 20.3$  ps). This is in reasonable agreement with the measured single-shot precision of about 28 ps (SNR  $\approx 100$ ), since the calculation excludes implementation losses such as INL errors, the effect of which can be quite large (Mäntyniemi *et al.* 2002a, 2002b, Mäntyniemi 2004).

As explained earlier, precision can be improved by averaging a number of measurement results, which improves performance in proportion to  $1/\sqrt{N}$ , where  $N$  is the number of measurements to be averaged. If  $N = 10\,000$ , for example, the standard deviation will be 0.28 ps, which in a 20 m sensor fibre corresponds to about 1.8  $\mu\epsilon$ , according to Equation (8). On the other hand, if  $N = 100$ , the standard deviation will be 2.8 ps or 18  $\mu\epsilon$ . These figures match well with the results achieved in practical measurements.

Equation (8) also indicates that the strain precision can be further improved by increasing the fibre length. This is an attractive method, because it enables a certain precision level to be achieved with a smaller number of measurements. As a result, the overall measurement time will be shorter.

The measurement time depends directly on the number of measurements used for averaging. With  $N = 10\,000$ , as above, the maximum pulsing frequency of 400 kHz results in a measurement time of 25 ms and a sampling rate of 40 Hz. When  $N = 100$ , the measurement time is considerably shorter, 0.25 ms, corresponding to a sampling rate of 4000 Hz.

Spatial resolution was studied by cutting a sensor fibre until the measurement system stopped working. The start pulse was taken from the output of a fused-type fibre coupler with a port configuration of  $1 \times 2$  and a coupling ratio of 50/50, while the other output was connected to the test fibre, the end of which served as the stop pulse. The measured minimum time delay was about 3 ns, corresponding to a fibre length of about 30 cm.

#### **4.2.2 Stability**

Drift refers to a deflection from the zero point produced e.g. by temperature changes and component ageing. Long-term measurements in particular use drift as an indicator of system stability. In commercial fibre-optic measurement systems such as low-coherence interferometer and Bragg grating systems, drift is usually minimized by means of a reference fibre or grating. The method is very simple: subtracting the result obtained with the sensor fibre from that of a reference fibre of equal length gives a measurement result which is free of most common-mode errors originating from the instrument and sensor.

The good stability of the TOF measurement system developed here is derived from the following factors: use of a reference fibre, continuous amplitude control, stable reflectors, complete single-channel operation, unsynchronized laser pulsing

with respect to the time clock, high measurement speed, averaging and a software filter.

As explained earlier, the reference fibre is connected in series with the sensor fibre by means of connectors which produce three timing pulses for the time-measurement unit. To minimize walk error, the peak voltage amplitudes of the pulses are continuously monitored and adjusted if necessary to the most stable region of the walk error curve, which is about 100 mV. The voltage amplitudes are adjusted by controlling the APD bias voltage, which is common to all three pulses in a sensor. When a number of sensors are connected in series, each sensor/reference pair has its own APD voltage within a range of about 40–60 V, corresponding to a dynamic range of about 3.5 / 1.

Good stability requires that all the timing pulses, both optical and electrical, should have a common signal path. The current TDC circuit does not support this kind of operation, however, since it divides each pulse into a separate TDC channel, as explained in Section 4.1.4. This problem can be overcome by making two separate measurements, one for the sensor fibre and another for the reference fibre. When measuring the reference fibre, the operation of the TDC must be disabled until the reference pulses arrive at the receiver. This disabling procedure, which is based on counting the timing pulses, is also used for separating the sensor/reference pairs from each other.

It is generally known that the results in a measurement system based on averaging should be uncorrelated (Reed 1964). This means in a TDC-based time measurement system that triggering of the probe pulse should not be synchronized with the clock oscillator used for time measurement. If the oscillators are synchronized, timing hits accumulate within particular interpolator channels, producing a non-Gaussian measurement distribution. As a result, the averaging procedure fails to achieve the full gain. This problem exists even if different oscillators and frequencies are used in the time-measurement circuit and the processor which controls the laser pulser. This is due to the fact that clock frequencies drift with respect to each other and become synchronized at a certain frequency for a length of time that depends on factors such as frequency difference, temperature, etc. The problem has been solved in the TOF system described here by introducing a jitter into the laser pulsing with the aid of a wide-band noise circuit with a frequency range filtered to about 5 MHz–15 MHz. Also included in the jitter circuit is an RC oscillator ( $f = 5$  MHz), which forces the probe pulses to be sent within a certain time window, thereby preventing unexpected measurement de-

lays. The jitter achieved is about one hundred nanoseconds in time scale, which far exceeds the clock cycle period of the TDC.

High measurement speed enhances stability, because it allows high-speed switching between the sensor and reference fibre, thereby enabling even dynamic common mode errors to be eliminated. A software filter, on the other hand, improves stability by removing results that fall outside the acceptable distribution range due to a noise trigger, for example.

The stability of the TOF measurement system was studied by means of a temperature chamber which allowed the temperature of the measurement device to be altered, while the sensor and reference fibres remained at room temperature. The fibres, with a length of 30 m, were loosely assembled on the same test bench in an identical manner, to ensure that they were exactly at the same temperature. This is extremely important in TOF measurement, since a temperature change can greatly affect the refractive index of a fibre and thus the resulting measurement. A round-trip delay change of  $2.3 \text{ ps} / ^\circ\text{C}$ , for example, has been measured with an acrylate-coated fibre of length 30 m. The drift observed in the TOF system developed here is present in Figure 35 as a function of time and temperature in a measurement that lasted about 14 hours.

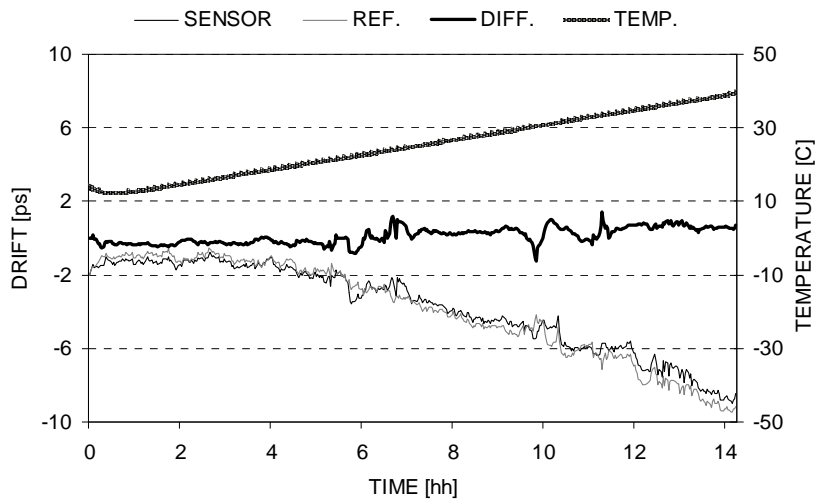


**Fig. 35. Drift of the TOF measurement system as a function of time and device temperature (Paper IX).**

During this measurement the temperature within the chamber was changed linearly in the range of +10 °C ... +40 °C. As the figure clearly indicates, the sensor and reference fibres exhibit similar behaviour, and a considerable improvement in stability takes place when the common mode effects are eliminated. Hence the peak-to-peak variations in the sensor and reference fibres are roughly 9 ps, while that of the difference curve is only about 3 ps. The changes in the sensor and reference curves are largely caused by the temperature drift in the TDC, which is of the order of 0.2 ps / °C (Mäntyniemi 2004). Part of the small variation in the difference curve may be explained by walk error, since amplitudes tend to change continuously as a function of temperature. Although this effect is compensated for by changing the bias voltage, there is a certain range, of the order of a few millivolts, within which an amplitude change is accepted. This is a necessary precaution that prevents the control loop from oscillating.

It should be noted that the device temperature is fairly stable under normal circumstances and the amount of drift is considerably less. For example, using a similar fibre to the above a peak-to-peak variation of about 0.3 ps has been achieved at room temperature in an experiment that lasted over 2 days and used an average number of 10 million.

The effects of polarization on the stability of the TOF system were also studied under laboratory conditions. It was assumed that random changes in polarization state due to temperature changes or mechanical loading of the fibre, for example, may affect the pulse shape or amplitude, causing a measurement error. Polarization effects were examined by controlled bending of an interconnection cable ( $\phi = 3$  mm) placed between the sensor and the TOF device with a radius range large enough not to introduce microbending into the fibre. For comparison, the measurement was carried out in two ways: with and without a polarization scrambler. The optical properties of the polarization scrambler, i.e. the length of the polarization-preserving fibre, were matched by the manufacturer with the spectrum of the laser diode used in the TOF system. In this test the polarization scrambler was connected close to the receiver.

The measurements were designed to study changes in time delay and amplitude in relation to the bending radius. Small amplitude changes of the order of a few millivolts were measured repeatedly without the polarization scrambler, but this effect was never observed with a polarization scrambler. Although the measured time delay did not change in either case, the test proves that pulse amplitudes are subject to polarization changes within fibres. Potential walk error can nevertheless be filtered with an adequate polarization scrambler.

### 4.2.3 Dynamic range and sensor networks

The maximum number of reflectors ( $N_{MAX}$ ) and sensors in a fibre can be calculated from the optical power range of the measurement system and the reflectivity and transmission loss of the reflector, using the formulae

$$\begin{aligned}
 OPR &= 2 \cdot (N_{MAX} - 1) \cdot A + B \\
 \rightarrow N_{MAX} &= (OPR + 2A - B) / 2A; \\
 A &= 10 \cdot |\log(100 - R) / 100| + ATTN; \\
 B &= 10 \cdot |\log(R / 100)|;
 \end{aligned}
 \tag{10}$$

where  $OPR$  is the optical power range of the measurement system, i.e. the difference between the pulse power sent into the fibre ( $\approx +10$  dBm) and the minimum detectable power level of the receiver ( $\approx -30$  dBm) that gives a signal-to-noise ratio (SNR) of 10,  $A$  is the transmission loss,  $B$  the reflection loss and  $R$  the reflectivity of the reflector (Figure 36).  $ATTN$  represents an extra loss in the reflector, in addition to the transmission loss, when a fibre connector is used.

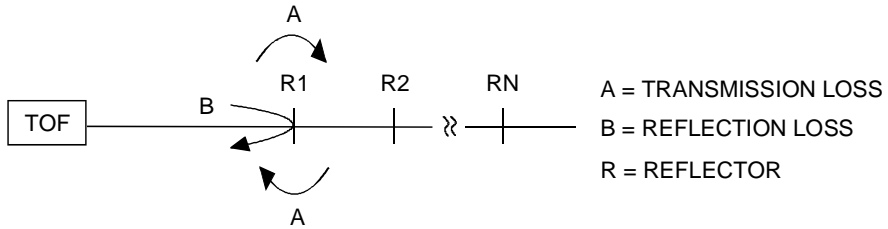


**Fig. 36. Transmission and reflection losses in a sensor fibre.**

A typical fibre connector used in the TOF system has a reflectivity ( $R$ ) and attenuation ( $ATTN$ ) of about 0.1% and 0.2 dB, respectively, giving 30 dB for reflection loss ( $B$ ) and 0.204 dB for transmission loss ( $A$ ). Substituting these figures into Equation (10) together with the optical power range ( $OPR$ ) of about 40 dB, we obtain a figure of 25 for  $N_{MAX}$ . Thus the maximum number of sensors is 8, since each sensor/reference pair needs 3 reflectors, as discussed earlier.

The sensor number can be considerably increased by using a reflector with no inherent loss ( $ATTN \approx 0$ ), such as a wideband Bragg grating, as tested in Paper VII. Using the above figures and 1% for reflectivity ( $R$ ), we obtain 0.04 dB for  $A$ , 20 dB for  $B$ , and 251 for  $N_{MAX}$ , which corresponds to 83 sensors. This is good enough for many sensing applications, but if a more comprehensive system is needed a fibre optic switch can be used.

It is worth noting here that, due to the limited dynamic range of the system's electrical AGC ( $\approx 3.5/1$ ), the use of a large number of sensors prevents some reflection pulses from being adjusted to the optimal voltage level of the walk curve. This is not a fundamental problem, however, since successive reflection pulses with approximately similar amplitudes have a common mode walk behaviour which cancels out the main part of this error without any amplitude control. On the other hand, gain control can also be performed with a device allowing a much larger adjustment range, such as a MEMS-type fibre-optic attenuator having a typical attenuation range of 30 dB (1000 /1).

**4.2.4 Measurement of strain in a bridge deck using long gauge-length TOF sensors**

A time-typical concrete-reinforced bridge built in 1958 was selected as the target for monitoring with the high precision TOF measurement system developed here (Figures 37 and 40). Located on highway E8 between Oulu and Raahe in Finland, the bridge crosses the River Siikajoki at Revonlahti. With a length of 90 m and a width of 15 m, the bridge has four openings, two traffic lanes and a separate bicycle lane built afterwards.

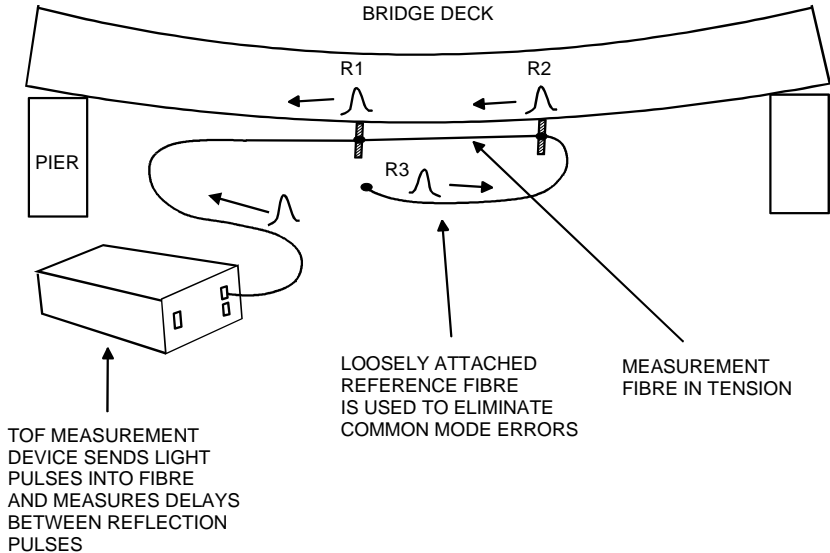


**Fig. 37. Principle of bridge measurement using long gauge-length TOF sensors.**

The shape of the bridge deck has undergone considerable changes over the years, and there are numerous visible cracks in the coating as well. An impending renovation will seek to restore its shape using a post-tensioning method. For the present study, several long gauge-length TOF sensors and reference devices were installed under the bridge deck to produce longitudinal strain information, as presented in Figure 37. A set of measurements will be carried out not only before and after the renovation, but also during the post-tensioning process.

### *Long gauge-length TOF sensors*

A long gauge-length TOF sensor used in the bridge measurement consists of optical fibres, a protective plastic tube and two mounting boxes, as shown in Figure 38. The plastic tube includes two fibres: a strain fibre and a reference fibre, which are connected in series by means of fibre optic connectors. Of the two fibres, the strain fibre is in tension, while the reference fibre is loosely coupled. Essentially, the reference fibre is used to eliminate common mode errors such as the effects of temperature on the refractive index. A typical gauge length is 2 m, but the figure may range from about 0.50 m up to 100 m or beyond, depending on the application.

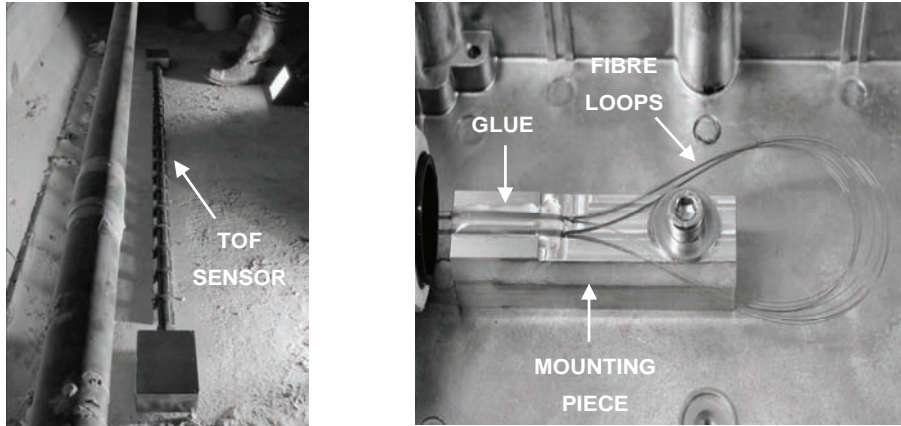


**Fig. 38. (Left) Photograph of a long gauge-length TOF sensor. (Right) Inside view of a mounting box.**

The fibre used is a standard single mode fibre with a polyimide coating that is attached with Loctite Hysol 9481 glue to an aluminium mounting piece with separate grooves for the strain and reference fibres, as seen in Fig. 38. The height of the mounting piece is such that the egress of the fibres is exactly in the middle of the plastic tube. This is done to avoid contact between the tube and the strain fibre, which may cause errors. There is a screw located in the mounting piece for attaching the sensor to the structure to be measured.

The long gauge-length TOF sensor measures the integral strain between attachment points, making the precision of the measurements directly proportional to the gauge length. Use of a fixed gauge length allows precision to be improved by coiling the excess fibre between the attachment points so that several fibre loops are subject to tension. Precision is then directly improved in relation to the number of loops. This fibre loop structure is also shown in Figure 38.

### *Calibration tests*

All the sensors installed on the bridge were calibrated on a test bench which enabled accurate alteration of the fibre length by means of a stepping motor. Each sensor measuring 2 m in length contained 5 loops of the strain and reference fibres. For comparison, one TOF sensor tube contained two commercial fibre Bragg gratings (FBG), one for measuring strain and the other for reference. The FBGs were assembled in the middle of the sensor tube and attached by their fibre pigtailed in the same way as the TOF strain and reference fibres, so that the distance between the gratings and the attachment point was about 1 m in both directions. This manner of assembly allows integral elongation to be measured with a point-type sensor such as an FBG, provided that strain is homogeneously distributed along the fibre path and that the fibre can move freely between the attachment points.

Calibration was based on measuring the primary strain response, i.e. the change in the time delay of the TOF sensor and wavelength of the FBG, and deriving the correct calibration coefficients from the results. It was assumed that the test bench is stable and that the movement of the stepping motor is extremely precise. The FBG results were measured using a Micron Optics' interrogation device FBG-IS Version 3, which has a precision of  $\pm 5 \mu\epsilon$  (rms value). The stepping motor, Model CMA-25PP manufactured by Newport, offers minimum incremental motion and bi-directional repeatability of  $0.3 \mu\text{m}$  and  $4 \mu\text{m}$ , respectively. The amount of pre-elongation in the calibration measurement was 0.5%, the elonga-

tion step was 50  $\mu\text{m}$  and the elongation range 0–1000  $\mu\text{m}$ , indicating that the maximum strain with a sensor length of 2 m was 500  $\mu\text{e}$  relative to the bias-point (Figure 39).

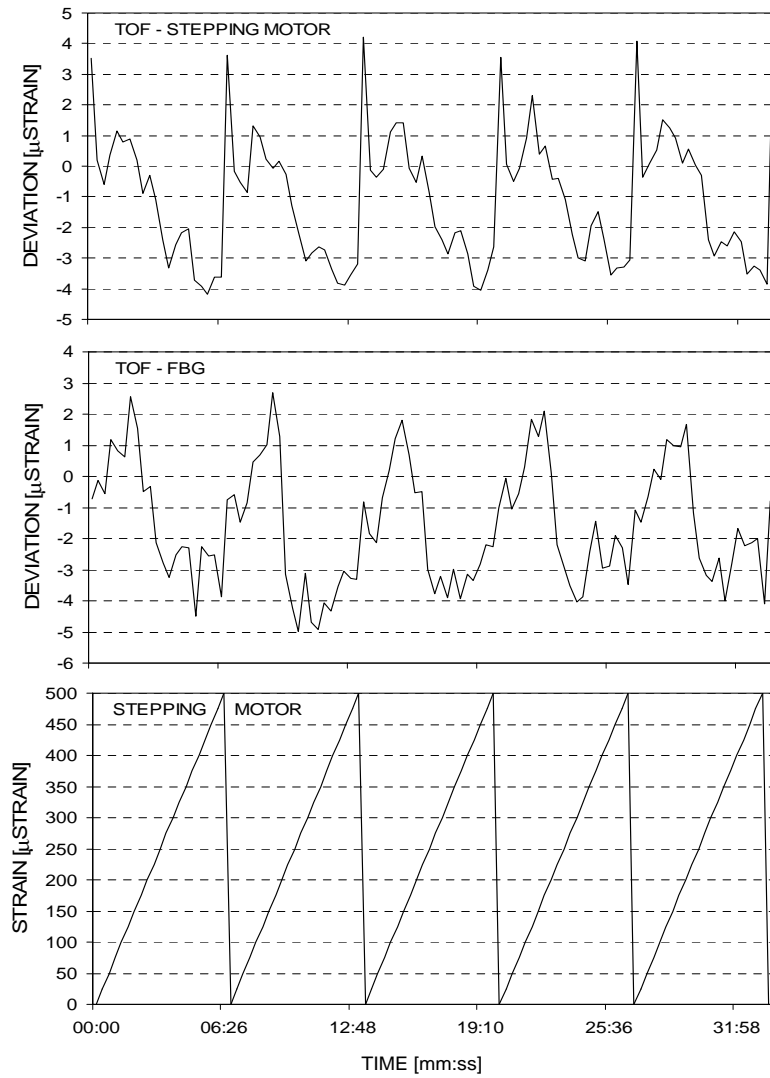


**Fig. 39.** Deviation of the TOF sensor results from the reference stepping motor and FBG sensor after calibration.

The measurements established that the response of the FBG sensor is linear in this elongation range, while the response of the TOF sensor is slightly non-linear, especially in the high strain region. Imperfect sensor design was a possible cause of this phenomenon but it was not studied in detail because such a high strain was not expected in this particular application, and because its effect could be calibrated out with an appropriate formula. The deviation of the TOF sensor from the reference stepping motor and the FBG using the defined calibration factors is shown in Figure 39. Also indicated in Fig. 39 is the position of the stepping motor (converted to  $\mu\text{Strain}$ ), showing five linear elongation cycles during an experiment that lasted about half an hour.

As the measurements show, the maximum deviation of the TOF sensor relative to the stepping motor is less than  $\pm 1\%$  ( $4.0 \mu\epsilon / 500 \mu\epsilon \cdot 100\% = 0.80\%$ ) while a comparison between the TOF and FBG produces a similar result within a difference of less than  $\pm 5 \mu\epsilon$ . Moreover, a study of successive elongation cycles reveals that the difference curve of the TOF sensor and the stepping motor is almost symmetrical. One may therefore deduce that the precision of the measurements can be slightly improved by changing the calibration formula or using a correction table.

### *Bridge measurements*

Four TOF sensors, a pair of FBGs and one temperature sensor were installed on the bridge. A transmitter-type temperature sensor (MKTS / Pt100) manufactured by Müller and offering a precision of  $0.2 \text{ }^\circ\text{C}$  was installed in the concrete inside the bridge to produce reference information. Three long gauge-length TOF sensors, one of them including the FBGs, were attached to the underside of the bridge deck along its longitudinal axis, so that sensors were located in the middle of the first and second openings (Fig. 40). In addition, one TOF sensor was attached on the edge of the bridge deck close to the first pier, in a spot with several surface cracks, against which the sensor was orthogonally installed (not shown in the figure).

The mounting boxes of the TOF sensors were attached to the bridge by means of stainless wedge anchors ( $\phi = 10 \text{ mm}$ ,  $l = 10 \text{ cm}$ ), one of which was needed at each end. To allow for pre-elongation ( $\epsilon = 0.5\%$ ), the distance between the anchor points was about  $1 \text{ cm}$  longer than the actual sensor length ( $2 \text{ m}$ ). Before attaching the sensors, stainless metal plates were glued to the concrete with HIT HY-150, manufactured by Hilti, to enable flat surface attachment.

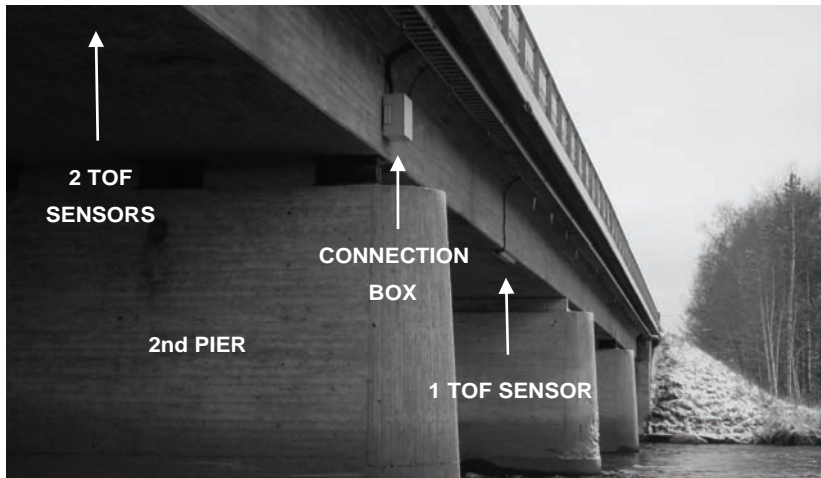


**Fig. 40. Photograph of the measured bridge.**

Both dynamic and static strains were of interest in the actual measurements. Dynamic strain is usually caused by traffic loading, whereas static strain is induced by temperature changes. A result recorded by a TOF sensor, when a truck crossed the bridge is shown in Figure 41.

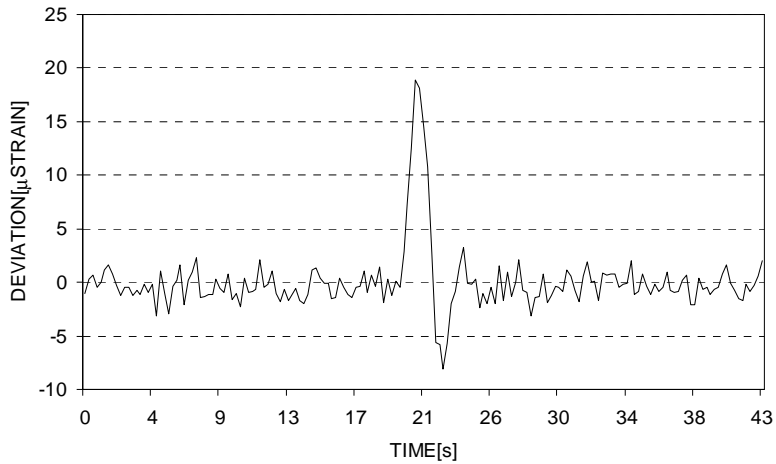


**Fig. 41. Strain in the bridge deck upon traffic loading. TOF measurement curve (Paper IX).**

As the driving time between the piers, spaced 20 m apart, is about one second at 60 km/h, the sampling frequency of the measurement system, in agreement with the Nyquist criterion, must exceed 2 Hz when measuring dynamic effects. To improve the dynamic margin, a sampling frequency of 4 Hz was used, corresponding to a maximum averaging number of 100 000 at a pulsing frequency of 400 kHz. This enabled a precision of 90 fs to be achieved which, according to Equation (8), corresponds to about 0.6  $\mu\epsilon$ .

As shown in Figure 41, the maximum strain for the truck is about 18  $\mu\epsilon$  and the averaged precision is roughly 0.8  $\mu\epsilon$  (rms value), derived from the peak-to-peak noise of about 5  $\mu\epsilon$  ( $5 \mu\epsilon / 6 \approx 0.83 \mu\epsilon$ ), which is in reasonable agreement with the value calculated above and the result measured by the FBG.

The results obtained with the TOF sensor and FBG are compared in Figure 42 with the thermal elongation of the bridge deck derived from the measured temperature using a coefficient of 12  $\mu\epsilon / ^\circ\text{C}$  for concrete. The measurements were carried out for more than three weeks at a sampling rate of 1 minute using ten million single shot measurements for each TOF sample.

Comparison with the calculated thermal elongation curve shows that, although the trends are nearly identical, the measured responses are slower and their amplitudes are smaller. This can be partly explained by temperature differences between the location of the temperature sensor and the locations of the optical fibre sensors. Alternatively, the observed difference may also be produced by a temperature difference between the reference and sensor fibres, caused by the fact that the loose reference fibres were in touch with the internal surface of the plastic tube, the temperature of which almost exactly follows the outside temperature, while the elongated sensor fibre is subject to slower temperature changes. Finally, the observed difference may also be produced by the existence of a crack between the attachment points.

A close look at the measured curves reveals that the curves measured by the TOF sensor and the FBG during the first 12 days were almost identical, with the maximum difference well below 10  $\mu\epsilon$ . After that the curves are still quite similar in shape, but they gradually diverge from each other so that there is a maximum offset of about 20  $\mu\epsilon$ . This phenomenon has not been studied in detail, but it is possible that the reference fibre, in either the FBG or TOF case or both, occasionally attaches to the internal surface of the sensor tube or the actual sensor fibre, which causes tension in the reference fibre and thus leads to crosstalk errors.

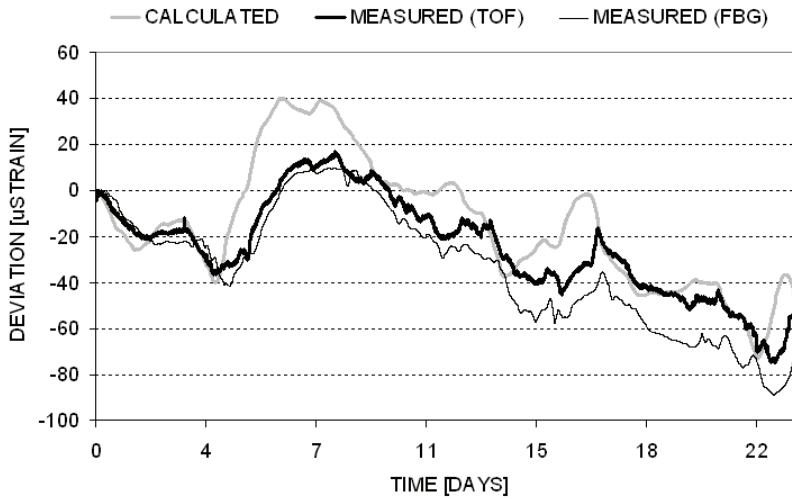


**Fig. 42. Thermal elongation of the bridge deck. Measurement curves from the TOF and FBG sensors and calculated model (Paper IX).**

### **4.3 Comparison of the TOF measurement system with commercial devices**

In this section the performance of the TOF device developed here will be compared with that of commercial fibre-optic strain measurement systems. The comparison may not be quite relevant in every aspect, as the information shown in Table 1 has been collected from the website of various manufacturers who may have tested their products in different ways and under different conditions. As there are a number of interrogation devices and sensors for this wide application area, no exact performance parameters are given, but only some figures that are representative of the technology.

It is in general difficult to rate measurement systems, as they may vary considerably in their operation principles and fields of application. The principal difference between the systems lay in the sensor length, which can range from a few millimetres in an FBG system up to tens of metres in a low-coherence interferometer. As the TOF measurement system is integral in nature, it can be directly compared only with the microbending system, low-coherence interferometer, high-resolution OTDR and BOTDA system.

**Table 1. Comparison of fibre-optic strain measurement systems.**

	FBG system <sup>1</sup>	EFPI System <sup>2</sup>	Micro-bending system <sup>3</sup>	BOTDA System <sup>4</sup>	Low coherence interferometer <sup>5</sup>	High-resolution OTDR <sup>6</sup>	TOF system
Precision [ $\mu\epsilon$ ]	< 0.3	< 0.3	1	10	1	6/60 <sup>(7,8)</sup>	1/10 <sup>(8)</sup>
Sampling rate [Hz]	> 100	> 10	< 100	DC	DC	DC	> 5 <sup>(9)</sup>
Gauge length [m]	0.01–2	0.01–0.1	0.1–10	0.5–20	0.2–20	0.1–100	0.3–100
Serial sensors	10–100	1	1	> 10000	1	> 10	> 10
Point/integral	point	point	integral	int./distr.	integral	integral	integral
Device cost	low	low	low	high	medium	medium	low <sup>(10)</sup>

<sup>1</sup> Micron Optics: [www.micronoptics.com](http://www.micronoptics.com)

<sup>2</sup> FISO Technologies: [www.fiso.com](http://www.fiso.com)

<sup>3</sup> OSMOS: [www.osmos-group.com](http://www.osmos-group.com)

<sup>4</sup> Omnisens: [www.omnisens.ch](http://www.omnisens.ch)

<sup>5</sup> Smartec: [www.smartec.ch](http://www.smartec.ch)

<sup>6</sup> Opto-Electronics: manufacturer changed, see [www.tempo-textron.com](http://www.tempo-textron.com) (model OFM20)

<sup>7</sup> calculated from time measurement resolution of 1 ps

<sup>8</sup> with fibre length of 20m / 2m

<sup>9</sup> for 1 sensor at a time

<sup>10</sup> estimated from manufacturing cost

Comparison with the low-coherence interferometer and microbending system shows that the precision and gauge-length are almost equal in all these approaches. The sampling rate of about 5 Hz in the TOF system clearly exceeds that of the interferometer, which only allows DC-type measurement, but is considerably less than 100 Hz characteristic of a microbending system. Of these three measurement systems, only the TOF device allows serial multiplexing.

It is apparent that the performance of the TOF system is better than that of a BOTDA system in terms of measurement speed and precision, but the multiplexing capability of a truly distributed BOTDA system with thousands of serial sensors is incomparably better than that of the TOF system or any other measurement method.

Since the operation of a high-resolution OTDR is based on time interval measurement, its area of application is similar to that of the TOF measurement system developed here. Although parameters such as gauge-length and number of sensors are almost equal, a closer look at the table reveals that the measurement speed and precision of the TOF system are an order of magnitude better than those of the OTDR.

The gauge-length of a point-type FBG and external Fabry-Perot interferometric sensor (EFPI) can be enlarged with a suitable package. Such sensors are commercially available from Micron Optics and Fiso Technologies, for example. Comparison between the FBG and TOF systems shows that the performance of

the FBG system is better in terms of precision, measurement speed and number of sensors, but the truly integrating TOF system offers a wider range of gauge-lengths extending up to 100 m or beyond, including sensor arrays with a curved shape, which is not possible with a basically point-type FBG approach.

The speed and precision of an EFPI measurement system are also better than those of the TOF system, but the latter offers a higher multiplexing capability than a basically single-channel EFPI system and allows the measurement of longer sensor fibres.

As the TOF measurement system developed here is not a commercial product, it is not relevant to give exact price information in Table 1 but only relative accounts for categorizing the sensing technologies. As a general rule a measurement system that allows serial multiplexing is a good choice in terms of cost per sensor and ease of installation. In this sense the TOF system is a potential alternative for intrinsically single-channel measurement approaches, while its use of a standard single mode fibre as a sensor makes it more attractive than an FBG system, for instance.

In conclusion, the TOF measurement system developed here is a real alternative to the established fibre-optic measurement technologies. When comparing technologies, it should also be noted that, apart from the FBG system, the TOF device is the only alternative that allows serial multiplexing at reasonable cost.

The most outstanding benefit of the TOF system, however, is its capability for measuring integral changes with serial-type, long gauge-length sensors, including ones that are embedded in a composite structure, which is otherwise only possible with a BOTDA device. One potential area of application for such measurements is comprehensive crack monitoring e.g. in FRP composite blades and ropes. As a cost-effective alternative, the TOF measurement system may nevertheless be of wider interest, particularly for static measurement applications.

## 5 Discussion

This thesis deals with the development of microbending sensors and their testing in various field applications. It also covers the development of fibre-optic TOF interrogation systems and their applications.

As regards the microbending approach, strain in a road structure could not be reliably measured even though the microbending sensor based on a pin structure showed a repeatable response with a reasonable precision of about  $100\ \mu\epsilon$  under laboratory conditions. As the measurement errors were mostly attributed to poor sensor design and a low signal-to-noise ratio in OTDR measurements, it is obvious that modifying the sensor structure would allow an adequate strain precision to be achieved even in harsh environments.

In another road experiment a measurement system based on an optical through-power technique and a continuous microbending sensor as well as the speckle sensor was found useful for producing on/off-type information for traffic monitoring applications such as traffic counts and the control of traffic lights. As simple measurement systems, they may also have potential for wider areas of application. The use of a thin, flexible telecommunication cable as a sensor makes the speckle approach in particular an interesting measurement system the potential of which warrants further investigation.

It was also observed that standard telecommunication fibres can be embedded inside FRP composite containers during the filament winding process. The fact that they form a continuous microbending structure with the surrounding glass matrix makes thin acrylate-coated fibres in particular capable of indicating the state of cure during manufacture and the health of the structure during the service life. These are important issues, as uncertainty regarding their material properties is a significant barrier to the wider acceptance of composite structures.

Several versions of the pulsed time-of-flight (TOF) measurement system were developed for interrogating a sensor network consisting of multiple long gauge-length strain sensors. A novice TOF system based mainly on commercial electronics was comprehensively tested under laboratory conditions, indicating that the best strain precision of about  $100\ \mu\epsilon$  can be achieved with a polyimide-coated sensor. The experiments showed that the novice TOF system could produce relevant strain information on optical cables and composite specimens under laboratory conditions, but that it suffered from poor stability, poor spatial resolution and low measurement speed, which made it unsuitable for field measurements.

The high-precision, TOF measurement system developed as part of the present work is capable of measuring both dynamic and static strains with a precision and measurement speed adequate for studying such phenomena as the behaviour of a bridge deck. Achieving an averaged precision that is better than  $1 \mu\epsilon$ , as demonstrated in laboratory and field measurements, the system is comparable to established fibre-optic measurement systems, such as the low-coherence interferometer and the microbending system. With a sampling rate of a few hertz, however, it is not as fast as a typical FBG or microbending system. Nonetheless, the measurement frequency exceeds that of an interferometer or a BOTDA system, the sampling rate of which is of the order of several seconds up to several minutes. In terms of the number of multiplexed sensors, the TOF system is comparable to a typical FBG system, and its ability to read tens of sensors in series makes it an attractive alternative to a low-coherence interferometer or microbending system, which are single-channel in nature. With a wide range of sensor lengths (0.3–100 m), the TOF system can be compared to a BOTDA or a low-coherence interferometer.

In view of the anomalies between the measurement curves of TOF and FBG sensors and the calculated thermal expansion of the bridge, it is difficult to estimate the long-term accuracy of the TOF measurement system developed here. The greatest challenge for the future will be to find out all the phenomena which affect its stability. The differing temperature and strain behaviour of the refractive indices of differently biased sensor and reference fibres is one possible error source. The main problem with the sensor centres on designing a structure that guarantees an equal temperature distribution over the sensor and reference fibres and avoids contact between the two. The slightly non-linear behaviour observed in the calibration measurement should also be studied further.

As for the measurement device, it suffers from a somewhat low signal-to-noise ratio in dynamic measurements, although the noise can be reduced considerably by using a time measurement circuit with a single-shot precision exceeding that of the existing system. With the aid of state-of-the art TDC technology (Jansson *et al.* 2006) the single-shot precision can be improved from about 30 ps to 15 ps, which means that a quarter of the number of measurements would need to be averaged to achieve a given precision ( $30\text{ps}/\sqrt{N} = 15\text{ps} \rightarrow N = 4$ ). Furthermore, by replacing the existing FPGA circuit with a faster commercial-available component, it would be possible to accelerate the reading procedure by a factor of about 2–3. The combined effects of these two factors offer about a 10-fold improvement in the measurement speed.

In conclusion, the TOF measurement system developed here can best be applied to the monitoring of large structures such as bridges and dams where both dynamic and static strains and their derivatives such as cracks, deflections and displacements are to be measured at many locations. It might also be an attractive tool for the composites industry and for end-users who may find its ability to measure multiple integral sensors useful for investigating delaminations, for example. As a cost-effective alternative, this fibre-optic TOF measurement system may also arouse wider interest e.g. in the safeguard applications where it could be used as an intrusion alarm for fences. Additionally, TOF measurement system may have potential in the optical telecommunication, where it could be used for determining dispersion, refractive index and other optical parameters as well.



## 6 Summary

This thesis focused on the developing of fibre-optic time-of-flight and amplitude-based measurement systems for structural monitoring. The sensors and interrogation devices developed in the course of the work were used for studying dynamic and static phenomena in various road structures, concrete bridges and fibre-reinforced containers and other composite specimens.

Strain in a steel mesh used for reinforcing a frost-susceptible road structure was studied with microbending sensors consisting of a pin structure and a polyimide-coated multi-mode or single mode fibre. Using a gauge-length of about 10 cm and a commercial time domain reflectometer (OTDR) in a quasi-distributed fashion, it was shown that the responses of the optical fibre sensors were similar in shape to those of commercial strain gauges, but that the absolute measurement values typically deviated by several tens of per cent, which was attributed to the low dynamic range, crosstalk between the multi-mode sensors and the poor signal-to-noise ratio of an OTDR.

In another road experiment continuous microbending and speckle sensors were found useful for providing on/off-type information for traffic control.

In a study of composite containers the aim was to develop a continuous monitoring system for evaluating the state of cure during the manufacturing process. It was assumed that this information would be useful in terms of yield and product quality. The industrial partner was also interested in monitoring delaminations due to external loading during service life.

Standard multi-mode and single mode fibres with different nylon and acrylate coatings were used as sensors in conjunction with optical through-power techniques and OTDRs. Fibres with a typical length of a few hundreds of metres were embedded inside the walls of containers during the normal filament winding process. The experiment showed that the curing process can be monitored by measuring changes in the through-power. It also became apparent that the location of external damage can be determined with a distributed optical fibre sensor and an OTDR. The best results in this experiment were achieved with thin acrylate-coated fibres.

Several versions of the pulsed time-of-flight (TOF) measurement system were developed for interrogating arrays of multiple long gauge-length sensors. The first version, based on the electronics used in commercial rangefinders, had a precision below 100  $\mu\text{m}$  (1 ps), which was found adequate for measuring strain in an optical cable or in a composite plate, but it suffered from poor stability, poor

spatial resolution and a low sampling rate, which made it unsuitable for most practical measurements.

The next version had a much higher bandwidth and made use of a new TDC circuit implemented on a CMOS chip. The spatial resolution of this new system was an order of magnitude better, about 0.3 m, compared with 5 m in the earlier system, and the single-shot precision was also improved by a factor of two, from about 60 ps to 30 ps.

The most recent measurement system is a modification of the high-bandwidth version mentioned above. The main difference is that the reading procedure of the TDC is realized by a programmable FPGA circuit instead of the much slower computer used in earlier versions. In addition, the system provides continuous amplitude control, which together with a reference fibre has led to a considerable improvement in stability.

The performance of the existing TOF measurement system was tested on a highway bridge near Oulu, Finland, using longitudinal sensors attached under the bridge deck. Using a sensor and reference fibre with a gauge-length of 2 m and 5 fibre loops, a strain precision of less than  $1 \mu\epsilon$  and a measurement frequency of 4 Hz could be achieved, which proved adequate for detecting passing trucks. The response of the TOF system in a static measurement situation was similar in shape to that of a commercial FBG measurement system, despite a slightly varying offset between the measurement curves. The difference in the results was attributed to possible mechanical crosstalk between the sensor and reference fibres in either the FBG or the TOF sensor.

Results achieved in numerous laboratory and field tests indicate that the performance of the fibre-optic TOF measurement system developed here is comparable to that of other interrogation systems such as a low-coherence interferometer, a microbending system and the FBG system. Comparison with other transit time-based measurement systems shows that the results achieved in this thesis far exceed the performance of all the earlier fibre-optic TOF systems used for structural monitoring.

As a truly integrating measurement approach, this TOF system is also a potential candidate for the commercial market. The fact that it allows static and dynamic measurements of multiple long gauge-length sensors, including ones embedded inside an FRP composite structure, makes the TOF system unique among measurement approaches. Such an ability makes it an attractive tool for the composite industry, but as a cost-effective alternative, it may also arouse wider interest, e.g. in the safeguard and telecommunication applications.

## References

- Alavie A, Maaskant R, Stubbe R, Othonos A, Ohn M, Sahlgren B & Measures R (1995) Characteristics of fiber grating sensors and their relation to manufacturing techniques. *Proc SPIE* 2444: 528–535.
- Bakis C, Bank L, Brown V, Cosenza E, Davalos J, Lesko J, Machida A, Rizkalla S & Triantafillou T (2002) Fiber-reinforced polymer composites for construction – State-of-the-art review. *Journal of Composites for Construction* 6(2): 73–87.
- Bao X, DeMerchant M, Brown A & Bremner T (2001) Tensile and compressive strain measurement in the lab and field with the distributed Brillouin scattering sensor. *Journal of Lightwave Technology* 19(11): 1698–1704.
- Barnoski M & Jensen S (1976) A novel technique for investigating attenuation characteristics. *Applied Optics* 15(9): 2112–2115.
- Bennett K & McLaughlin L (1995) Monitoring of corrosion in steel structures using optical fiber sensors. *Proc SPIE* 2446: 48–59.
- Bergman L, Eng S & Johnston A (1983) Temperature stability of transit time delay for a single-mode fibre in a loose tube cable. *Electronics Letters* 19(21): 865–866.
- Berthold J (1997) Sensors in industrial systems. In: Dakin J & Culshaw B (ed) *Optical Fiber Sensors – Applications, Analysis, and Future Trends*. Artech House, USA.
- Bertolini G (1968) Pulse shape and time resolution. In: Bertolini G & Coche A (eds.) *Semiconductor Detectors*. North-Holland Publishing Co, Amsterdam.
- Blue Road Research Inc. [ONLINE]. Available: <http://www.blueroadresearch.com>.
- Bogue R (2005) UK start-up poised to take the fibre optic sensor market by storm. *Sensor Review* 25(1): 24–27.
- Braunstein J, Ruchala J & Hodac B (2002) Smart structures: Fiber-optic deformation and displacement monitoring. *Proc First International Conference on Bridge Maintenance, Safety and Management (IABMAS)*, Barcelona, Spain, Available on CD (ISBN: 84-95999-05-6).
- Brininstool M (1987) Measuring longitudinal strain in optical fibers. *Optical Engineering* 26(11): 1112–1119.
- Butter C & Hocker G (1978) Fiber optics strain gauge. *Applied Optics* 17(18): 2867–2869.
- Calvert S & Mooney J (2004) Bridge structural health monitoring system using fiber grating sensors: development and preparation for a permanent installation. *Proc SPIE* 5391: 61.
- Cauchi S, Cherpillod T, Morison D & McClarty E (2007) Fiber-optic sensors for monitoring pipe bending due to ground movement. *Pipeline & Gas Journal* (January 2007).
- Chan T, Yu L, Tam H, Ni Y, Liu S, Chung W & Cheng L (2006) Fiber Bragg grating sensors for structural health monitoring of Tsing Ma bridge: Background and experimental observation. *Engineering Structures* 28(5): 648–659.
- Culshaw B (1988) Basic concepts of optical fiber sensors. In: Dakin J & Culshaw B (eds) *Optical Fiber Sensors: Principles and Components*. Artech House, USA.
- Culshaw B (1996) *Smart Structures and Materials*. Artech House, USA.

- Culshaw B (2004) Optical fiber sensor technologies: opportunities and – perhaps – pitfalls. *Journal of Lightwave Technology* 22(1): 39–50.
- Dakin J (1993) Distributed optical fiber sensors. *Proc SPIE* 1797.
- Dakin J & Culshaw B (1988) *Optical Fiber Sensors: Principles and Components*. Artech House, USA.
- Delepine-Lesoille S, Merliot E, Boulay C, Quétel L, Delaveau M & Courteville A (2006) Quasi-distributed optical fibre extensometers for continuous embedding into concrete: design and realization. *Smart Materials and Structures* 15(4): 931–938.
- Doyle C (2003) Fibre Bragg grating sensors – An introduction to Bragg gratings and interrogation techniques [ONLINE]. Available: <http://www.smartfibres.com/Attachments/Smart%20Fibres%20Technology%20Introduction.pdf>. (Cited 2007/12/12).
- Doomink J, Phares B, Zhou Z, Jinping O, Graver T & Xu Z (2004) Fiber Bragg grating sensing for structural health monitoring of civil structures [ONLINE]. Available: <http://www.micronoptics.com/pdfs/FBGsensingSHMcivil.pdf>. (Cited 2007/12/12).
- Everall L & Lloyd G (2006) Optical interrogation system and sensor system. U.S. Patent 7,046,349.
- Fields J & Cole J (1980) Fiber microbend acoustic sensor. *Applied optics* 19(19): 3265–3267.
- Fiso Technologies Inc. [ONLINE]. Available: <http://www.fiso.com>.
- Fixter L & Williamson C (2006) State of the Art Review – Structural Health Monitoring, [ONLINE]. Available: <http://amf.globalwatchonline.com> (see Smart.Mat/latest news).
- Fogale Nanotech [ONLINE]. Available: <http://www.fogale.fr/pages/index.php>. (Cited 2007/12/12).
- FOS (2004) Fiber-sensor specialist breaks the price barrier. *Fiber Optic Sensors & Systems* 18(4): 1–4 [ONLINE] Available: [http://www.ipi.com.au/ipi/IPI.nsf/LookupPDF/igss/\\$file/igss.pdf](http://www.ipi.com.au/ipi/IPI.nsf/LookupPDF/igss/$file/igss.pdf). (Cited 2007/12/12).
- Fox-Tek Inc. [ONLINE]. Available: <http://www.fox-tek.com>.
- Gao J, Shi B, Zhang W & Zhu H (2006) Monitoring the stress of the post-tensioning cable using fiber optic distributed strain sensor. *Measurement* 39(5): 420–428.
- Gu X, Chen Z & Ansari F (2000) Embedded fiber optic crack sensor for reinforced concrete structures. *ACI Structural Journal* 97(3): 468–476.
- Guoliang J, Van Vickle P, Peters K & Knight V (2007) Oscillator interrogated time-of-flight optical fiber interferometer for global strain measurements. *Sensors and Actuators* 135(2): 443–450.
- Habel W, Hofmann D & Hillemeier B (1997) Deformation measurements of mortars at early ages and of large concrete components on site by means of embedded fiber-optic microstrain sensors. *Cement and Concrete Composites* 19(1): 81–102.
- Habel W, Feddersen I & Fitschen C (1999) Embedded quasi-distributed fiber-optic sensors for the long term monitoring of the grouting area of rock anchors in a large gravity dam. *Journal of Intelligent Material Systems and Structures* 10(April): 330–339.
- Hampshire T & Adeli H (2000) Monitoring the behavior of steel structures using distributed optical fiber sensors. *Journal of Constructional Steel Research* 53(3): 267–281.

- Hartog A, Conduit A & Payne D (1978) Variation of pulse delay with stress and temperature in jacketed and unjacketed optical fibres. *Optical and Quantum Electronics* 11(May): 265–273.
- Horiguchi T, Rogers A, Michie W, Stewart G & Culshaw B (1997) Distributed sensors: Recent developments. In: Dakin J & Culshaw B (eds) *Optical Fiber Sensors – Applications, Analysis, and Future Trends*. Artech House, USA.
- Hornung S, Kashyap R, Reeve M, Russell J & Titchmars J (1983) Axial strain in optical-fiber cable manufacture and duct installation. *Journal of Lightwave Technology* 1(2): 359–362.
- Idriss R, Kodindouma M, Kersey A & Davis M (1997) Multiplexed Bragg grating optical fiber sensors for damage evaluation in highway bridges. *Smart Materials and Structures* 7: 209–216.
- Inaudi D (1997) Fiber optic smart sensing. In: Rastogi P (ed) *Optical Measurement Techniques and Applications*. Artech House, USA.
- Inaudi D & Vurpillot S (1999) Monitoring of concrete bridges with long-gage fiber optic sensors. *Journal of Intelligent Material Systems and Structures* 10(4): 280–292.
- Inaudi D, Casanova N, Vurpillot S, Glisic B, Kronenberg P & Lloret S (2000) Lessons learned in the use of fiber optic sensor for civil structural monitoring [ONLINE]. Available: <http://www.smartec.ch> (see Applications / Bibliography). (Cited 2007/12/12).
- Inaudi D (2002) Photonic sensing technology in civil engineering applications. In: López-Higuera J (ed) *Optical Fibre Sensing Technology*. John Wiley & Sons, England.
- Inaudi D & Glisic B (2005) Application of distributed fiber optic sensory for SHM. 2<sup>nd</sup> International Conference on Structural Health Monitoring of Intelligent Infrastructure [ONLINE]. Available: <http://www.smartec.ch> (see Applications/Bibliography). (Cited 2007/12/12).
- Inaudi D & Glisic B (2006) Integration of distributed strain and temperature sensors in composite coiled tubing. *Proc SPIE* 6167.
- Insensys Ltd. [ONLINE]. Available: <http://www.insensys.com>.
- Insensys (2005) Vortex induced vibration on riser pipes [ONLINE]. Available: [http://www.insensys.com/dynamicdata/data/docs/deepstar\\_case\\_study\\_january\\_2005.pdf](http://www.insensys.com/dynamicdata/data/docs/deepstar_case_study_january_2005.pdf). (Cited 2007/12/12).
- International Vocabulary of Basic and General Terms in Metrology (1994). Beuth Verlag GmbH, Berlin, Germany.
- ISHMII [ONLINE]. Available: <http://www.ishmii.org/> (see SHM Guidelines). (Cited 2007/12/12).
- ISHMII (2002) Monitoring and Safety Evaluation of Existing Concrete Structures – State-of-the-Art Report [ONLINE]. Available: <http://www.ishmii.org/> (see SHM Guidelines / FIB Task Group 5-1 SHM Guidelines (Europe)). (Cited 2007/12/12).
- Jacobs G (2004) High-definition surveying – 3D laser scanning: Versatility – The other “hidden” instrument inside laser scanners. *Professional Surveyor* 24(10).
- Jaeger B, Sansalone M & Poston R (1997) Using impact echo to assess tendon ducts. *Concrete International* 19(2): 42–46.

- Jansson J, Mäntyniemi A & Kostamovaara J (2006) A CMOS time-to-digital converter with better than 10 ps single-shot precision. *IEEE J Solid-State Circuits* 41(6): 1286–1296.
- Johnson M & Ulrich R (1978) Fiber-optical strain gauge. *Electronics Letters* 14(6): 432–433.
- Kaisto I, Kostamovaara J, Manninen M, & Myllylä R (1983) Optical range finder for 1.5–10 m distances. *Applied Optics* 22(20): 3528–3264.
- Kajorncheappunngam S, Gupta R & GangaRao H (2002) Effect of aging environment on degradation of glass-reinforced epoxy. *Journal of Composites for Construction* 6(1): 61–69.
- Kao K & Hockham G (1966) Dielectric fibre surface waveguides for optical frequencies. *Proceedings of the Institution of Electrical Engineers* 113(7): 1151–1158.
- Kashyap R & Reeve M (1980) Single-ended fibre strain and length measurement in frequency domain. *Electronics Letters* 16(18): 689–690.
- Kashyap R, Reeve M, Hornung S, Bandurek G & Nevett J (1982) Measuring of strain relief in an experimental optical fibre cable. *Electronics Letters* 18(6): 263–265.
- Katz S (1998) Factors affecting strain gauge selection for smart structure application. *Proc SPIE* 3330: 20–27.
- Kercel S & Muhs J (1992) Repeatable sensitivity of optical-time-domain reflectometry-based strain measurement. *Proc SPIE* 1757: 60–73.
- Kersey A, Berkoff T & Morey W (1993) Multiplexed fiber Bragg grating strain-sensor system with a fiber Fabry-Perot wavelength filter. *Optics Letters* 18(16): 1370–1372.
- Kersey A (1995) Fiber optic sensor multiplexing techniques. In: Udd E (ed) *Fiber Optic Smart Structures*. John Wiley & Sons, USA.
- Kersey A, Davis M, Patrick H, LeBlanc M, Koo K, Askins C, Putnam M & Friebele E (1997) Fiber grating sensors. *Journal of Lightwave Technology* 15(8): 1442–1463.
- Kersey A (1997a) Multiplexing techniques for fiber-optic sensors. In: Dakin J & Culshaw B (eds) *Optical Fiber Sensors – Applications, Analysis, and Future Trends*. Artech House, USA.
- Kersey A (1997b) Optical fiber sensors. In: Rastogi P (ed) *Optical Measurement Techniques and Applications*. Artech House, USA.
- Kilpelä A & Kostamovaara J (1997) Laser pulser for a time-of-flight laser radar. *Review of Scientific Instruments* 68(6): 2253–2258.
- Kilpelä A, Ylitalo J, Määttä K & Kostamovaara J (1998) Timing discriminator for pulsed time-of-flight laser rangefinding measurements. *Review of Scientific Instruments* 69(5): 1978–1984.
- Kostamovaara J & Myllylä R (1986) Time-to-digital converter with an analog interpolation circuit. *Review of Scientific Instruments* 57(11): 2880–2885.
- Kunzler M, Udd E, Taylor T & Kunzler W (2003) Traffic monitoring using fiber optic grating sensors on the I-84 freeway & future uses in WIM. *Proc SPIE* 5278: 122.
- Kurashima T, Horiguchi T & Tateda M (1990) Distributed-temperature sensing using stimulated Brillouin scattering in optical silica fibers. *Optics Letters* 15(18): 1038.

- Lawrence C, Nelson D, Bennett T & Spingarn J (1997) Determination of process-induced residual stress in composite materials using embedded fiber optic sensors. *Proc SPIE* 3042: 154–167.
- Lee C & Taylor H (1988) Interferometric optical fibre sensors using internal mirrors. *Electronics Letters* 24(4): 193–194.
- Lee C & Taylor H (1995) Sensors for smart structures based on the Fabry-Perot interferometer. In: Udd E (ed) *Fiber Optic Smart Structures*. John Wiley & Sons, USA.
- Li C, Sun Y, Zhao Y, Liu H, Gao L, Zhang Z & Qiu H (2006) Monitoring pressure and thermal strain in the second lining of a tunnel with a Brillouin OTDR. *Smart Materials and Structures* 15(5): 107–110.
- Lin Y, Chang K, Lai J & Wu I (2004) Applications of optical fiber sensor on local scour monitoring. *Proc IEEE Sensors 2004* vol 2: 832–835.
- Lou K, Zimmermann B & Yaniv G (1994) Combined sensor system for process and in-service health monitoring of composite structures. *Proc SPIE* 2191: 32–45.
- Lou K, Yaniv G, Hardtmann D, Ma G & Zimmermann B (1995) Fiber optic strain monitoring of bridge column retrofitted with composite jacket under flexural loads. *Proc SPIE* 2446: 16–24.
- López-Higuera J (2002) *Handbook of Optical Fibre Sensing Technology*. John Wiley & Sons, England.
- Lyöri V (1993) *Kuitututkalla Luettava Hajautettu Kuituanturi*. Oulu, Finland. Master's thesis, University of Oulu, Department of Electrical Engineering.
- Lyöri V (2000) *Valopulssin Kulkuaikamittaukseen Perustuva Kuituoptinen Venymänmittaus*. Oulu, Finland. Licentiate thesis, University of Oulu, Department of Electrical and Information Engineering.
- MacLean A, Moran C, Johnstone W, Culshaw B, Marsh D & Andrews G (2001) A distributed fibre optic sensor for liquid hydrocarbon detection. *Proc SPIE* 4328.
- Measures R (2001) *Structural Monitoring with Fiber Optic Technology*. Academic Press, USA.
- Meier U (2000) Composite materials in bridge repair. *Applied Composite Materials* 7(2–3): 75–93.
- Michie C, Culshaw B, Konstantaki M, McKenzie I, Kelly S, Graham N & Moran C (1995) Distributed pH and water detection using fiber-optic sensors and hydrogels. *Journal of Lightwave Technology* 13(7): 1415–1420.
- Micron Optics Inc. [ONLINE]. Available: <http://www.micronoptics.com>.
- Morey W, Meltz G & Glenn W (1989) Fiber optic Bragg grating sensors. *Proc SPIE* 1169: 98–107.
- Morey W, Ball G & Meltz G (1994) Photoinduced Bragg gratings in optical fibers. *Optics and Photonics News (Feb)*: 7–14.
- Morin A, Caron S, Van Neste R & Edgecombe M (1996) Field monitoring of the ice load of an icebreaker propeller blade using fiber optic strain gauges. *Proc SPIE* 2718: 427–438.
- Myllylä R (1978) A modern positron lifetime spectrometer. *Nuclear Instruments and Methods* 148: 267–271.

- Mäntyniemi A, Rahkonen T & Kostamovaara J (2002a) An integrated 9-channel time digitizer with 30 ps resolution. *IEEE International Solid State Circuits Conference Vol 1*: 266–267.
- Mäntyniemi A, Rahkonen T & Kostamovaara J (2002b) A nonlinearity corrected CMOS time digitizer IC with 20 ps single-shot precision. *IEEE International Symposium on Circuits and Systems Vol 1*: 513–516.
- Mäntyniemi A (2004) An Integrated CMOS High Precision Time-to-Digital Converter Based on Stabilised Three-Stage Delay Line Interpolation. Oulu, Finland. Doctoral thesis, University of Oulu, Department of Electrical and Information Engineering.
- Määttä K, Kostamovaara J & Myllylä R (1993) Profiling of hot surfaces by pulsed time-of-flight laser range finder techniques. *Applied Optics* 32(27): 5334–5347.
- Niewisch J & Bartelt H (1994) Optical fiber sensor array for dynamic variables. *Sensors and Actuators* 42(1–3): 562–566.
- Niklès M, Vogel B, Briffod F, Grosswig S, Sauser F, Luebbecke S, Bals A & Pfeiffer T (2004) Leakage detection using fiber optics distributed temperature monitoring. *Proc SPIE* 5384.
- Nissilä S, Kostamovaara J & Myllylä R (1991) Thermal characteristics of optical delay in fibers used in pulsed laser rangefinding. *Journal of Lightwave Technology* 9(11): 1464–1466.
- OMEGA (1998) *Transactions in Measurement and Control, Volume 3 – Force-Related Measurements* [ONLINE]. Available: [http://www.omega.com/literature/transactions/Transactions\\_Vol\\_III.pdf](http://www.omega.com/literature/transactions/Transactions_Vol_III.pdf). (Cited 2007/12/12).
- Omnisens SA [ONLINE]. Available: <http://www.omnisens.ch>.
- OSMOS SA [ONLINE]. Available: <http://www.osmos-group.com>.
- Pinto N, Frazão O, Baptista J & Santos J (2006) Quasi-distributed displacement sensor for structural monitoring using a commercial OTDR. *Optics and lasers in Engineering* 44(8): 771–778.
- Pluciński J, Wierzba P & Kosmowski B (2005) Time-of-flight fiber optic sensors for strain and temperature measurement. *Proc SPIE* 5952.
- Pospisil K, Stryk J, Korenska M & Pazdera L (2003) Selected acoustic methods for nondestructive testing [ONLINE]. Available: <http://www.ndt.net/article/ndtce03/papers/p060/p060.htm>. (Cited 2007/12/12).
- Rastogi P (1997) *Optical Measurement Techniques and Applications*. Artech House, USA.
- Reed S (1964) Evaluation of measurement. In: Bleuler E & Haxby R (eds) *Electronic Methods*. Academic Press, USA.
- Roberts G, Meng X & Brown C (2006) Kinematic GPS trials measure 3D displacements – to millimeter precision – of Scotland’s Fort Road Bridge. *Sensors Weekly* [ONLINE]. Available: <http://www.sensormag.com/sensors/article/articleDetail.jsp?id=323336&sk=&date=&pageID=3>. (Cited 2007/12/12).
- Roctest Ltd. [ONLINE]. Available: <http://www.roctest.com>.
- Rogers A (1999) Distributed optical-fibre sensing. *Measurement Science and Technology* 10(8): 75–99.

- Russel P & Archambault J (1996) Fiber gratings. In: Culshaw B & Dakin J (eds) *Optical Fiber Sensors: Components and Subsystems*. Artech House, USA.
- Rizkalla S & Hassan T (2002) Effectiveness of FRP for strengthening concrete bridges. *Journal of the International Association for Bridge and Structural Engineering* 12(2): 89–95.
- Shibata N, Katsuyama Y, Mitsunaga Y, Tateda M & Seikai S (1983) Thermal characteristics of optical pulse transit time delay and fiber strain in a single-mode optical fiber cable. *Applied Optics* 22(7): 979–984.
- Smartec SA [ONLINE]. Available: <http://www.smartec.ch>.
- Smart Fibres Ltd. [ONLINE]. Available: <http://www.smartfibres.com>.
- Smith D & Williams J (2002) Direct measurement of large strains in synthetic fiber mooring ropes using polymeric optical fibers. *Offshore Technology Conference 2002* [ONLINE]. Available: <http://www.ornl.gov/sci/fossil/Publications/RECENT%20PUBS/FEAC322.pdf>. (Cited 2007/12/12).
- Sørensen H, Canning J, Lægsgaard J & Hansen K (2006) Control of the wavelength dependent thermo-optic coefficients in structured fibres. *Optics Express* 14(14): 6428–6433.
- Talat K (1990) Smart skins and fiber-optic sensors application and issues. *Proc SPIE* 1370: 103–114.
- Tateda M, Tanaka S & Sugawara Y (1980) Thermal characteristics of phase shift in jacketed optical fibers. *Applied Optics* 19(5): 770–773.
- Tatekura K, Yamamoto H & Ejiri Y (1982) Strain of optical fibres of an optical submarine cable on the sea bed. *Electronics Letters* 18(10): 414–415.
- Udd E (1991a) The emergence of fiber optic sensor technology. In: Udd E (ed) *Fiber Optic Sensors - An Introduction for Engineers and Scientists*. John Wiley & Sons, USA.
- Udd E (1991b) *Fiber Optic Sensors - An Introduction for Engineers and Scientists*. John Wiley & Sons, USA.
- Udd E (1995) *Fiber Optic Smart Structures*. John Wiley & Sons, USA.
- Valis T, Hogg D & Measures R (1992) Fiber-optic Fabry-Perot strain rosettes. *Smart Materials and Structures* 1(3): 227–232.
- Van Steenkiste R & Springer G (1997) *Strain and Temperature Measurement with Fiber Optic Sensors*. Technomic Publishing Company, USA.
- Williams J, Smith D & Muhs J (2006) Measurement of large strains in ropes using plastic optical fibers. U.S. Patent 6,999,641.
- Yokogawa Electric Co. [ONLINE]. Available: <http://www.yokogawa.com/tm>.
- Zhang W, Gao J, Shi B, Cui H & Zhu H (2006) Health monitoring of rehabilitated concrete bridges using distributed optical fiber sensing. *Computer-Aided Civil and Infrastructure Engineering* 21: 411–424.
- Zhao Y & Ansari F (2001) Quasi-distributed fiber-optic strain sensor: principle and experiment. *Applied optics* 40(19): 3176–3181.
- Zimmermann B, Claus R, Kapp D & Murphy K (1989) Optical time domain reflectometry for local strain measurements. *Proc SPIE* 1170: 534–541.

- Zimmermann B, Claus R, Kapp D, Murphy K (1990) Fiber-optic sensors using high-resolution optical time domain instrumentation systems. *Journal of Lightwave Technology* 8(9): 1273–1277.
- Zimmermann B & Claus R (1991) Multi-segment OTDR based fiber strain sensors for dynamic structures. *Proc SPIE* 1586: 92–95.
- Zimmermann B & Claus R (1993) Spatially multiplexed optical fiber time domain sensors for civil engineering applications. In: Ansari F (ed) *Applications of Fiber Optic Sensors in Engineering Mechanics*. ASCE, USA.
- Zumberge M & Husmann E (1998) A time-of-flight fiber optic borehole strain sensor in Antarctica [ONLINE]. Available: <http://gravity.ucsd.edu/research/Arcstrain/arcstrain.html>. (Cited 2007/12/12).
- Zumberge M, Elsberg D, Harrison W, Husmann E, Morack J, Pettit E & Waddington E (2002) Measurement of vertical strain and velocity at Siple Dome, Antarctica, with optical sensors. *Journal of Glaciology* 48(161): 217–225.

## Original papers

- I Lyöri V, Suopajarvi P, Nissilä S, Kopola H & Suni H (1994) Measurement of stress in a road structure using optical fibre sensors. Proc. First World Conference on Structural Control, Los Angeles, USA, 1: WA3 40–48.
- II Suopajarvi P, Pennala R, Heikkinen M, Karioja P, Lyöri V, Myllylä R, Nissilä S, Kopola H & Suni H (1998) Fibre optic sensors for traffic monitoring applications. Proc. SPIE, 5<sup>th</sup> Annual International Symposium on Smart Structures and Materials, San Diego, USA, 3325: 222–229.
- III Suopajarvi P, Lyöri V, Nissilä S, Kopola H & Johansson R (1995) Indicating cure and stress in composite containers using optical fibers. Optical Engineering 34(9): 2587–2591.
- IV Lyöri V, Määttä K, Nissilä S, Kopola H, Englund M & Mitrunen A (1996) A high resolution reflectometer for measuring dynamic strain in a single mode optical fibre. Proc. International Conference on Applications of Photonic Technology 2, Montreal, Canada: 751–756.
- V Lyöri V, Määttä K, Nissilä S, Kopola H & Englund M (1997) A high precision Fresnel-OTDR for distributed fibre-optic sensor network applications. Proc. 12<sup>th</sup> International Conference on Optical Fiber Sensors, Williamsburg, USA: 520–523.
- VI Lyöri V, Määttä K, Myllylä R, Jurvakainen M, Lahtinen H, Peltomäki P, Pramila A, Heikkinen M, Suopajarvi P & Kopola H (2000) A fibre-optic time-of-flight laser radar for measuring integral strain in a composite structure. Proc. SPIE, 14<sup>th</sup> International Conference on Optical Fiber Sensors, Venice, Italy, 4185: 210–213.
- VII Lyöri V, Mäntyniemi A, Kilpelä A, Duan G, & Kostamovaara J (2003) A fibre-optic time-of-flight radar with a sub-metre spatial resolution for the measurement of integral strain. Proc. SPIE, International Conference on Smart Structures and Materials, San Diego, USA, 5050: 322–332.
- VIII Lyöri V, Kilpelä A, Duan G, Kostamovaara J & Aho T (2006) Monitoring of a bridge-deck using long-gage optical fiber sensors with a pulsed TOF measurement technique. Proc. 3<sup>rd</sup> International Conference on Bridge Maintenance, Safety and Management (IABMAS), Porto, Portugal, published on CD (ISBN 0 415 40315 4).
- IX Lyöri V, Kilpelä A, Duan G, Mäntyniemi A & Kostamovaara J (2007) Pulsed time-of-flight radar for fiber-optic strain sensing. Review of Scientific Instruments 78(2): 024705.

Original papers have been reprinted with kind permission of the following publishers: IASCM (I), SPIE (II, III, VI, VII), Springer Science and Business Media (IV), OSA (V), Taylor & Francis (VIII) and AIP (IX).

Original papers are not included in the electronic version of the dissertation.



ACTA UNIVERSITATIS OULUENSIS  
SERIES C TECHNICA

272. Aikio, Janne P. (2007) Frequency domain model fitting and Volterra analysis implemented on top of harmonic balance simulation
273. Oiva, Annukka (2007) Strategiakeskeinen kyvykkyyden johtaminen ja organisaation strateginen valmius. Kahden johtamismallin testaus
274. Jokinen, Hanna (2007) Screening and cleaning of pulp—a study to the parameters affecting separation
275. Sarja, Tiina (2007) Measurement, nature and removal of stickies in deinked pulp
276. Tóth, Géza (2007) Computer modeling supported fabrication processes for electronics applications
277. Näsi, Jari (2007) Intensified use of process measurements in hydrometallurgical zinc production processes
278. Turtinen, Markus (2007) Learning and recognizing texture characteristics using local binary patterns
279. Sarpola, Arja (2007) The hydrolysis of aluminium, a mass spectrometric study
280. Keski-Säntti, Jarmo (2007) Neural networks in the production optimization of a kraft pulp bleach plant
281. Hamada, Atef Saad (2007) Manufacturing, mechanical properties and corrosion behaviour of high-Mn TWIP steels
282. Rahtu, Esa (2007) A multiscale framework for affine invariant pattern recognition and registration
283. Kröger, Virpi (2007) Poisoning of automotive exhaust gas catalyst components. The role of phosphorus in the poisoning phenomena
284. Codreanu, Marian (2007) Multidimensional adaptive radio links for broadband communications
288. Perkkiö, Miia (2007) *Utilitas* restauroinnissa. Historiallisen rakennuksen käyttötarkoituksen muutos ja funktionaalinen integriteetti
289. Nissilä, Mauri (2008) Iterative receivers for digital communications via variational inference and estimation
290. Toivonen, Tuukka (2007) Efficient methods for video coding and processing

Book orders:  
OULU UNIVERSITY PRESS  
P.O. Box 8200, FI-90014  
University of Oulu, Finland

Distributed by  
OULU UNIVERSITY LIBRARY  
P.O. Box 7500, FI-90014  
University of Oulu, Finland

S E R I E S E D I T O R S

**A**  
**SCIENTIAE RERUM NATURALIUM**  
*Professor Mikko Siponen*

**B**  
**HUMANIORA**  
*Professor Harri Mantila*

**C**  
**TECHNICA**  
*Professor Juha Kostamovaara*

**D**  
**MEDICA**  
*Professor Olli Vuolteenaho*

**E**  
**SCIENTIAE RERUM SOCIALIUM**  
*Senior Assistant Timo Latomaa*

**E**  
**SCRIPTA ACADEMICA**  
*Communications Officer Elna Stjerna*

**G**  
**OECONOMICA**  
*Senior Lecturer Seppo Eriksson*

**EDITOR IN CHIEF**  
*Professor Olli Vuolteenaho*

**EDITORIAL SECRETARY**  
*Publications Editor Kirsti Nurkkala*

ISBN 978-951-42-8701-5 (Paperback)

ISBN 978-951-42-8702-2 (PDF)

ISSN 0355-3213 (Print)

ISSN 1796-2226 (Online)

